Biocatalytic Halocyclization of Amides Enables

By Vanadium Haloperoxidases

by

Kayla Merker

A Thesis Presented in Partial Fulfillment
of the Requirements for the Degree
Master of Science

Approved October 2022 by the
Graduate Supervisory Committee:

Kyle Biegasiewicz, Chair
Laura Ackerman-Biegasiewicz
Jeremy Mills

ARIZONA STATE UNIVERSITY

December 2022

ABSTRACT

Marine algae are a rich source of bioactive halogenated natural products. The presence of these marine natural products has largely been attributed to their biosynthesis by organisms in these environments through a variety of different halogenation mechanisms. One of the key contributors in these halogenation processes are from the vanadium haloperoxidases (VHPOs) class of enzymes. VHPOs perform an electrophilic halogenation through the oxidation of halide ions with hydrogen peroxide as the terminal oxidant. This technique produces an electrophilic halide equivalent that can directly halogenate organic substrates. Despite the numerous known reaction capabilities of this enzyme class, their construction of intramolecular ring formation between a carbon and nitrogen atom has remained unreported.

Herein, this study presents a development of a ‘new to nature’ chemical reaction for lactam synthesis. In pursuit of this type of reaction, it was discovered that wild type VHPOs (e.g., Curvularia inaequalis, Corallina officinalis, Corallina pilulifera, Acaryochloria marina) produce halogenated iminolactone compounds from acyclic amides in excellent yields and selectivity greater than 99 percent yield. The extension to chlorocyclizations will also be discussed.

DEDICATION

This thesis is dedicated to the memory of Roberta Merker. She was my constant source of support and encouragement during the challenges of my life. I am truly thankful to have had her in my life. She was my true inspiration and had molded me into the woman I am today. Although, she was unable to see me graduate during my undergraduate and graduate career, I know she would have been proud. This is for her.

ACKNOWLEDGMENTS

I have been extremely fortunate to have had the support of the department, friends, and colleagues. Without this support, this thesis would not have been possible.

First, I would like to thank my supervisor Dr. Kyle Biegasiewicz for his support and patience in guiding me during my graduate career. Working in your lab and knowing you as an individual has been a privilege. I am truly grateful for this opportunity. His experience has been invaluable, and I have learned much from him. Without his assistance and involvement, this thesis would have never been accomplished. I am excited to share what I have gained from his lab, as these skills will be with me for many years.

I would also like to thank my committee, including Prof. Laura Ackerman-Biegasiewicz and Prof. Jeremy Mills. I would also like to thank Prof. Nick Stephanopoulos for allowing me to collaborate with his group on total synthesis projects. Additionally, I would like to thank Arizona State University for providing the studentship that allowed me to do the research recorded in this master's thesis.

I am also thankful to my colleagues who have continuously helped me during these past two years, providing friendship, great conversation, and encouragement; Logan Hessefort, Jackson Tennet, and Manik Sharma. Also, a special thank you to Lauren P.T. Ramos for their personal and professional support during my time at the University. For many memorable evenings out and in, and always listened to me when I needed someone to talk to. I will always appreciate our friendship.

I want to thank my partner and best friend, Christian Sutherlin, for providing me with unfailing support and continuous encouragement throughout my years of study and through the process of researching and writing this thesis. Thank you for taking the time to proofread the earlier drafts of my thesis and for your many constructive suggestions. This accomplishment would not have been possible without them.

Finally, I thank God for letting me through all the difficulties. I have experienced His guidance day by day, and He is the one who let me finish my degree. I will keep trusting Him for my future challenges and endeavors. Thank you.

TABLE OF CONTENTS

Page

LIST OF TABLES v

LIST OF FIGURES vi

LIST OF SCHEMES ix

BACKGROUND/LITERATURE REVIEW

Introduction 1

Chemical and Biological Halogenation 5

Nucleophilic Halogenation 11

Radical Halogenation 12

Electrophilic Halogenation 15

Halofunctionalization of Olefins 22

Vanadium Haloperoxidases 31

BIOCATALYTIC HALOCYCLIZATION OF AMIDES ENABLED BY VANADIUM HALOPEROXIDASES

Project Design 40

Results and Discussion 42

Substrate Formation, 3–6 42

NBS Lactonization, 7–10 43

Enzymatic Halocyclization, 11–18 45

Summary and Conclusion 59

Experimental Procedures 61

General Information 61

Substrate Synthesis 63

Synthesis of Wittig, 1 63

Synthesis of Acid Chloride, 2 65

Synthesis of Amide Substrates, 3–5 66

Synthesis of NBS Substrates, 7–10 70

Page

Screening Procedure, 11–14 74
Physical Data 76
NMR Analyses 76
LCMS Analyses 85
REFERENCES 89

LIST OF TABLES

Table Page

1. Enzymatic Analysis with Ci, Co, Cp and Am with (3) 47

2. Enzymatic Analysis with Ci, Co, Cp and Am with (4) 50

3. Enzymatic Analysis with Ci, Co, Cp and Am with (5) 53

4. Enzymatic Analysis with Ci, Co, Cp and Am with (6) 56

LIST OF FIGURES

Figure Page

1. Class of Lactam Compounds 1

2. Biologically Active Lactam-containing Compounds.....2

3. Anticancer Halogenated Compounds Approved by the FDA in the United States in 2021.....6

4. Strategies for Enabling Stereoselectivity for Maintaining Catalyst/Halirenium Ion Association.....24

5. Crystal Structure of the Vanadium Chloroperoxidase from *C. inaequalis*, with a Close-up View of its Active Site 33

6. Amide Substrates, 3–6 41

LIST OF SCHEMES

Scheme Page

1. Synthesis of (+)-pramanicin 3

2. Halofunctionalization of Unactivated Alkenes in the Presence of HFIP 8

3. Comparison of Biocatalytic and Chemocatalytic Routes of Sitagliptin Phosphate .10

4. Halogenation of SAM by X-mediated by a Nucleophilic Halogenase 12

5. Generalized Mechanistic Radical Rebound Pathway of C-H Halogenation 13

6. Catalytic Cycle of Non-heme Iron α-ketoglutarate-dependent Halogenases 14

7. WelO5 Chlorination 15

8. Generalized Mechanistic Electrophilic Pathway of C-H Halogenation 16

9. HOX Generation and Utilization with (a) Heme-iron-dependent Haloperoxidases

(b) Vanadium-dependent Haloperoxidases. 18

10. FDH-mediated Electrophilic Halogenation 20

11. Racemization by Interalkene Halonium Transfer 23

12. Type I Example of Chiral Lewis Base Catalysis Mechanism.....25

13. Type 2 Chiral Ion Pairing Catalysis by Haloetherification.....26

14. Type 3 Hydrogen Bonding Catalysis by Bromocyclization of Olefins 27

15. Enantioselective Interactions Type 4 (a) LA Catalyzed and (b) Directed

Halocyclization 29

16. Proposed Catalytic Cycle of Vanadium-dependent Haloperoxidases 35

17. VBrPO Catalyzed Reaction with Nerolidol and Nerol 36

18. Biocatalytic Pathway to Napyradiomycin B1 (III). 38

Scheme Page

19. Proposed Reaction Sequence for the Vanadium Bromoperoxidase Catalyzed Reaction 40

20. Synthesis of Amide Starting Materials, 3–6 43

21. Iminolactone Product Standards, 7–10 45

22. Actual Reaction Sequence for the Enzyme Catalyzed Reaction with (3).....58

Introduction

Lactams are well-recognized as one of the most privileged compound types in modern drug design and discovery. This class of cyclic amides are classified based on ring size (β-four membered lactam, γ-five membered lactam, δ-six membered lactam, $\boldsymbol{\varepsilon}$-seven membered lactam) as well as their structural topologies such as, isolated, fused, spiro, and bridged (Figure 1).[1] These compounds have established themselves as promising leads in antimicrobial activity as early as the twentieth century and have demonstrated further applications in therapeutics, including the treatment of diabetes, cancer, and infectious diseases.[1,2] For example, the β-lactam class of compounds is one of the most influential families of natural microbial products applied in modern medicine.[2]

Figure 1. Class of Lactam Compounds.[1]

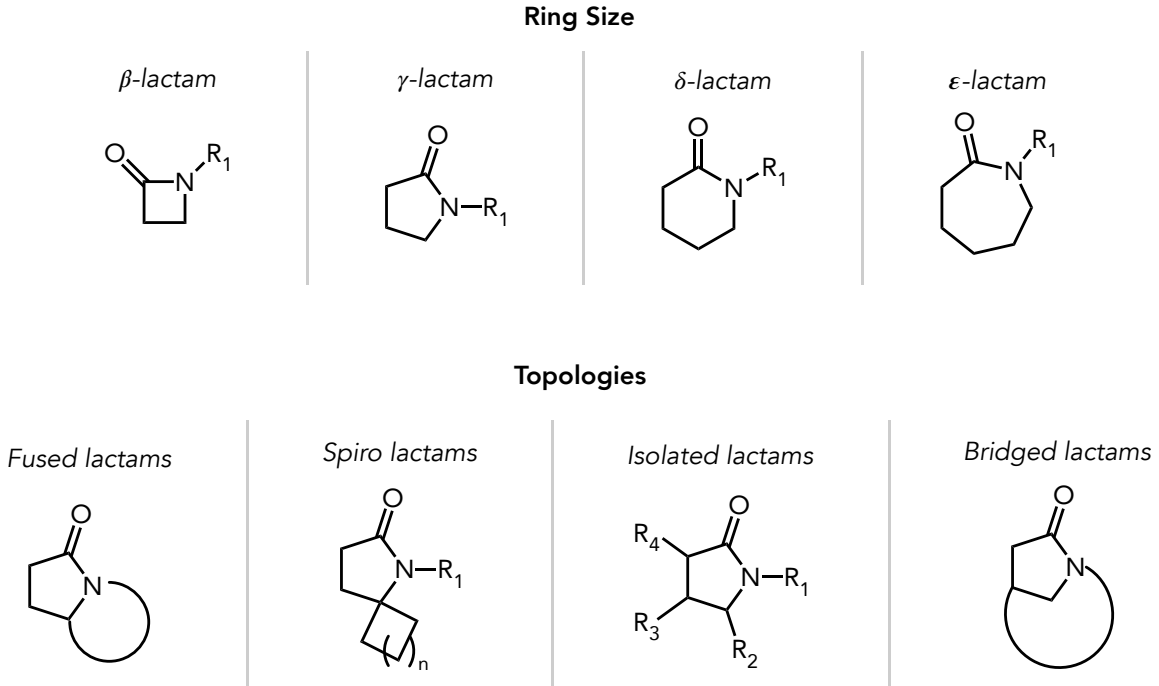

In the early twentieth century, the antibiotic penicillin was discovered and used to control and eliminate intractable infections.[2] Interestingly, the β-lactam class of compounds accounts for $15 billion in US sales and roughly about 65 percent of all antibiotic prescriptions.[3] Although penicillin was one of the first lactam compounds discovered in modern medicine, research has supported several other lactam systems.[4] Several biologically active lactam-containing molecules present in medications today are shown below in Figure 2.[1]

Figure 2. Biologically Active Lactam-containing Compounds.[1]

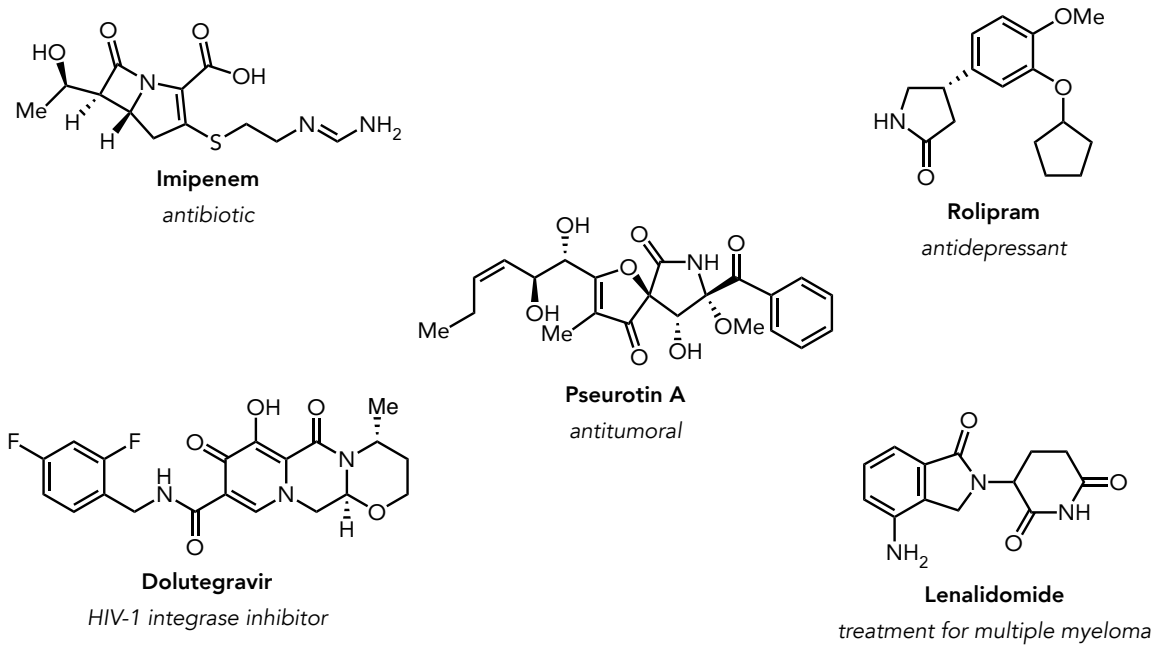

Several lactams have received considerable attention in medicinal chemistry over the past decade due to their conformationally restricted scaffolds. Their inherent peptidomimetic features have been helpful in achieving greater potency, selectivity, and metabolic stability of peptide-based drugs.[1] Of those, γ-lactams have become a primary

interest in medicinal chemistry. Their broad range of biological and structural activity has also been found in many natural compounds, including bacteria, plants, fungi, and animal sources.[5] The γ-fused and isolated lactams also have a more extensive activity profile than compounds with spiro- or bridged-lactams.[1] Additionally, both-fused and isolated lactams account for over 1,600 unique scaffolds and thousands of biologically active compounds.[1] Various synthetic strategies have been developed to access the structural moiety; however, the most intuitive method is the intramolecular amide formation between a carboxylic group and an amine.[6] For example, the start of a total synthesis of (+)-pramanicin **II** began from *L*-glutamic acid **I**, and the condensation of an amine with a carboxylic acid formed γ-lactam **III** after reduction (Scheme 1).[5, 6] Interestingly, the stereochemistry of naturally occurring pramanicin could be established due to their discovery.

Scheme 1. Synthesis of (+)-pramanicin.[5,7]

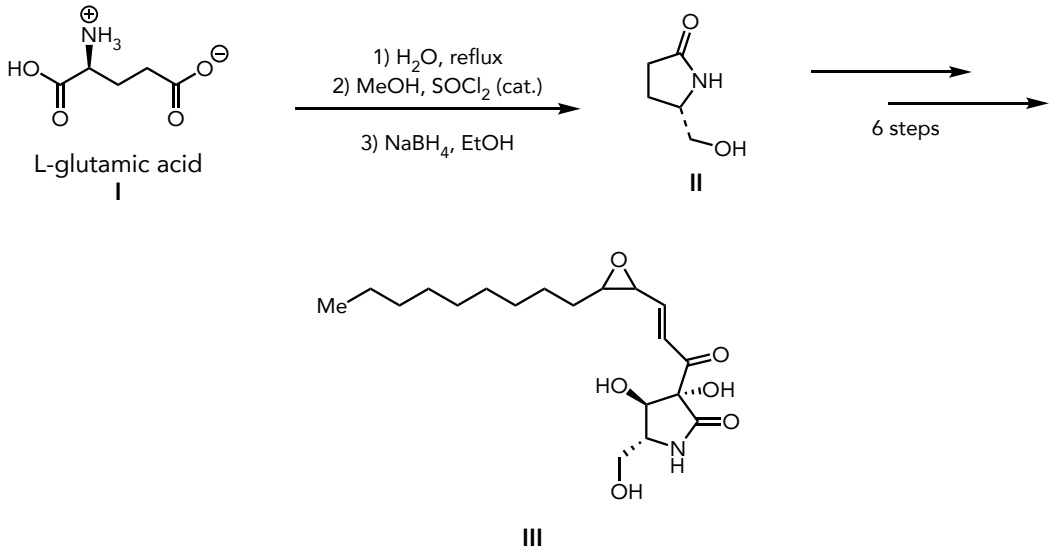

The percentage of lactam-containing compounds continues to increase in several databases. Drugs approved for clinical use were obtained from DrugBank, natural products were received by the Universal Natural Product Database (UNPD), and molecules annotated with biological activity were obtained from ChEMBL version 23.[1] However, halogenating lactams may potentially be clinically important as it can impact the functionality of biological activity. For example, there are several β-lactams present in many important antibiotics.[4] By halogenating β-lactams they could potentially be effective against β-lactamase positive bacteria because the β-lactamase may not recognize the new halogenated β-lactam. Additionally, halogenating other classes of lactams can lead to decreased resistance to these drugs by pathogenic microorganisms. For example, in a previous study by Bhuma *et al.*, they attempted to study the effects of halogenating δ-lactams, such as Nojirimycin, a transpeptidase inhibitor.[8] Their claim was that halogenating lactam derivatives will potentially increase their potency as pharmaceutical drugs.[8] However, their results showed that halogenating these iminosugars did not have an increase in microbial enzymatic inhibition.[8] However, in a recent study in 2021, researchers studied the effects of halogenating δ-lactones.[9] It has been shown that -lactones cause bacterial cell death through disruption of lipopolysaccharide (LPS).[9] The LPS constitutes the outer membrane of most gram-negative bacteria.[9] Their research showed that halogenating lactones with fluorine increased their antibacterial effects against *E. coli*.[9] Therefore, further research needs to be done to show a potential relationship between halogenation of lactams and increased drug potency.

Chemical and Biological Halogenation

Halogenation of organic substrates is a fundamental transformation in organic chemistry. In 2014, it was reported that halogenated compounds constitute roughly 20 percent of active pharmaceutical ingredients (APIs) and 30 percent of current agrochemicals.[10] The beneficial effects of carbon-halogen bonds within the structure of organic compounds have played a role in increasing their durability, stability towards biodegradation and oxidation, higher biological activity, and membrane permeability of their respective unhalogenated structure. Although chlorinated and brominated molecules predominate in natural metabolites, synthetic APIs and agrochemicals with fluorine and chlorine are more abundant. Despite the high incidence of chlorine and fluorine atoms in the final structure of APIs, brominations and iodinations are often carried out to generate of synthetic intermediates.

During the first decade of the 21st century, the significance of halogen-containing drugs continues to emerge as some compounds contain one or more halogen atoms. In 2021, 50 new chemical entities were approved by the FDA for clinical use.[11] Ultimately, 25 percent of all FDA approved drugs in 2021 were halogenated.[10] The revenue generated by cancer drugs continues to rise yearly and is expected to double by 2026.[12] In 2021, oncology drugs reached $176 billion in sales.[11] Below consists of common halogenated anticancer drugs that were approved by the FDA within the past year (Figure 3).[10]

Figure 3. Anticancer Halogenated Compounds Approved by the FDA in the United States in 2021.[10]

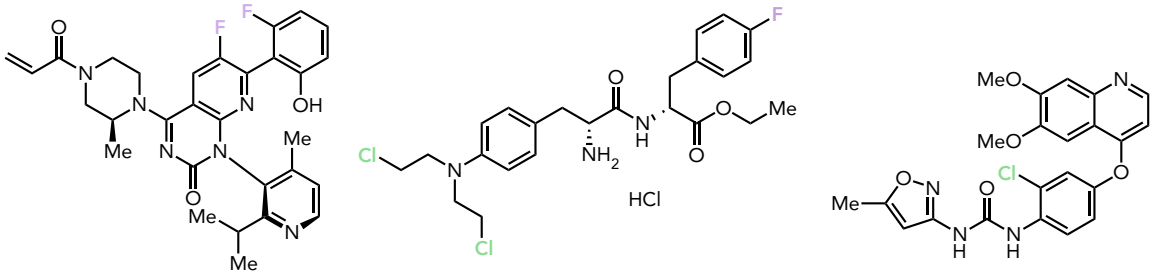

Sotorasib
NSCLC and colorectal cancer

Melphalan flufenamide as HCl salt
multiple myeloma

Tivozanib
renal cell carinoma

One of the most active areas in chemical synthesis has been in the installation of halogens at early and late stages. They are valuable for the preparation of organometallic reagents, utility in cross couplings, and radical precursors in radical-mediated transformations.[13] By far the most prevalant is in the transition metal-catalyzed cross-coupling involving an organo(pseudo)halide electrophile that couples with a nucleophilic partner, such as an organometallic reagent, an alkene, or a heteroatom.[13] Palladium, Nickel, and Copper are common transition metal catalysts for these transformations, and their reactivity is frequently tempered by phosphines, N-heterocyclic carbenes, or other ancillary ligands.[13] Cross-coupling reactions with organometallic nucleophiles include Suzuki-Miyaura, Negishi, Kumada, Stille, Giese, and Hiyama-type. Transition-metal directed and undirected C-H bond halogenation was developed and found to be a sustainable approach in organic synthesis to obtain the organo-halogen compound. In 2014, Paik and co-workers reported recent progress in first-row transition metal-catalyzed methods associated with directed and undirected strategies for C-H halogenation (X = Cl, Br, and I).[14] Additionally, Reeves discusses detailed progress of

synthetic methodologies in orango-fluorination.[Error! Bookmark not defined.] Although there are strategies to control cross-coupling chemoselectivity; substrate steric or electronic biases can deactivate specific sites and enable atypical chemo selectivity. [13]

Inexpensive and atom economic halogenations involve using elemental halogens (X_2) or hydrogen halides (HX).[10] However, these reagents used in organic synthesis have significant drawbacks due to their highly corrosive and toxic nature and high reactivity. Synthetic chemists have developed halogenating reagents that avoid using X_2 and HX. A commonly used replacement features the *N*-halosuccinamide (NXS) reagents used as a substituent of X_2 (X = Br, Cl, I), but the preparation of this reagent requires the use of the corresponding elemental halogen. These reagents have found utility in halocyclization reactions involving numerous functional groups including carboxylic acids, alcohols, and amides.[15] For example in the context of halolactamization, Gandon, Leboeuf, and co-workers wanted to incorporate a strategy that would allow both to activate the halide reagent, NXS, and prevent the deactivation of the halide source.[16] They accomplished this while operating under mild reaction conditions using hexafluroroisopropanol (HFIP) (Scheme 2).[16] The purpose of this additive is to effectively activate the N-halosuccinamide reagent and prevent halide deactivation with amine functional groups.[16] However, reactivity was limited for arenes and oxygen nucleophiles. Since they are less nucleophilic than amines, they are less prone to reducing the electrophile in a side reaction.[16]

Scheme 2. Halofunctionalization of Unactivated Alkenes in the Presence of HFIP. [16]

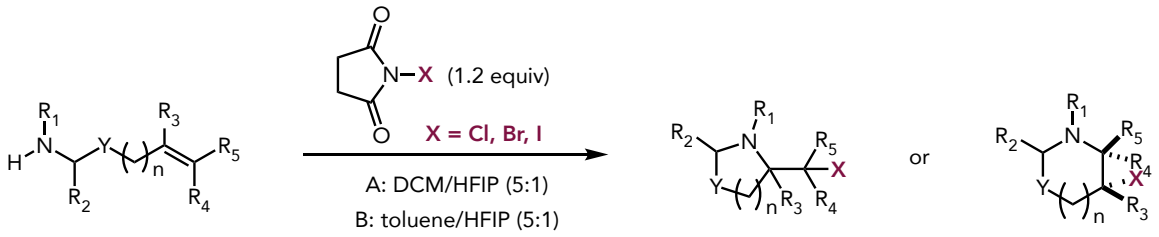

All these methods prove to be viable in developing halogenated products, but they still seem to be significant drawbacks in synthetic chemistry. Hazardous waste, toxic reagents, and selective and reactive introduction of halogens using conventional approaches often remain current challenges in the field.[17] Each of these examples can also impact the tolerance of functional groups and limit the substrate scope.[17] However, there has been a rise in alternative methods, such as biocatalysis, for generating halogenated analogs of biologically active metabolites. There has been a great interest in investigating the biosynthesis of halogenated natural products and the biotechnological potential of halogenating enzymes as they offer excellent catalyst-controlled selectivity without the need for protecting groups or hazardous materials.[17]

Biocatalysis is one of the most promising technologies for sustainable synthesis in pharmaceutical, biotechnological, and industrial use. Many of the catalytic mechanisms of enzymatic catalysis similar to those of classical chemical catalysis. However, biocatalysis offers several benefits in the field of synthetic organic chemistry. Firstly, the reactions typically occur in a milder temperature range, using less energy. Under industrial conditions when performing with a large scale of chemicals, energy consumption and reliability of catalysts are crucial factors that influence the final price of

the product. Biocatalytic reactions can be carried out in an aqueous environment, reducing solvents' use and the disposing/recycling cost. In contrast, over the years, biocatalytic reactions in biphasic systems and pure organic solvents allow a higher substrate loading, prevent the hydrolysis of water-sensitive compounds, and shift the thermodynamic equilibrium of many reactions.[18] Additionally, a majority of these reactions aren't air-sensitive, while many homogenous and heterogeneous catalysts will be oxidized and deactivated by air or at room temperature.[18] Another advantage of biocatalysts is the application of unique enzymatic features, allowing chemo-, regio-, and enantioselective chemical reactions. This tool offers the possibility to redesign synthetic pathways for the preparation of essential molecules and to obtain them at higher yields. These features are critical in the pharmaceutical and fragrance industries, where getting biologically active chiral compounds is vital. For example, Merck and Codexis collaborated and developed a chemoenzymatic route for the synthesis of the type 2 diabetes drug sitagliptin (Januvia).[19] The mechanism relied on an enzyme-catalyzed transamination with a highly engineered R-selection transaminase (Scheme 3).[19] Additionally, Huffman *et al.* reports the development of a nine-enzyme biocatalytic cascade for the synthesis of human HIV treatment, islatravir.[20, 21] Both studies are prime examples of directed evolution being used in organic synthesis and highlight biocatalysis as a revolutionary industrial chemical process.

Scheme 3. Comparison of Biocatalytic and Chemocatalytic Routes of Sitagliptin Phosphate.[19]

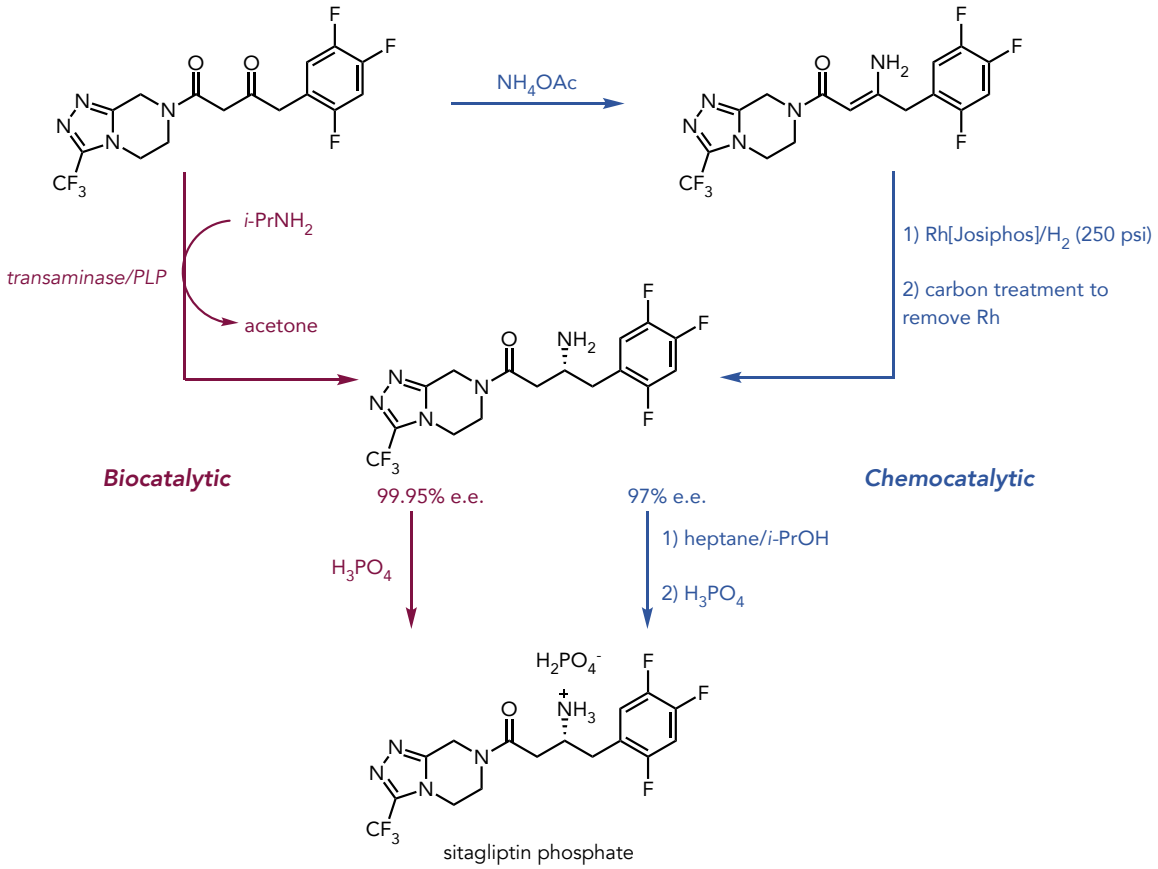

Halogenases are a class of enzymes that cleave and activate halogens for introduction into an organic compound.[22] The first halogenating enzymes to be discovered were the heme-dependent haloperoxidases in the 1960s; vanadate-dependent haloperoxidases followed in the 1980s.[22] Since then, there has been substantial progress with new families of halogenases being discovered and biochemically and structurally characterized. Halogenation is divided into three mechanistic classes according to the chemical nature of the active halogenating agent. These classes include nucleophilic substitution, radical rebound, and electrophilic halide species.[22] However, a further

subdivision within the broader categories is based on the exact catalytic species and cofactor, which enables halogen oxidation.

Nucleophilic Halogenation (X^-)

Halide anions are generally not considered viable nucleophiles, especially in aqueous solutions. However, some halogenases use (partially) desolvated X^- anions in substitution reactions at carbon centers as nucleophiles. [22] The enzymatic construction of C-F bonds proceeds through a different route of formation than the C-Cl, C-Br, and C-I bonds.[23] Once fluoride is in solution, it is surrounded by water. This allows for access to the naked fluoride ion for nucleophilic attack.[24] This drawback could limit biodistribution and cause a harmful environment to produce organisms from fluorinated metabolites. Fluoroacetate is generated by a fluorinase, adenosyl fluoride synthase (FIA), which O'Hagan and co-workers discovered.[25] FIA is currently one of the only enzymes that accepts fluorine and chlorine halide substrates.[24] However, another enzymatic class, SalL, can mediate chlorination in salinosporamide biosynthesis.[24, 26] This class of enzymes were also found to be closely related to FIA but does not accept fluorine halide substrates.[26] Literature supports that SaIL can only accept chlorine, bromine, and iodine halide substrates.[24, 26] Both, FIA and SalL are members of a rare group of nucleophilic halogenases that have facilitated enzymatic halogenation of adenosines, which utilize *S*-adenosyl-L-methionine (SAM) as a substrate.[24]

The mechanistic understanding utilizes nucleophilic halogenases to catalyze the attack of halide anions as nucleophiles to the electrophile, SAM. The energy cost of desolvation of the halide ion in the active site appears to be compensated by pairing with

a side chain hydroxyl of a serine residue in that active site.[24] The reaction is formulated with the halide ion attacking the polarized carbon-sulfur bond at the sulfonium cation site of SAM, taking advantage of that good leaving group to drive C-X bond formation in a simple nucleophilic substitution (Scheme 4).[24] Conversely, the enzyme can catalyze a reverse reaction to break the C-X bond. This method of reactivity of the nucleophilic halide ion differs from the other enzymatic strategies used for biological halogenation.

Scheme 4. Halogenation of SAM by X-mediated by a Nucleophilic Halogenase. [24]

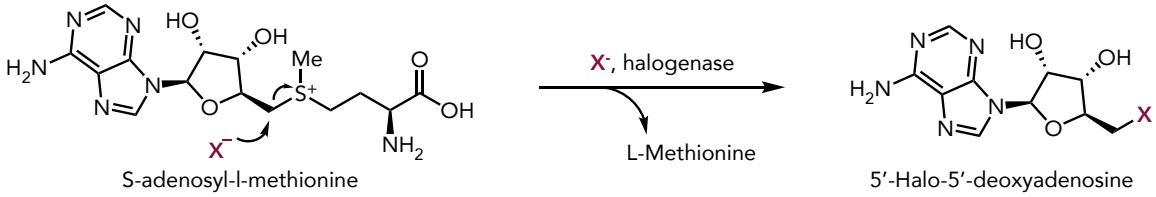

Radical Halogenation (X•)

The low chemical reactivity of substrates with aliphatic carbons suggests a different approach to catalysis may be required. The radical rebound pathway is employed to achieve energetically less favorable halogenations.[24] The general pathway (Scheme 5) proceeds through the hydrogen atom abstraction (HAA) from the substrate C-H bond by high valent metal-oxo species to give alkyl radical.[14] Next, the radical interacts with the halogen atom attached to the metal center through a halide radical rebound process, resulting in the formation of the halogenated product.[14]

Scheme 5. Generalized Mechanistic Radical Rebound Pathway of C-H Halogenation.[14]

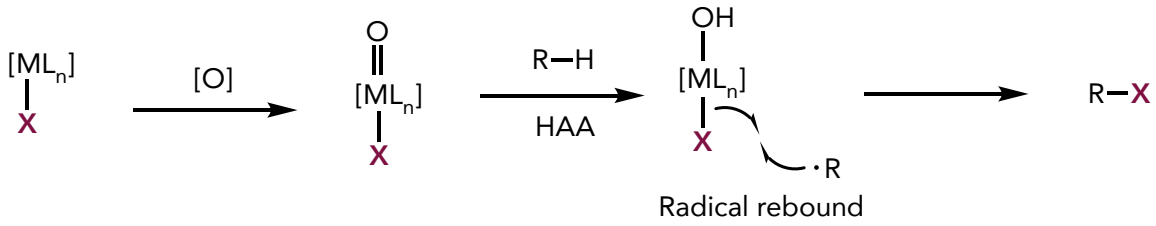

The most common halogenase family used in this mechanistic pathway are non-heme iron/ α-ketoglutarate-dependent halogenases.[22] More specifically, the enzymes classified in this family depend on the metal cofactor iron (II) complex to install a halogen at non-activated carbon centers.[14, 22, 24] Non-heme iron α-ketoglutarate-dependent halogenases have evolved from their hydroxylase counterparts. Understanding of the catalytic cycle mediated by non-heme iron α-ketoglutarate-dependent halogenases is informed by studying hydroxylases. The analogy between biological hydroxylation and halogenation in the context of flavoprotein catalysts is that when nature carries out hydroxylation of inactivated carbon sites, it turns to iron enzymes and generates high-valent oxoiron species as powerful oxidants.[22, 24] Iron in two microenvironments can serve this catalytic oxygenation purpose in biology.

A non-heme iron center, α-ketoglutarate, and oxygen are needed in the catalytic cycle mediated by non-heme iron α-ketoglutarate-dependent halogenases. The cycle begins with an octahedral Fe^{II} coordinated in a bidentate fashion by α-ketoglutarate, and a weakly bound water ligand is later replaced by molecular oxygen.[22, 24,27] Additionally, the facial triad in this class of enzymes consists of two-histidine residues and one carboxylate structural moiety, either an aspartate or glutamate residue.[27] In Scheme 6, the

water ligand is initially displaced by substrate binding, causing the subsequent reaction of **II** with molecular oxygen. In non-heme iron halogenases, **III** undergoes oxidative decarboxylation and generates the Fe^{IV}=O oxidant **IV** with a chloride (or bromide) ligand in the coordination sphere of the catalytic iron. After radical hydrogen abstraction, the halogenase contains a Fe^{III} with both an -OH and a -Cl ligand **V** as potential sources of •OH or •Cl transfer to the alkyl radical. Catalytic chlorination (or bromination) is observed as the outcome, and the metal center returns to its Fe^{II} state.

Scheme 6. Catalytic Cycle of Non-heme Iron α-ketoglutarate-dependent Halogenases.[24]

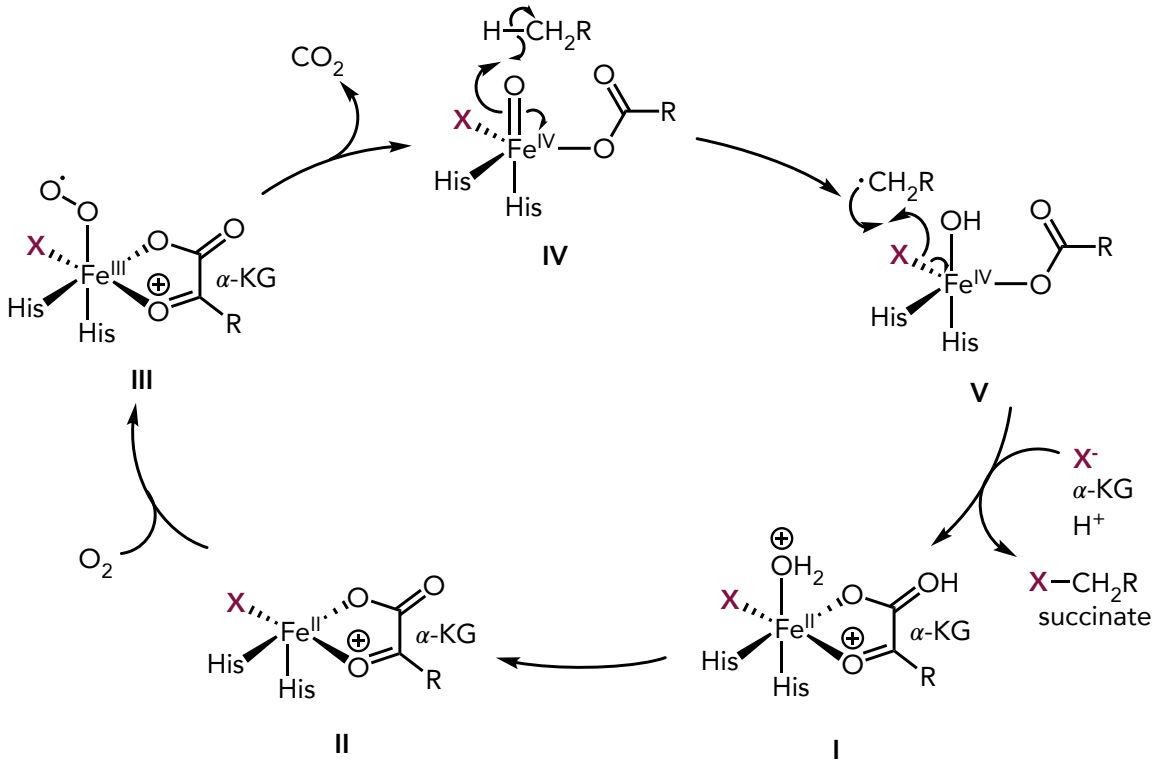

Significant conformational changes are observed within these by non-heme iron α-ketoglutarate-dependent proteins. These changes occur directly after oxygen binding

and the subsequent decarboxylation event, orientating the substrate for the observed regioselective halogenation. However, non-heme iron α-ketoglutarate-dependent halogenases appeared to be challenging to handle *in vitro* due to the oxygen sensitivity of the iron core.[28] Recent advances suggest an iron reconstruction step can be performed to activate enzymes purified aerobically.[29] The first member of the non-heme iron enzyme, WelO5 was discovered in 2014 by Liu and Hillwig.[30, 31] WelO5 had evolved through sequence analysis and mutagenesis of the C-terminus sequence in AmbO5 (Scheme 7).[32] Both enzymes can aid in the formation of chlorine substitution with complex indole natural products and with an expanded substrate scope.[32, 33] These transformations create the possibility to use such proteins more readily in biotransformations.

Scheme 7. WelO5 Chlorination.[32]

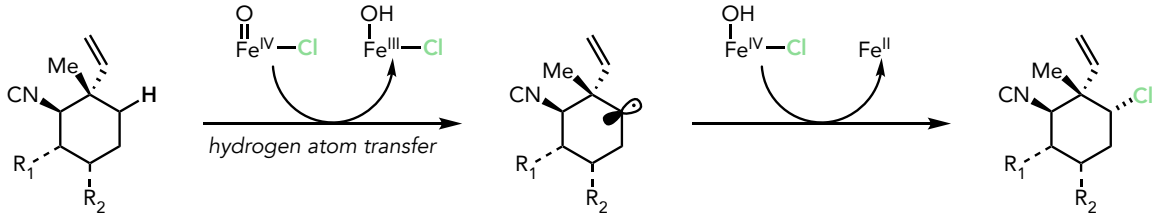

Electrophilic Halogenation (X^+)

Electrophile-type halogenases are responsible for the installation of a halogen at relatively electron-rich carbon centers, usually in alkenes or aromatic rings, also known as the electrophilic aromatic substitution reaction. The basic mechanistic understanding of this pathway (Scheme 8) involves the initial formation of a high valent metal-oxo species in the presence of an oxidant.[14, 22] Next it is followed by its interaction with a

halide source, most likely hypohalous acid (HOX), or hypohalite (OX^-), to generate an electrophilic hypohalite intermediate.[14, 22, 24] The organic substrate then reacts with this hypohalite intermediate to provide the halogenated product.[14, 22] Another note is that the known families of electrophilic halogenases use different oxidants to affect the two-electron oxidation of X^- to X^+.[22]

Scheme 8. Generalized Mechanistic Electrophilic Pathway of C-H Halogenation. [14]

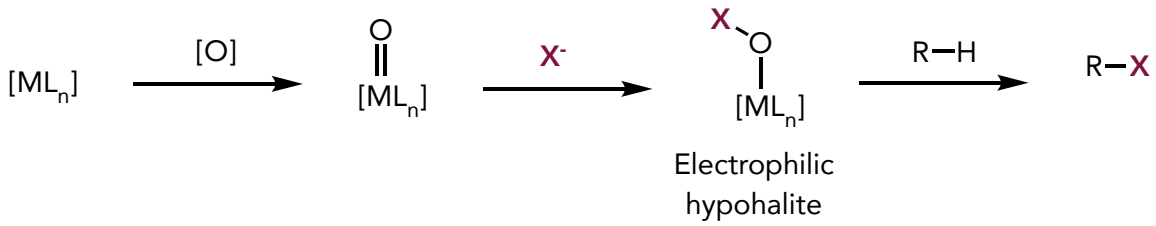

Halogenase families involved in EAS include heme-dependent and vanadium-dependent haloperoxidases and flavin-dependent halogenases.[22] The earliest studies of halogenation date back to 1959 when Hager discovered the initial characterization of a fungal chlorinating enzyme as a heme-dependent chloroperoxidase.[34] Since then, several discoveries of other classes of halogenating enzymes have utilized three different redox cofactors: vanadium, the dihydro form of FAD (FADH2), non-heme iron centers, as obligate cofactors in different types of halogenating systems. The heme- and vanadium-dependent enzymes use hydrogen peroxide as a substrate, classifying them as haloperoxidases.[22] However, the flavin-dependent and non-heme iron-dependent enzymes require dioxygen as a reducible co-substrate and will not react with hydrogen peroxide.[22, 24] From the two categories, oxygen is employed in two oxidation states as O_2

or H_2O_2. There are close parallels in the logic of halogen ions activated for C-X bond formation by the haloperoxidases and halogenases. Heme- and vanadium-dependent haloperoxidases generate bound hypohalite (-OH) intermediates.[24] These can react as X^+ equivalents with electron-rich substrates.[24] In the active site of the FADH2-dependent halogenase and the non-heme-dependent halogenases, the dihydrogen is reduced to generate the reactive X^+ species for halogenation. More importantly, the unifying theme for each category is that the oxidation of the ground state X^- ions provides the halogenating species for C-X bond formation.

Haloperoxidases are defined as enzymes that utilize hydrogen peroxide and a halogen to generate HOX. These enzymes are named by the most negative halogen for which they can affect oxidation. Haloperoxidases are the least selective out of all the enzymes enabling halogenation; this is because they catalyze the generation of free hypohalous acid, most of which is released by the enzyme. Heme-dependent haloperoxidases are a subset of haloperoxidases that contain a heme-iron cofactor coordinated to an axial cysteine ligand within the enzyme (Scheme 9a).[24] Hydrogen peroxide binds to the enzyme in its resting state (**I**) to form a heme-iron (IV) intermediate (**II**). The addition of halide to the ferryl oxygen (**III**) produces a heme iron (III)-OX species (**IV**). As a result, the free hypohalous acid (HOX) is formed, which is used to react with an electrophilic substrate.

Vanadium-dependent haloperoxidases are widely found in algae, fungi, and bacteria and utilize a vanadium cofactor bound by an axial histidine ligand (Scheme 9b).[24] The resting state of vanadium-dependent haloperoxidases is bound by the imidazole ring of a histidine residue (**I**). However, the protein-ligand is used to anchor the

redox cofactor in the active site. The mechanism below shows that the vanadate ion coordinates with the incoming hydrogen peroxide and gives rise to the formation of the peroxo complex (**III**). Next, the oxidation of the halite ion results in the V-OX species (**IV**). After hydrolysis, a hypohalous acid species (HOX) is formed as the electrophilic halogenating agent. Additionally, throughout the generation of the halogenating cycle, the vanadium ion does not change its oxidation state. Unlike the heme-dependent haloperoxidase catalytic cycle, the exact order of events of the vanadium-dependent catalytic cycle is not as known, but several sources have proposed the catalytic cycle.[22, 24] Additional information about vanadium-dependent haloperoxidases will be elaborated on in the next section of the thesis. The main difference between the heme-iron-dependent biocatalytic cycle is that the vanadium center in the vanadium-dependent biocatalytic cycle maintains its oxidation state throughout the process.[24]

Scheme 9. HOX Generation and Utilization with (a) Heme-iron-dependent Haloperoxidases (b) Vanadium-dependent Haloperoxidases.[24]

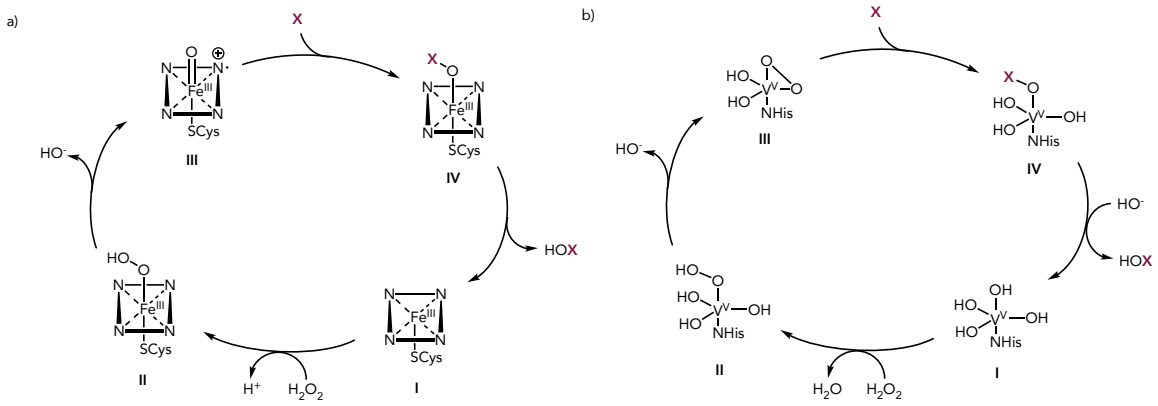

In 1995, a study by Dairi introduced flavin-dependent halogenases (FDHs) as the second series of halogenases.[35] Later work conducted by van Pée and colleagues established essential requirements for FDHs.[36] The result demonstrated regioselectivity with a halogenase requiring both flavin and molecular di-oxygen for pyrrolnitrin biosynthesis.[36] Flavin-dependent halogenases can be separated into two variants: (1) acting on free substrates and (2) requiring a substrate to tether to a carrier protein covalently.[24] Variant 1 is the most investigated and engineered FDH, which utilizes tryptophan halogenases to enable regioselective halogenation of tryptophan at the 5, 6, or 7 positions. Walsh and van Pée were the few scholars to introduce the mechanism of flavin-dependent tryptophan halogenase (Scheme 10).[37, 38] However, in comparison to one another, Walsh had proposed that a lysine residue reacts with HOX to form the haloamine intermediate, guiding the regioselectivity of halogenation.[37] In contrast, van Pée had presented a proximal glutamate residue and a lysine residue binding to HOX. Both examples promote a regioselective EAS reaction.[38]

Scheme 10. FDH-mediated Electrophilic Halogenation.[24]

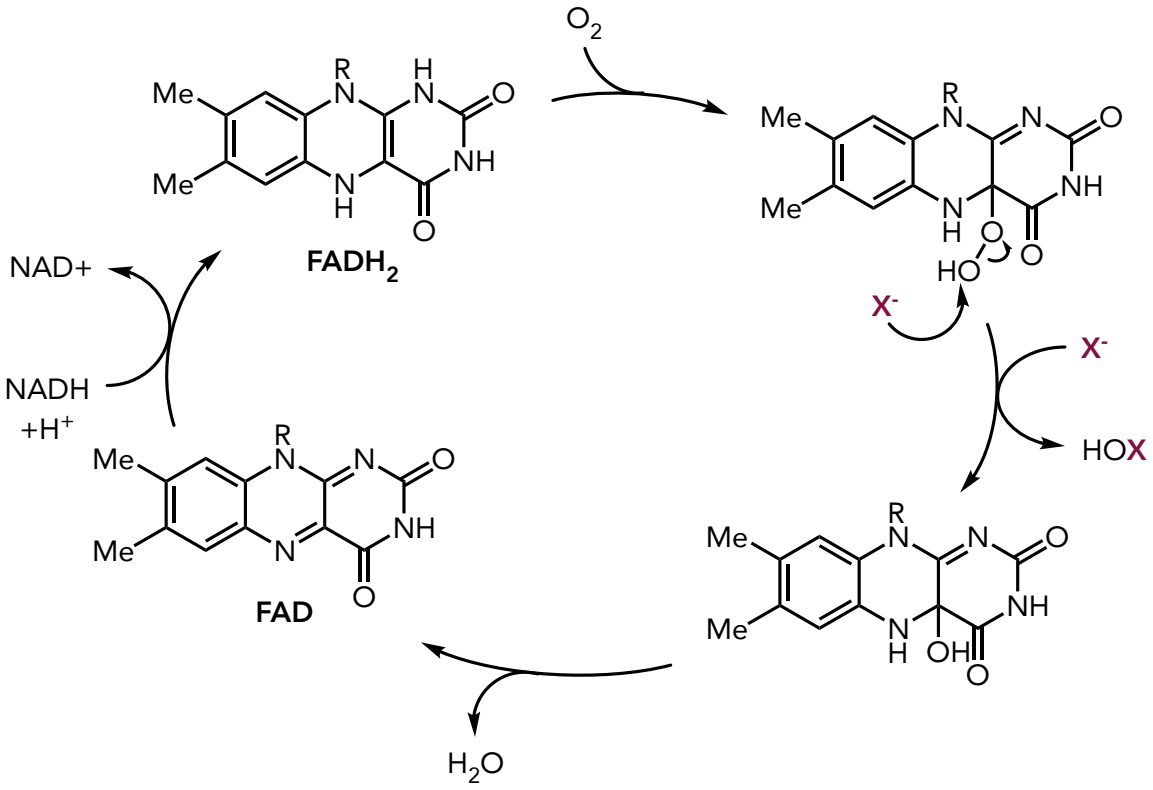

Each of these methods provides mechanistically unique approaches used by nature to introduce halogens into organic substrates. Several enzymatic families have been discovered and continue to be investigated. Enzymes can be inexpensive, biodegradable, safe catalysts that can be produced worldwide. The expense of enzymes is dependent on the materials used to make them; however, they are known to be more inexpensive than the development of an organometallic catalyst. Approaches such as protein engineering also allow one to overcome enzymes' limitations for fulfilling industrial functions. These include the level of expression, stability, catalytic activity, and the specification of enzymes that can be tuned by changing their amino acid sequence. Identifying halide binding sites in halogenase crystal structures can lead to new insight

into the enzyme mechanism and halide specification. Halide binding plays a significant role in regioselective halogenation reactions catalyzed by electrophilic, nucleophilic, and radical halogenases.[39] Interestingly, all three pathways can be used on chemically distinct and different substructures such as indole, phenol, pyrrole, and aliphatic moieties, dependent on the halogenation reaction performed. However, the major problem can be conclusively assigning the identity of an electron density peak as a halide; for example, bromine and iodine are heavier atoms than chlorine and fluorine, making them have anomalous signals and confirming their placement on the molecule.[40] After a halide site has been recognized, its application to the enzyme mechanism needs to be established. [39] The incorporation of biocatalysis has the potential to revolutionize synthetic design strategies. The application of enzymes in industry and the development of enzymatic routes has become more established throughout the years. However, the main limitation of the method is the lack of unnatural reactions that enzymes can perform. Biocatalysis will continue to grow and lead to future discoveries, applications, education, and occupations.

Halofunctionalization of Olefins

Halofunctionalizations of olefins performs a stereospecific cyclization process that result in a 1,2-*anti* arrangement of the halogen and nucleophile. From a mechanistic perspective, the process usually proceeds from forming an alkene complex with subsequent ionization to form a cyclic halonium (halirenium) ion.[15] Nucleophiles can then capture the halirenium. Olah and co-workers were the first scientists to observe halirenium ions in liquid sulfur dioxide (SO_2).[41] While utilizing the ^{1}H-NMR time scale between -60 and -80 degrees Celsius, the researchers discovered that all iodonium and bromonium ions, and several chloronium ions are cyclic, whereas the fluorine analogs demonstrated as acyclic β-fluorocarbenium ions.[41] The drawback of acyclic cations makes the process non-stereospecific in fluorofunctionalization reactions. An additional study was conducted by Brown and co-workers where they incorporated an olefin-to-olefin transfer process between adamantylidene adamantane and the isolable bromairanium and iodiranium ions derived from it.[42] At low temperatures, the 13C NMR spectra showed that the halonium ion has two perpendicular planes of symmetry.[42] Addition of the parent olefin causes line broadening of specific signals attributable to the carbon atoms above and below the planes that include the central C-C bond and are perpendicular to the above two planes.[42] The broadening suggests that small amounts of parent olefin can translocate the X^+ from the top side of a given halonium ion to its bottom.[19] Therefore, their work supports the hypothesis that the process occurs through a low-barrier associative displacement at the halogen (Scheme 11).[15]

Scheme 11. Racemization by Interalkene Halonium Transfer.[15]

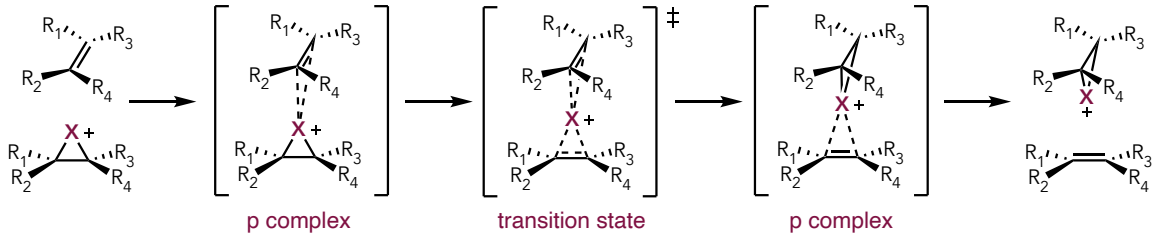

Catalytic halofunctionalization can be performed using a multitude of strategies including Brønsted acid-, Lewis acid-, Lewis base-, and phase transfer catalyst mediated processes. [15] Brønsted and Lewis acids increase the electrophilicity of halogen sources by binding and withdrawing electron density. Lewis bases are presumed to activate halogen sources by forming a polarized complex in equilibrium with a highly reactive cationic halogen species, following the general mechanism for Lewis base activation of Lewis acids. [15] However, phase transfer catalysis does not require the catalyst to activate the halogen source. Instead, the mechanism has the halogen source and starting material separated into different phases before being brought together by the catalyst. The biggest challenge in halofunctionalization reactions is engineering enantioselectivity.[15] Any successful strategy associated with bromo- or iodofunctionalization has shown an association between the chiral catalyst and the halirenium ion intermediate. Racemization of the halirenium ion leads to diastereomeric ion pairs, leading to different stabilities and reactivities. Currently, four tactics are known to maintain the halirenium ion association (Figure 4).[15]

Figure 4. Strategies for Enabling Stereoselectivity for Maintaining Catalyst/Halirenium Ion Association. [15]

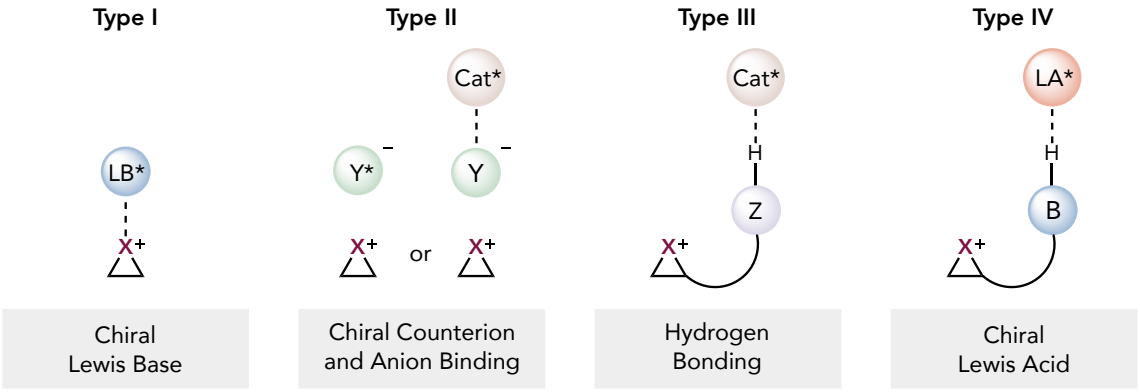

Type I demonstrates an association of the halirenium ion intermediate with a chiral Lewis base. [15] The Lewis base does not dissociate before nucleophilic capture of the halirenium ion. This tactic is suggested as most effective in combination with other control elements compared to the other catalytic enantioselective methods. [15] Wirth and peers developed one of the earliest works on enantioselective halocyclization using halogen/amine complexes.[43] The researchers utilized a new approach with ICI and a primary amine to obtain a reagent-controlled iodolactonization (Scheme 12a).[43] The rate-determining step in the reaction of bis(pyridinohalonium) triflates with alkenols are preceded by the reversible dissociation of one amine ligand to form the monoligand intermediate **II**, which possesses an accessible N-Br σ^* orbital (Scheme 12b).[43] Whereas the ligated reagent **I** is coordinatively saturated and unreactive with alkenes. A simple consideration of the lack of available orbitals suggests that this predissociation equilibrium is likely expected to all doubly ligated halogen sources.[43] This example

provided insight into the mechanism of halocyclization; however, none of the systems provided more than 65:35 e.r.[43]

Scheme 12. Type I Example of Chiral Lewis Base Catalysis Mechanism. [43]

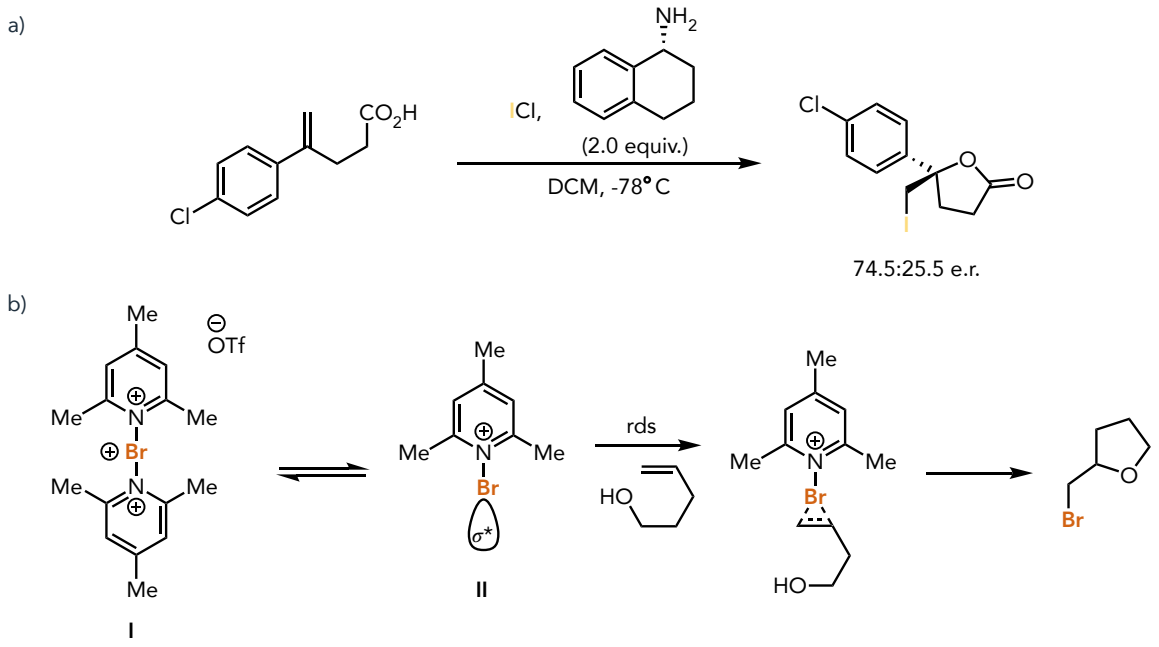

Type II, like Type I, expresses the interaction between the catalyst and the Lewis acidic haliraium ion as Coulombic. [15] The scheme shows a formation of an ion pair with a chiral anion. They use a Lewis or Brønsted acidic chiral catalyst to bind to an achiral counteranion derived from the halogen source. [15] The Coulombic interactions between the two sources can be an advantage as this guarantees the continuous association of ion pairs in nonpolar media; this tactic can also be called the chiral ion-pair strategy.[15] Henecke and co-workers utilize a new approach to enantioselective haloetherifcation with the combination of N-haloamides as a halogen source and chiral phosphate counter ions as catalysts (Scheme 13).[44] The enantioselectivities achieved in the research were moderate,

and their substrate scope is limited due to the symmetry requirements of the meso intermediate.[44] The haliranium ion is achiral (meso). The observation of enantioselectivity demonstrates that the phosphate catalyst is associated with the halirenium intermediate during nucleophilic capture as it most distinguishes enantiotropic, electrophilic sites. The authors propose that phosphoric acid catalyzes the reactions by acting as an anionic Lewis base, potentially involving a phosphate hypoiodite intermediate. [44]

Scheme 13. Type 2 Chiral Ion Pairing Catalysis by Haloetherification.[44]

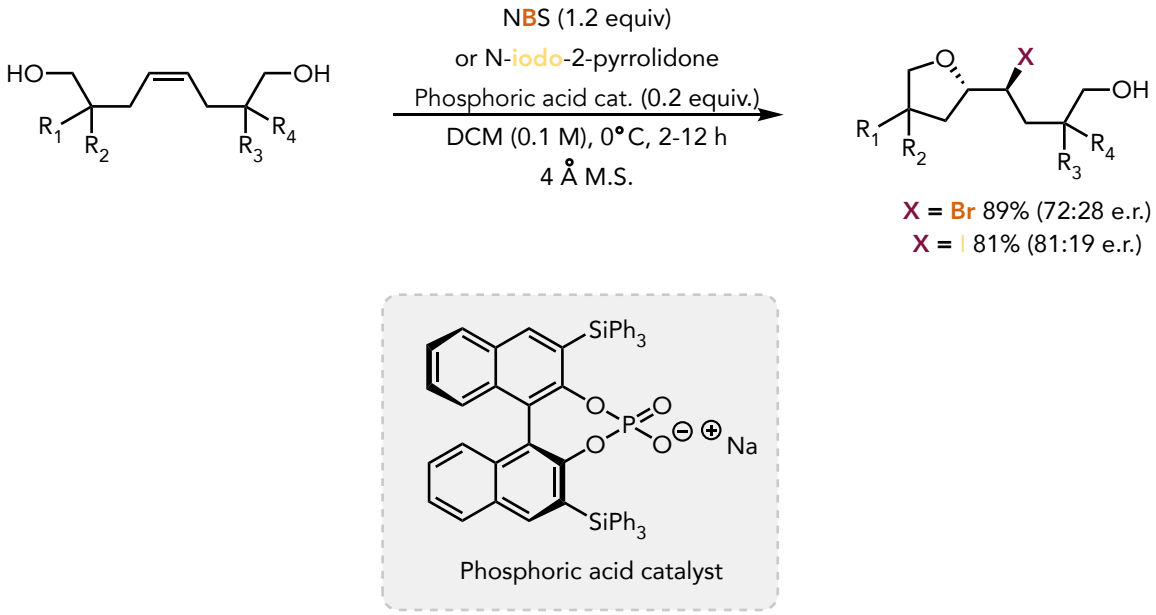

In comparison, Type 3 and 4 strategies differ vastly from Type 1 and 2. The two tactics utilize a secondary site on the substrate as the locus of association of the chiral catalysts instead of the haliraium ion. [15] Type III is accomplished by the assimilation between hydrogen-bond donors (HBD) such as alcohols, carboxylic acids, and

sulfonamides into the substrate, and hydrogen-bond acceptors (HBA) like phosphoryl groups and tertiary or heteroaromatic amines into the catalyst. [15] Shi and co-workers utilize a chiral phosphoric acid as the sole catalyst in their system (Scheme 14).[45] The authors rationalized their model's method as a Type III tactic by observing selectivity. The substrate acted as an HBD, and NBS served as an HBA by accepting hydrogen from the catalyst. [45] Additionally, the results demonstrated moderate to good enantioselectivities of up to 91 percent in the bromocycloetherification from a series of unconjugated alkenols, providing extensive and exclusively the product of *exo*-cyclization (bromofurans).[45]

Scheme 14. Type 3 Hydrogen Bonding Catalysis by Bromocyclization of Olefins.[45]

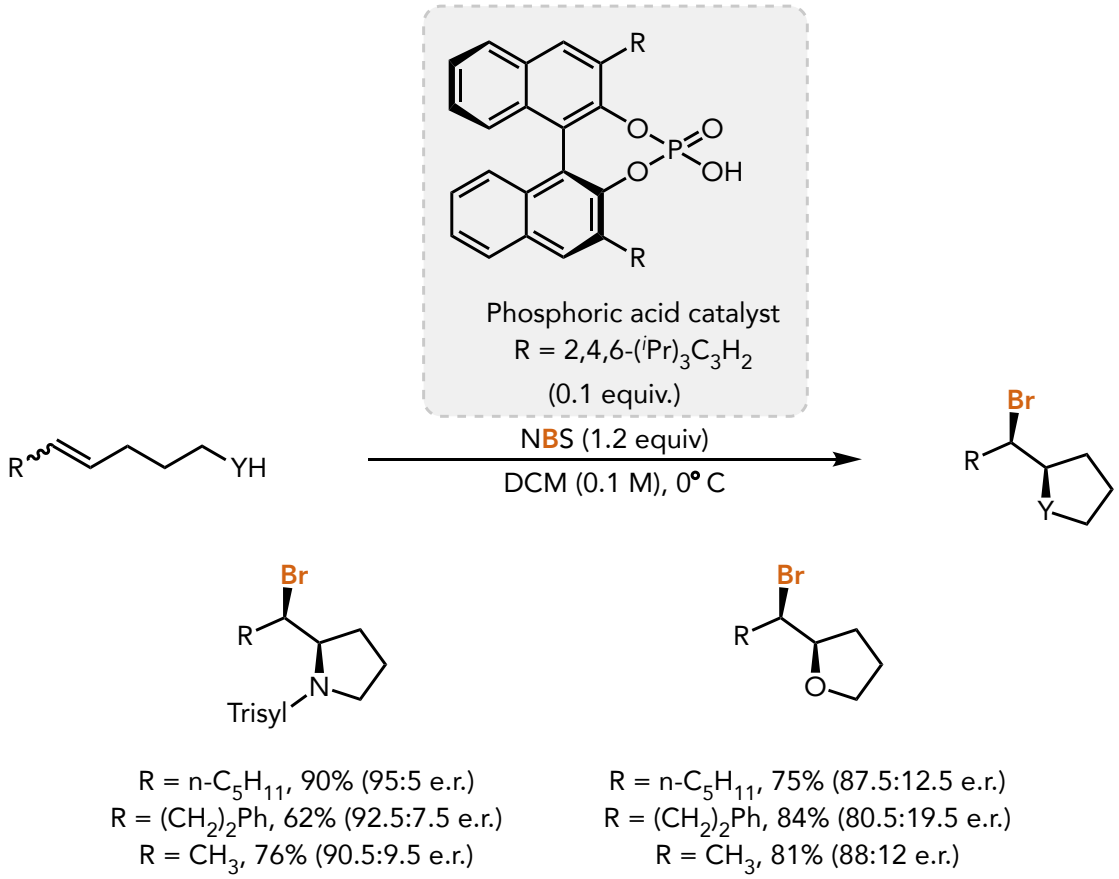

Lastly, Type 4 uses the interaction between a substrate with a Lewis basic site and a chiral Lewis acid to provide an environment to activate the capture of the halirenium ion.[15] Interestingly, the Lewis acid in this scheme can activate the nucleophile or the electrophile. Literature suggests titanium-based Lewis acids are best used to activate stabilized nucleophiles to transform enantioselective cyclization. Taguchi and co-workers started this example in 1995 by using a titanium/taddol complex with unsaturated malonate **I** to complete an iodocarbocyclization (Scheme 15a).[46] The electrophile, iodonium ion aids in the efforts for the reaction to proceed with high enantioselectivity.[46] The fused butyrolactone is achieved after the displacement of iodide from one of the diastrophic ester groups.[46] However, a disadvantage to this approach is having the carboxyl group act as the nucleophile. This causes the enantioselectivity of the product to be significantly reduced, even when it is present in a stoichiometric amount of a chiral complex.[47] Conversely, the literature supports that the activation of the halogen source is mainly performed with salen complexes of cobalt (II) and chromium (III).[15, 47] For example, a report in 2003 demonstrated a very high yield and good enantioselectivity when using a Co^{II}/salen complex to catalyze the iodoetherification of (Z)-5-substituted-5-pentenols (Scheme 15b).[48] Interestingly, the same starting material used in the reaction was also cyclized with a $Cr^{III}Cl$/salen complex and resulted in equal or greater enantioselectivity at one-quarter of the loading.[49] Additional research from Gao and co-workers confirmed high yields and moderated to good enantioselectivity while utilizing the Co^{II}/salen complex to the iodolactonization of 4-substituted-5-pentenoic acids.[50]

Scheme 15. Enantioselective Type 4 Interactions (a) LA Catalyzed and (b) Directed Halocyclization.[46, 48]

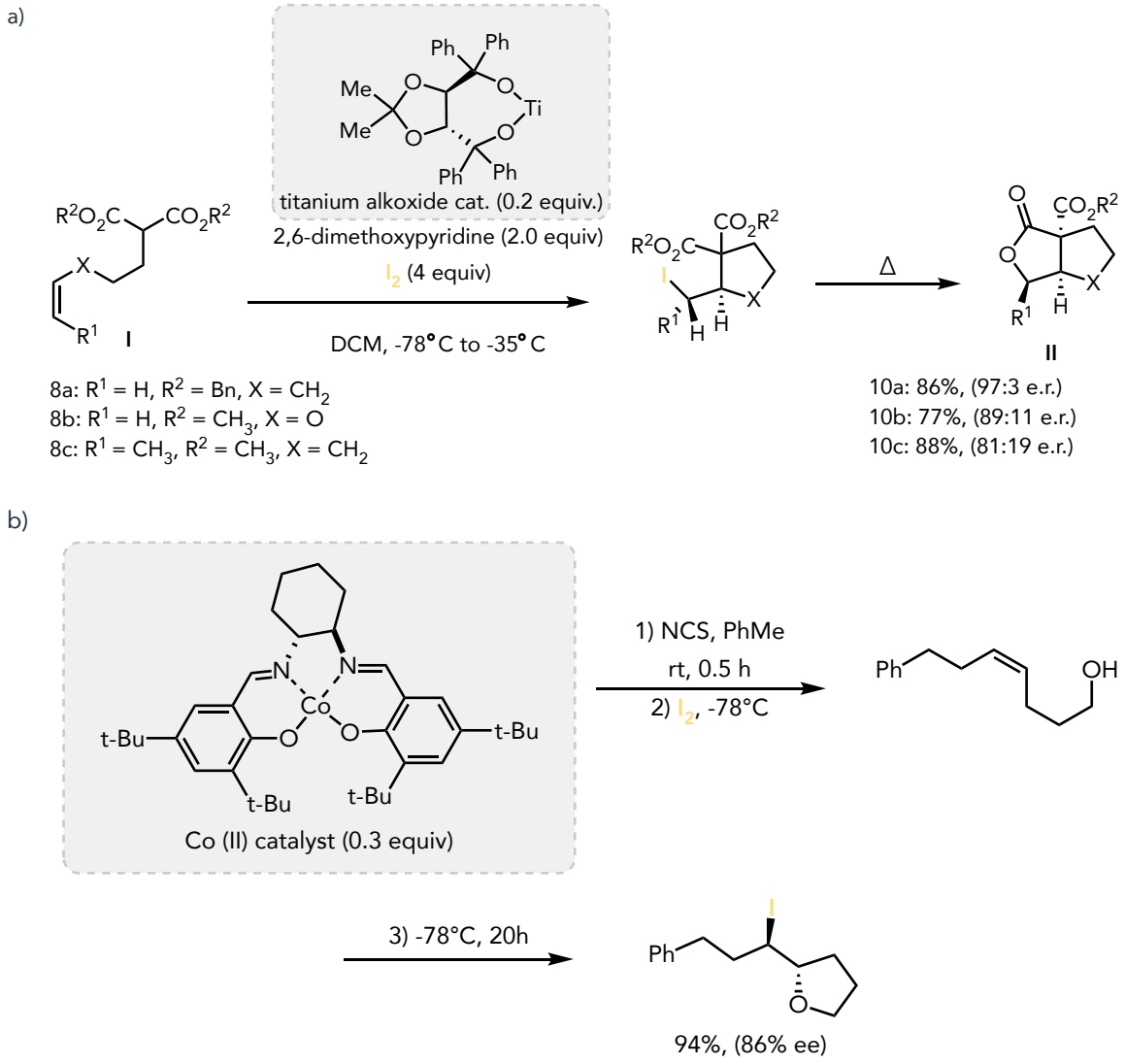

Substantial progress has been made on the four tactics, including enantioselective forms of certain halofunctionalization. In some of the above examples, lactam systems seem to be the most prevalent in halofunctionalization. Unfortunately, achieving this halofunctionalization with high enantioselective yields is not transparent. Additionally, studies should also consider specific enantioselective variants for dichlorination and

dibromination reactions. For halofunctionalization to be effective and safe, new methods must combine catalytic and stereocontrolling strategies. In addition, novel mechanisms must be discovered and developed. Furthermore, the configuration of specific ions, including bromiranium and iodiranium, challenges these new methods.[15] On the other hand, chloriranium ions allow for effective control of stereochemistry but also pose significant risks due to their hyperactivity.[15] Fluorofunctionalization reactions are less researched, but it has been shown that their products are of great importance. [15] New studies and research will continue to aid in discovering more effective halofunctionalization reactions. There has been a rise in success in combining biocatalysis of halogenase enzymes and synthetic organic methods.

Vanadium Haloperoxidases

As discussed previously, vanadium haloperoxidases and heme haloperoxidases are both similar as they undergo an electrophilic halofunctionalization. However, vanadium haloperoxidases are inherently different from the heme-dependent haloperoxidases, as they require another transitional metal and halides to break hydrogen peroxide. For example, in the catalytic cycle of Scheme 12b, it was observed that the oxidation state of the center metal does not change, whereas, in the heme haloperoxidase cycle, the heme cofactor is oxidized from the degradation of hydrogen peroxide.[51, 52] Additionally, literature shows that those high concentrations of hydrogen peroxide could hinder the catalyzation of haloperoxidases.[53] Another critical difference between the two reaction types is that some vanadium haloperoxidases can be applied to several applications. These applications include the degradation of lignocellulose, halocyclization, halogenation of organic substrates in a regiospecific manner, and antifouling.[52]

Vanadium is the second most abundant of all the transition metal elements and is commonly found in the ocean.[54, 55, 56, 57] Vanadium is also commonly found in the form of a vanadate oxyanion at a pH of 7.[55, 58, 59] Additional studies have confirmed that the cofactor can also be discovered in terrestrial fungi and marine bacteria. Between all the halogens used in vanadium haloperoxidases, bromide is present in high concentrations and is most prominent in marine environments. Vilter and co-workers discovered the first vanadium haloperoxidase in seaweed in 1983.[60] They had discovered a competitive kinetic transformation utilizing vanadium bromoperoxidase from the brown algae, *Ascophyllum nodosum.*[60] This enzyme is responsible for the biosynthesis of halogenated

natural products. However, additional products could be formed, as the hypobromous acid can diffuse from the active site and halogenate unbound substrates. [60] Other oxidized vanadium bromoperoxidase intermediates are bromine, tribromide, and enzyme-bound "bromonium ion equivalent."[61] Surprisingly, there are only few examples of natural systems known that utilize vanadium ion. Nitrogenases and haloperoxidases are the two types of enzymes that utilize a vanadium ion, but the focus of this section will be discussing the haloperoxidases.[55, 62, 63, 64, 65, 66] Since this discovery, several reports support vanadium haloperoxidases being found in seaweed, fungi, and lichen organisms.[56, 67, 68]

Only three vanadium haloperoxidases have had their crystal structure resolved: from the fungus *C. inaequalis*, VClPO, from the brown alga, *A. nodosum*, VBrPO, and from the red alga *C. officinalis*, VBrPO.[69, 70, 71, 72, 73, 74] Between the three vanadium haloperoxidase structures they have less than 30 percent sequence similarity. They all share a common active site structure consisting of two side-by-side four α-helix bundles with the vanadium active site located towards the bottom of the structure (Figure 5). [68, 69, 72, 73] Additionally, the negative charge of the oxygen of vanadate group is stabilized by hydrogen bonds to three positively charged residue around the center which are Arg_{360}, Arg_{490}, and Lys_{353}. Arg_{490} forms a salt bridge with residue of Asp_{292}. All vanadium haloperoxidase structures are bound is a trigonal bypryramidal form linked to the protein, a histidine ligand, whereas the other four ligands are oxygen based.[75] Mutation studies were reported by Hemrika and co-workers and demonstrated that replacing histidine with alanine prevented the cofactor from binding, therefore, solidifying its role as an "anchor".[4]

Figure 5. Crystal Structure of the Vanadium Chloroperoxidase from *C. inaequalis*, with a Close-up View of its Active Site.[58, 59, 62, 63, 76]

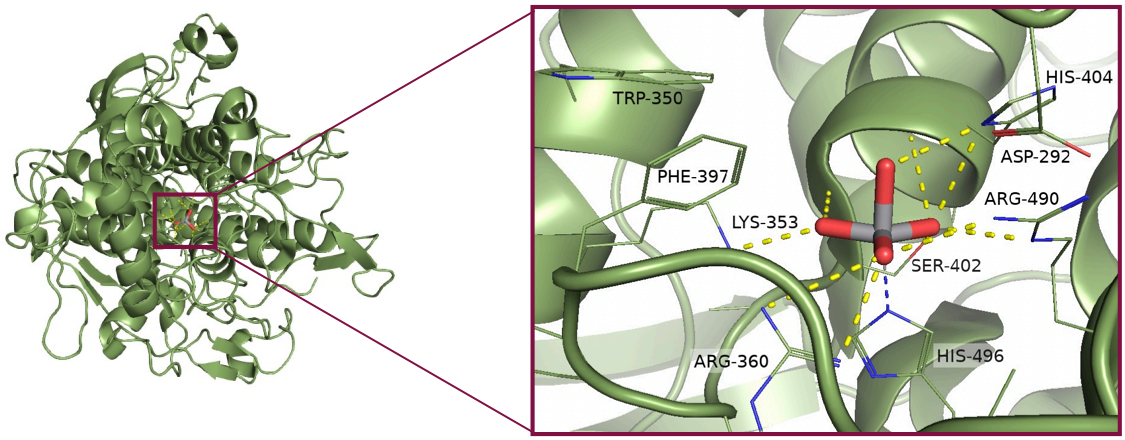

Vanadium has a tetrahedral anion vanadate intermediate that is structurally and chemically similar to the phosphate anion. Analysis of the sequences and active site of amino acids of vanadium haloperoxidases show high structural conversion and an overlap with several classes of acid phosphatases. The structure similarity between both reported having the volume of circumscribing spheres of 125 A and 102 A. [74, 77] Vanadate could be one of the alternative elements for substitution of phosphate enzymes. [74, 75] Interestingly, vanadium doesn't suffer from oxidative inactivation since it does not change its redox state through the catalytic cycle.[63,78, 79] Making this enzyme highly stable in extreme environments.[80] The pharmaceutical industry is highly supportive of utilizing vanadium haloperoxidases as sources of halogenating enzymes due to their resistant in high concentration of hydrogen peroxide substrate, hypohalous acid and in various organic solvents.[77] These haloperoxidases also have a tolerance with high temperature and can oxidize organic sulphides in the absence of halides.[81, 82, 83]

Although the mechanism for vanadium haloperoxidases is debatable in literature, sources agree that the oxidation state of vanadium remains the same throughout the catalytic cycle.[58] Scheme 16 demonstrates the simplified proposed mechanism from Moore *et al.* and a series of chemists in the field of biocatalysis.[52, 64, 84, 85] Coordination of hydrogen peroxide to the vanadium center is the first step in catalysis. The histidine residue attached to the metal center (**I**) activates the axial water molecule to deprotonate, allowing peroxide to bind. Research supports that the crystal structure of the peroxo-vanadium center demonstrates that the peroxide is coordinated in the equatorial plane and distorts the vanadium site to a tetragonal bipyramidal geometry.[71] After peroxide has bonded to the site (**II**), histidine is no longer hydrogen-bonded to any oxygen atoms of the cofactor, therefore, making lysine in the active site in direct contact with one of the oxygen atoms of the bound peroxide. This further activates the peroxide through charge separation. Next, a halide ion is introduced into the cycle and binds to the enzyme through a nucleophilic attack on the partially positive oxygen atom (**III**). This binding breaks the peroxide bond and creates the nucleophilic XO^- species, which leaves the coordination sphere as hypohalous acid after protonation from a water molecule. If an appropriate nucleophile is present, the generated hypohalous acid intermediate will react with the organic substrate, giving rise to a halogenated product, **IV** seen in the scheme below. If there is no substrate present, the oxidized halogen intermediate will react with another equivalent of hydrogen peroxide to generate dioxygen in the singlet state and the halide.

Scheme 16. Proposed Catalytic Cycle of Vanadium-dependent Haloperoxidases. [52, 64]

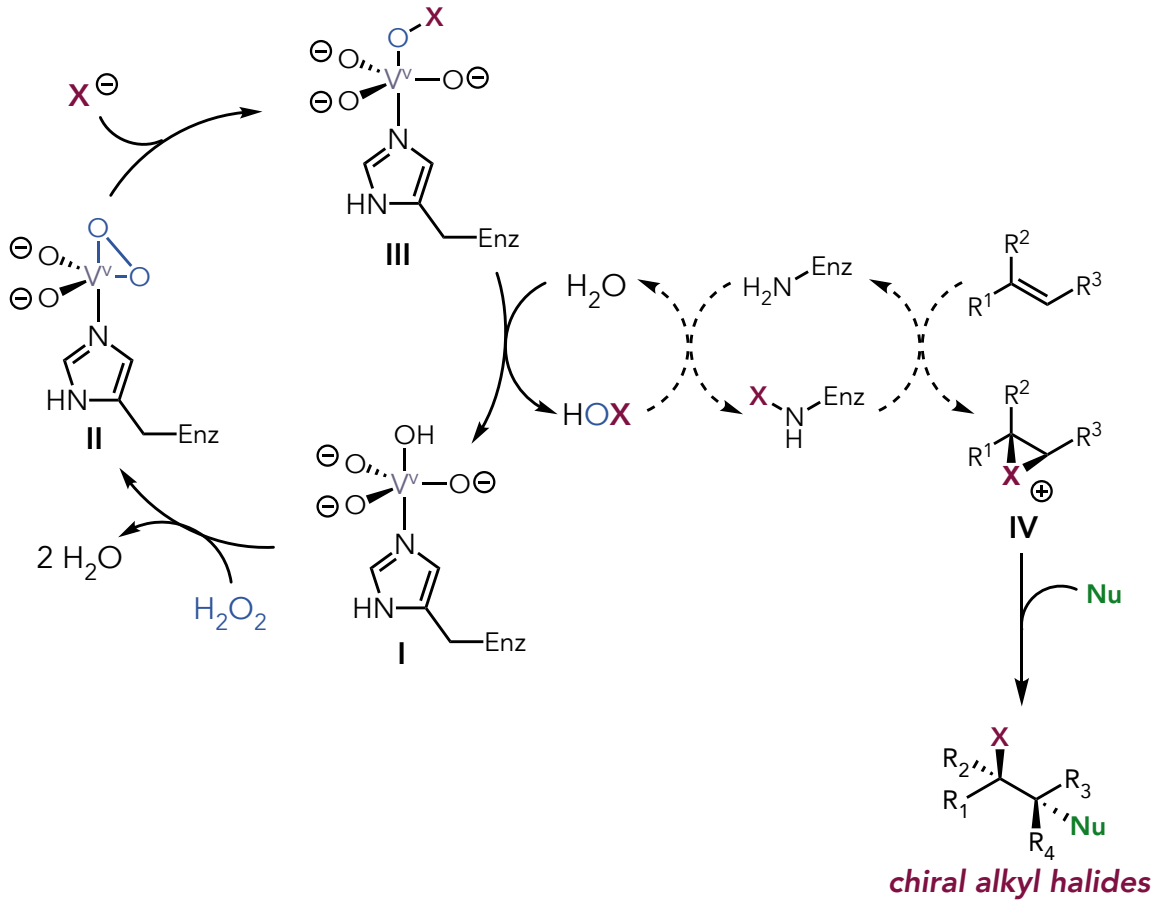

A majority of the characterized vanadium haloperoxidases are eukaryotic in origin and have been isolated as vanadium bromoperoxidase or chloroperoxidase.[72, 86] Vanadium haloperoxidases are typically named for the most electronegative halides they can oxidize. For example, a vanadium haloperoxidase could oxidize chloride, bromide, or iodide, making them vanadium chloroperoxidase, bromoperoxidase, or iodoperoxidase.[69, 78, 87] In marine red algae (species from *Corallina officinalis, Plocamium cartilagineum, Laurencia pacifica),* vanadium bromoperoxidase was isolated from catalyzing the bromination and cyclization of sesquiterpenes.[88, 89] Scheme 17 demonstrates that the

enzymes with nerolidol synthesized single diastereomers of β- and γ-synderol, whereas with nerol, the reaction was able to produce a mixture of diastereomers of monobromo eight-membered cyclic ether.[88] Researchers hypothesized that the formation of the eight-membered ether resulted from the initial V-BrPO catalyzed bromination reaction at the terminal olefin and was followed by an intramolecular nucleophilic attack by the alcohol.[89] Additionally, most of the other products reported are found in many bromocyclic terpene marine metabolites.[89]

Scheme 17. VBrPO Catalyzed Reaction with Nerolidol and Nerol. [76]

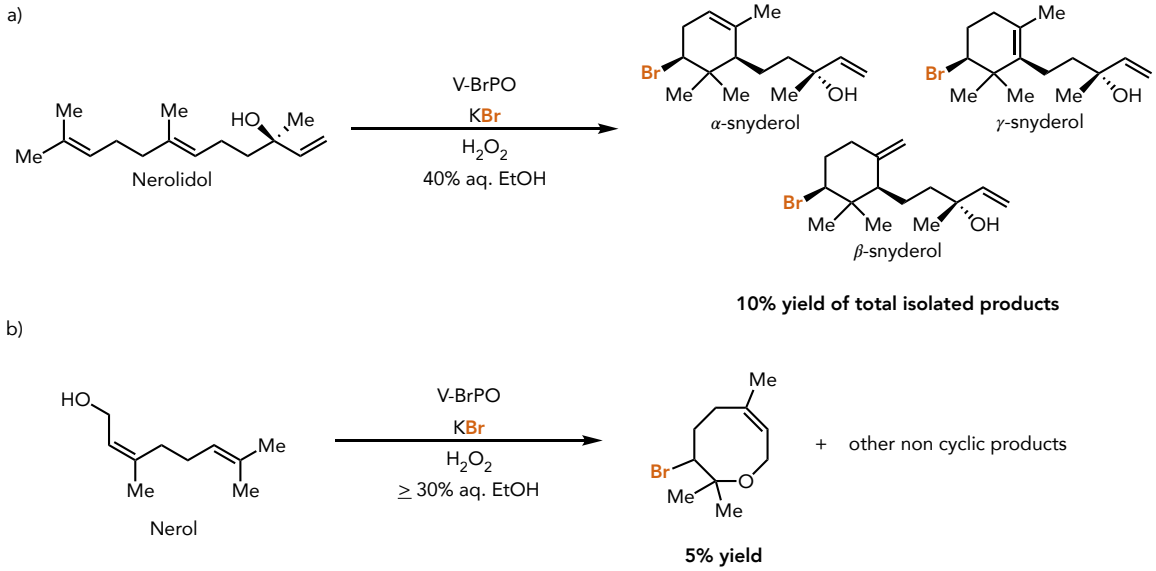

Vanadium haloperoxidases can also be found in bacteria and fungi to aid in synthesizing halogenated products. Previous examples favor vanadium bromoperoxidase in the synthesis of halogenated products, but subsequent studies show an example selecting vanadium chloroperoxidase for the same reaction. Winter and colleagues report

at least seven napyradiomycins from the expressed CNQ-525 gene cluster in *Streptomyces albus*.[90] Napyradiomycins are dihydroquinone antibiotics that show activity in fighting against MRSA.[91] Analysis of the napyradiomycin pathway shows three putative vanadium chloroperoxidase genes in *Streptomyces aculeolatus* NRRL 18422 and the marine bacterium *Streptomyces sp.* CNQ-525.[90] The vanadium chloroperoxidases obtained from these genes can cause the chloronium-induced cyclization of two terpene units in the meroterpenoid napyradiomycin biosynthetic pathway.[90] Recently, in 2018, Moore et al. reported a total enzymatic synthesis of napyradiomycins A1 and B1 (Scheme 18).[92] The biosynthesis highlights the utility of vanadium haloperoxidases enzymology in complex natural product generation.[92] Their work demonstrates NapH4 performing a chloronium-induced terpenoid cyclization to establish two stereocenters and a new carbon−carbon bond.[92] Additionally, NapH1 catalyzes chlorination and etherification reactions at two distinct stages of the pathway.[92] This study demonstrates a sustainable enantioselective approach to create complex halogenated metabolites, like napyradiomycin B1.[92] Additionally, the fungi *C. inaequalis* and *Embellisia didymospora* utilize vanadium chloroperoxidases in the terrestrial environment.[93, 94] *C. inaequalis* is a pathogen of *Zea mayes* and utilizes vanadium chloroperoxidases to produce hypohalous acids and hydroxyl radicals that damage plant cell walls.[95] The catalytic mechanism of vanadium chloroperoxidase from *C. inaequalis* has directed the catalytic mechanism of vanadium haloperoxidases. From the examples mentioned, brominium and chloronium-induced cyclization seem to be a common mechanism for producing enantiospecific halogenated compounds among vanadium haloperoxidases in marine algae, bacteria, and fungi.

Scheme 18. Biocatalytic Pathway to Napyradiomycin B1 (III).[92]

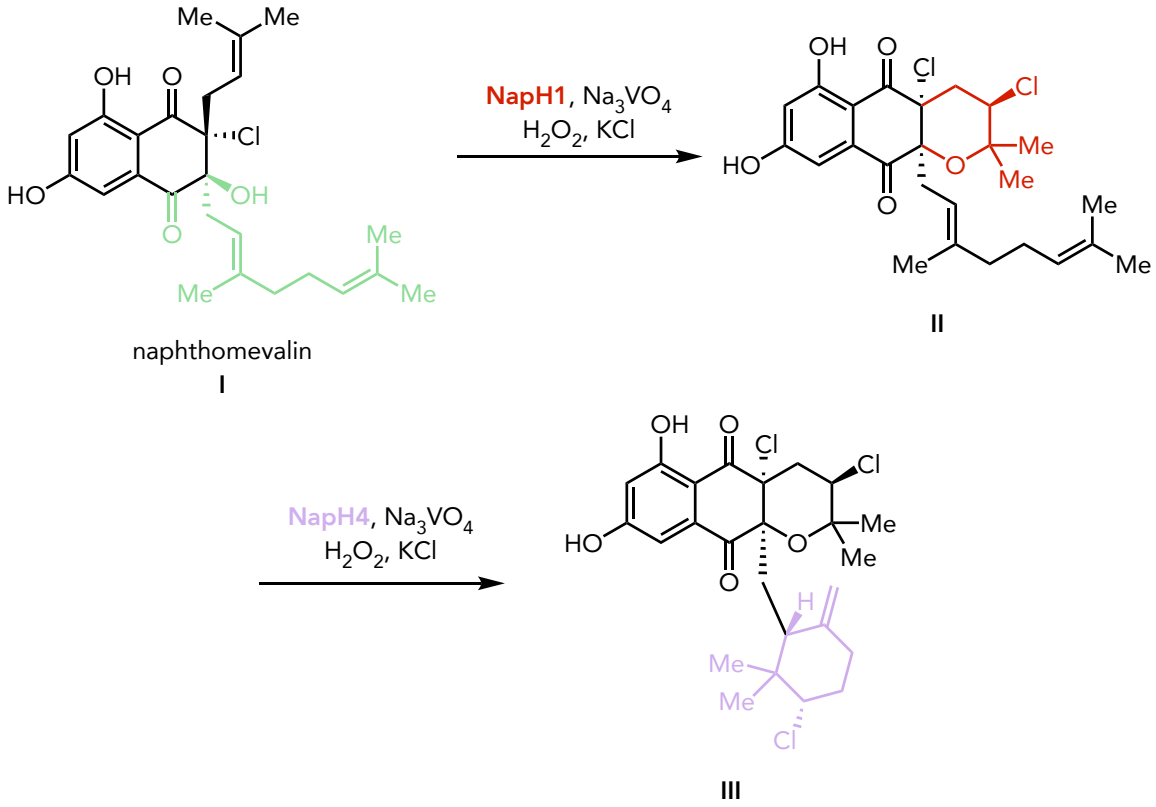

As the catalytic turnover of vanadium haloperoxidases far exceeds any synthetic catalyst for halide oxidation known to date, this family of proteins has attracted interest for bio-inspired catalyst design.[96, 97] Through observation it has been shown that many organisms are haloperoxidases involved in forming of organohalogens. Vanadium bromoperoxidases of marine algae synthesize brominated organics with antibacterial, antifouling, and cytotoxic activity.[88, 89] Additionally, studies have confirmed that vanadium chloroperoxidases and bromoperoxidases were found within two bacterial strains, *Pseudomonas* and *Streptomyces*.[90] There has been an increase in the number of bacteria screened for halogenation enzymes in the past decade, and there is still a need for more discovery. studies have confirmed that halogen-mediated reactions contribute

toward selective transformations, causing a change in the regio- and stereoselectivity.[98] Developments in modern chemistry have suggested utilizing biocatalysis, as it can aid in the changes of halogenated organic molecules that can control the formation and stereoselectivity of product formation. Most importantly, this method benefits green-chemical processes, and pharmaceutical applications have emerged based upon structural analogues of the active site of vanadium haloperoxidases has prompted further research in the function of these haloperoxidases.[55, 99, 100] For example, this thesis will discuss the cyclized products formed when utilizing several amide substrates and vanadium haloperoxidases. This research will help increase our knowledge of biocatalytic halocyclization of amides and be beneficial for creating several pharmaceutical compounds and natural products. The following steps were taken and analyzed:

1. Synthesize and purify amide substrates,
2. Screen each substrate with vanadium haloperoxidases *(Curvularia inaequalis, C Corallina officinalis, Corallina pilulifera, Acaryochloria marina)* and with a change of conditions
3. To compare yield and product formation, run each substrate using 1.2 equivalents of NBS.

Project Design

Despite the VHPOs established capabilities in halocyclization reactions, their utility in intramolecular ring formation of a C-N bond has remained unreported. This work intends to unlock the full potential of vanadium haloperoxidases to halogenate substrates such as alkenes and lactam rings. Additionally, the work will also discover new reactivity and substrate specificity. Our goal is to capitalize on the mechanistic machinery present in the VHPOs to perform a halolactamization reaction. The engineering involved in the enzymatic pocket could perform a different method of halocyclization than the previous synthetic approaches. By changing the reactions conditions, we predict a N-attack cyclization from the same substrates to afford a lactam product shown in Scheme 19.

Scheme 19. Proposed Reaction Sequence for the Vanadium Bromoperoxidase Catalyzed Reaction.

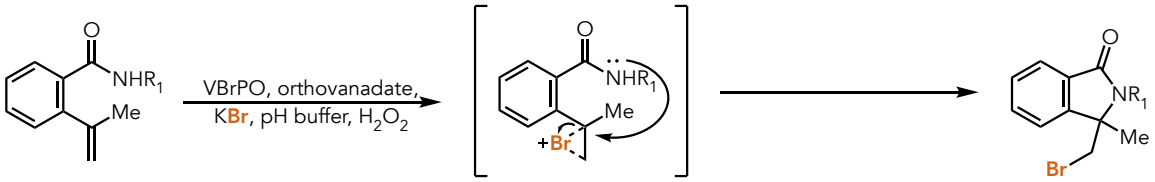

After the starting substrates have been synthesized (Figure 6) they will be screeneed individually with *C. inaequalis, C. officinalis, C. pilulifera,* or *A. marina*. Each enzyme will be pre-incubated with orthovanadate before being combined with the starting materials (**3–6**), potassium bromide, buffer solution, DI water, and hydrogen peroxide.

Figure 6. Amide Substrates (3-6).

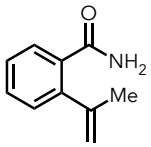

3

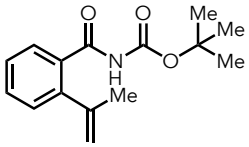

4

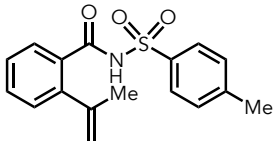

5

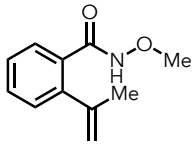

6

Results and Discussion

We began our reaction studies by synthesizing a suite of amides with an alkene appendage for cyclization (Scheme 20). Our sequence began with treatment of 2-(prop-1-en-2-yl)benzoic acid with methyltriphenylphosphonium bromide, anhydrous THF and potassium tert-butoxide to perform a Wittig olefination. Subsequent treatment with oxalyl chloride and DMF in DCM provided common precursor 2-(prop-1-en-2-yl)benzoyl chloride **(2)**. This intermediate could then be used to synthesize amides **3-6**. 2-(prop-1-en-2-yl)benzamide **(3)** was formed from **(2)** with ammonium hydroxide and TEA in DCM. The production of *tert*-butyl (2-(prop-1-en-2-yl)benzoyl)carbamate **(4)** was continued from **(3)** with DCE, oxalyl chloride, and tert-butanol. To make 2-(prop-1-en-2-yl)-*N*-tosylbenzamide **(5),** the reaction utilized **(2)** with 4-methylbenzenesulonamide, and powered KOH in DCM. Lastly, *N*-methoxy-2-(prop-1-en-2-yl)benzamide **(6)** was made from **(2)** with *o*-methylhydroxylamine hydrocholoride, TEA, EDCI, and HOBT in DCM.

Scheme 20. Synthesis of Amide Starting Materials (3–6).

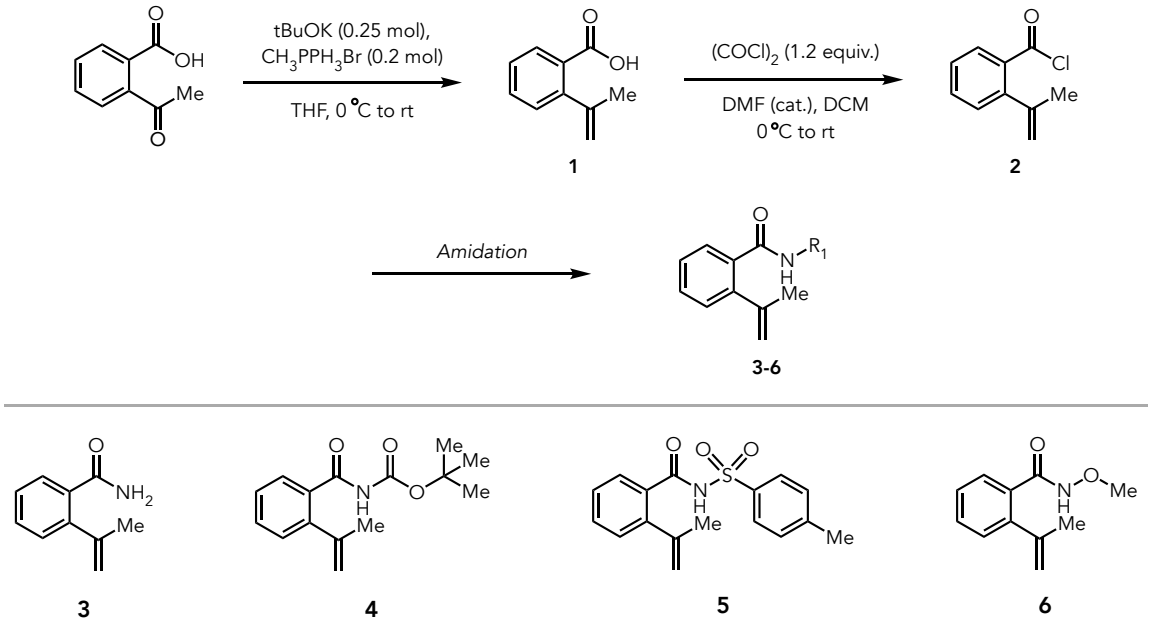

With our desired substrates in hand, we turned our attention to the development of a simple reagent-based protocol to prepare our product standards. We carried out the procedure of this room-temperature NBS-mediated bromocyclization of substrates **(3–6)** in DCM. After purification, a variety of vicinal brominated 5-membered iminolactones **(7–10)** shown in Scheme 21 were readily obtained in moderate yields within 1 h.

Product **(7)** produced from the NBS reaction obtained a 55 percent yield after purification. The compound was also characterized by mass spectrometry, *m/z* 242 and NMR. After collecting the ^{13}C NMR spectra of **(7)** the chemical shift for the carbonyl carbon is observed at δ 168.9 ppm. Additionally, to support the bromination of the lactone product, a signal for the proton alpha to the bromine was observed at δ 3.74 – 3.82 ppm (d, 1H).

The iminolactone **(8)**, produced from the NBS reaction obtained an 83 percent yield after purification. The compound was characterized by mass spectrometry, *m/z* 394, and NMR. The ^{13}C NMR spectra supports that the carbonyl carbon is observed at δ 171.2 ppm. Additionally, to support the bromination of product **(8)**, a signal for the proton alpha to the bromine is observed at δ 3.71 – 3.77 ppm (d, 1H).

Iminolactone, **(9)**, produced from the NBS reaction obtains roughly a 72 percent yield after purification. The compound was characterized by mass spectrometry, *m/z* 342, and NMR. The ^{13}C NMR spectra supports that the carbonyl carbon is observed at δ 166.1 ppm. The bromination of the product **(9)** was supported on the 1H NMR spectra at δ 3.94 – 4.60 ppm (d, 1H).

The NBS-mediated reaction obtained the iminolactone product (**10)** with a yield of 93 percent after purification. The compound was characterized by mass spectrometry, *m/z* 270, and NMR. The ^{13}C NMR spectra supports that the carbonyl carbon is observed at δ 154.5 ppm. On the ^{1}H NMR spectra the bromination of the lactone product reported a signal observed at δ 3.74 – 3.99 ppm (d, 1H) for the proton alpha to the bromine.

Scheme 21. Iminolactone Product Standards (7–10).

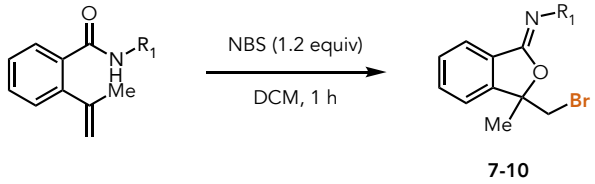

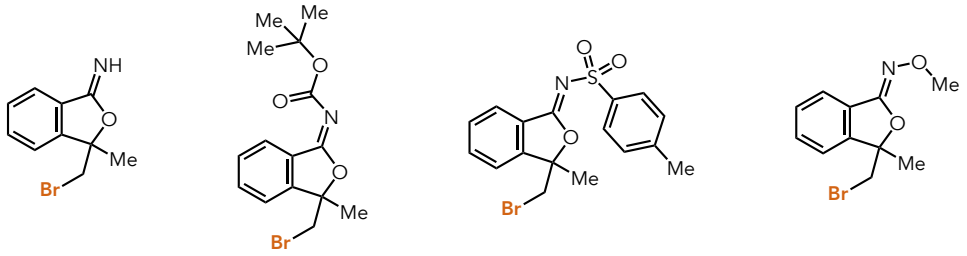

Upon completion of the above studies, we were interested in knowing if we could override the O vs. N-selectivity from the reagent-based methods utilizing vanadium haloperoxidases. The reaction of 2-(prop-1-en-2-yl)benzamide **(3)** with vanadium bromoperoxidases, *C. inaequalis, C. officinalis, C. pilulifera,* and *A. marina* in the presence of bromide ion and hydrogen peroxide produces the cyclized product **(11)** with a yield greater than 60 percent under standard conditions (Table 1). The final product was identified by mass spectrometry, *m/z* 240. When the enzyme was not pre-incubated with orthovanadate, the results contributed or harmed the conversion of the brominated product with yields ranging between 24 to 91 percent. As expected, when changing conditions independently with no enzyme, no halide, or no peroxide it resulted in no product formation. The enzymatic product was never confirmed on enantioselectivity nor was the product characterized by NMR. The biocatalytic route has a higher average of

product conversion than the NBS reaction, but the elution time and *m/z* of both products, **(7)** and **(11)**, are the same.

Additionally, the amide substrate **(3)** also reacted in the presence of a chloride ion instead of a bromide ion with the four vanadium haloperoxidases. Unfortunately, three out of four of the enzymes did not perform, whereas under standard conditions with *C. inaequalis* results presented a yield of 29 percent of the chlorinated product **(15)**. Products under standard conditions and with no orthovanadate were confirmed by mass spectrometry. Same as the previous methods written for bromoperoxidases, we changed the conditions independently to no enzyme, no halide, or no peroxide. This resulted in no product formation. Additionally, when the amount of halide or peroxide added in the reaction increased, the percent yield did not increase more than 5 percent for the desired iminolactone product. The cyclized product **(15)** was never confirmed on enantioselectivity, nor was the product characterized by NMR. Additionally, experiments utilizing NCS for the halocyclization were not conducted to compare product formation.

Table 1 shows the comparison of conversion of the enzymatic reactions with its starting substrate **(3)**. The LCMS analyses of and NMRs are represented in Physical Data.

Table 1. Enzymatic Analysis with Ci, Co, Cp and Am with (3).

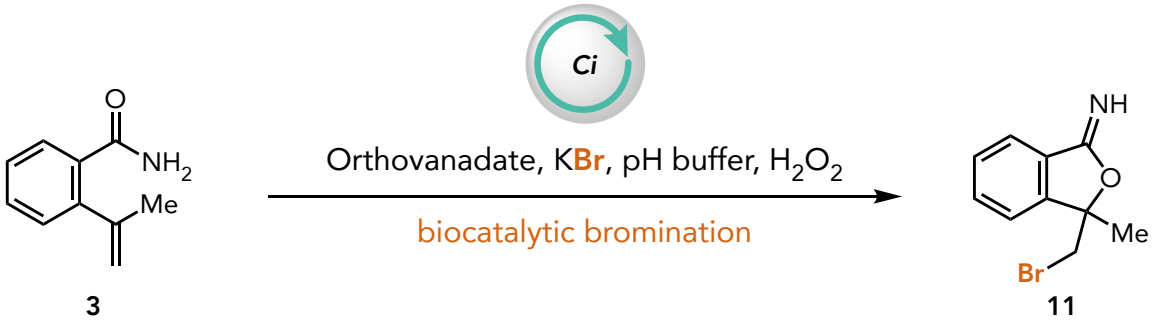

3 11

Peak	%	m/z	Ret. Time (min)
SM	>99	162	1.9
STD	85	240	3.6
No OV	91	240	3.6

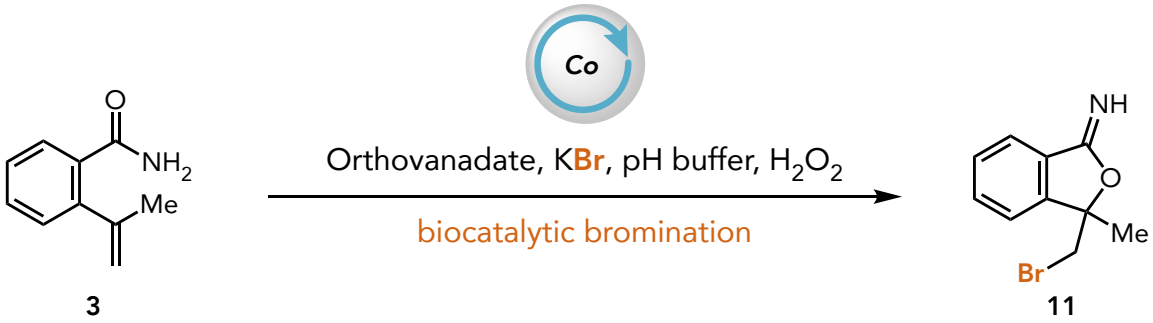

3 11

Peak	%	m/z	Ret. Time (min)
SM	>99	162	1.9
STD	65	240	3.6
No OV	85	240	3.6

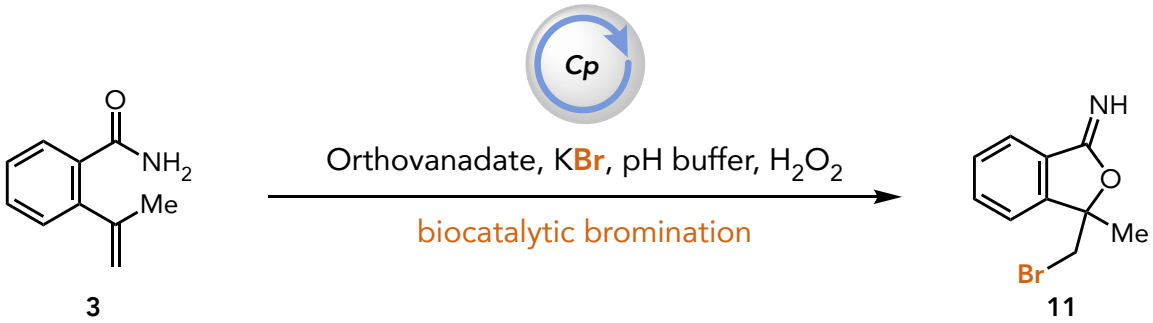

3 11

Peak	%	m/z	Ret. Time (min)
SM	>99	162	1.9
STD	79	240	3.6
No OV	60	240	3.6

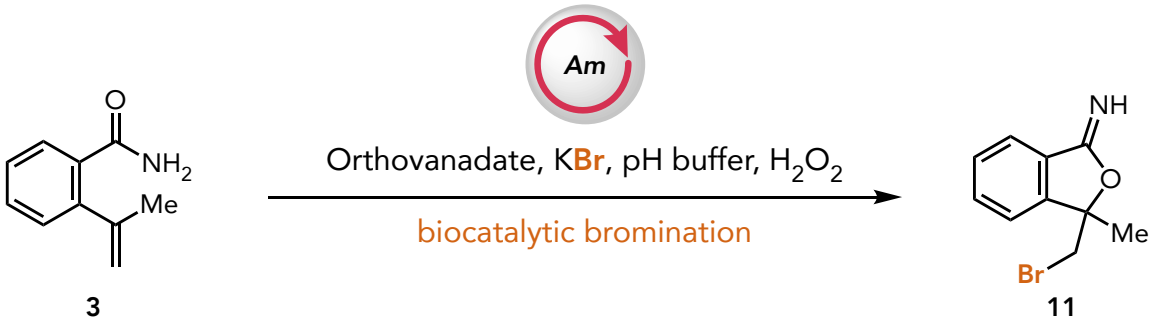

3 11

Peak	%	m/z	Ret. Time (min)
SM	>99	162	1.9
STD	59	240	2.6
No OV	24	240	3.6

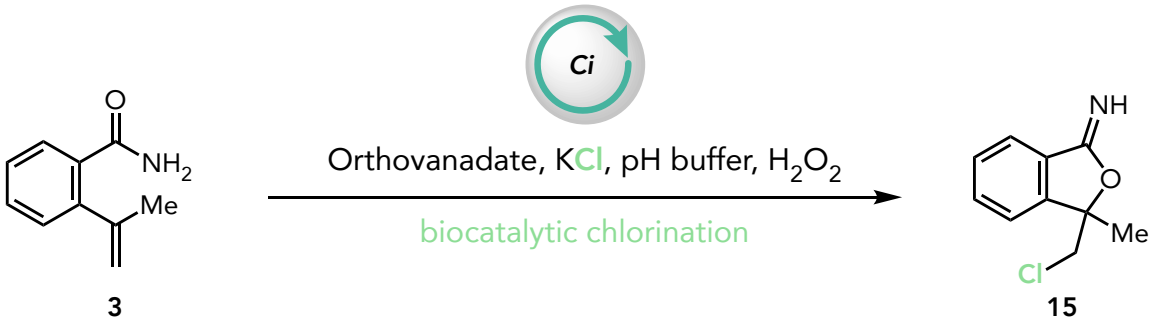

3 15

Peak	%	m/z	Ret. Time (min)
STD	29	271	3.5
No OV	28	271	3.5

When the enzymatic-mediated reaction carried out with *tert*-butyl (2-(prop-1-en-2-yl)benzoyl)carbamate **(4)**, with *C. inaequalis* and *C. officinalis,* there is a greater than 99 percent yield to produce the iminolactone **(12)** product (Table 2). The lactam product is identified by mass spectrometry, *m/z* 342, whereas the starting material **(4)** has a *m/z* 235. Additionally, when the enzyme was not pre-incubated with orthovanadate, the results did not affect the high conversion of the lactam product. In comparison, the results with *A. marina,* had both a lower yield under standard conditions and with no orthovanadate. Whereas *C. pilulifera*, had the opposite results of a higher yield with no orthovanadate and a low yield under standard conditions. When changing the conditions independently to no enzyme, no halide, or no peroxide it resulted in no product formation just as the previous method. The biocatalytic route has a higher average of product conversion than the NBS reaction when utilizing *C. inaequalis* and *C. officinalis*. However, the elution time and *m/z* of products **(8)** and **(12)** enzymatic-mediated and NBS-mediated are the same.

Additionally, the boc amide substrate **(4)** also reacted in the presence of a chloride ion with the four vanadium haloperoxidases. Unfortunately, none of the enzymes produced any significant yield. Additionally, we changed the conditions independently to no enzyme, no halide, or no peroxide. This also resulted in no product formation. When the amount of halide or peroxide added in the reaction increased, the yield remained as zero percent. Experiments utilizing NCS for the halocyclization were not conducted to compare product formation.

Table 2 shows the comparison of conversion of the enzymatic reactions with its starting substrate **(4)**. The LCMS analyses of and NMRs are represented in Physical Data.

Table 2. Enzymatic Analysis with Ci, Co, Cp and Am with (4).

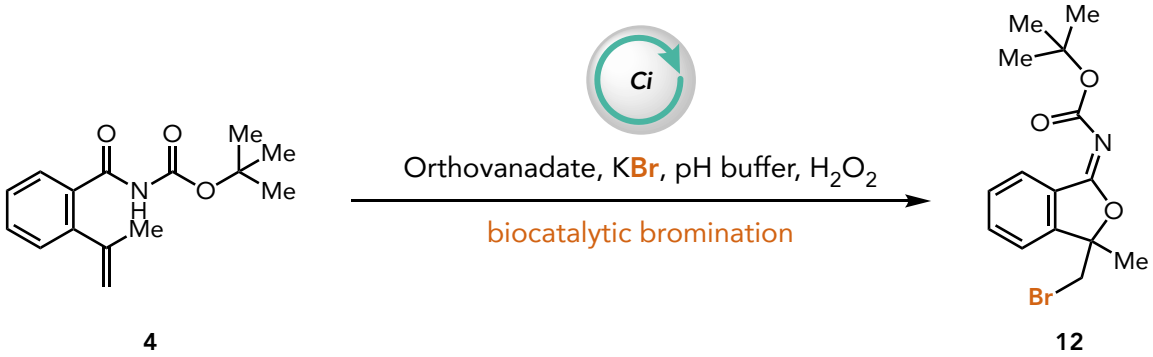

4 12

Peak	%	m/z	Ret. Time (min)
SM	>99	235	3.4
STD	>99	342	3.8
No OV	>99	342	3.8

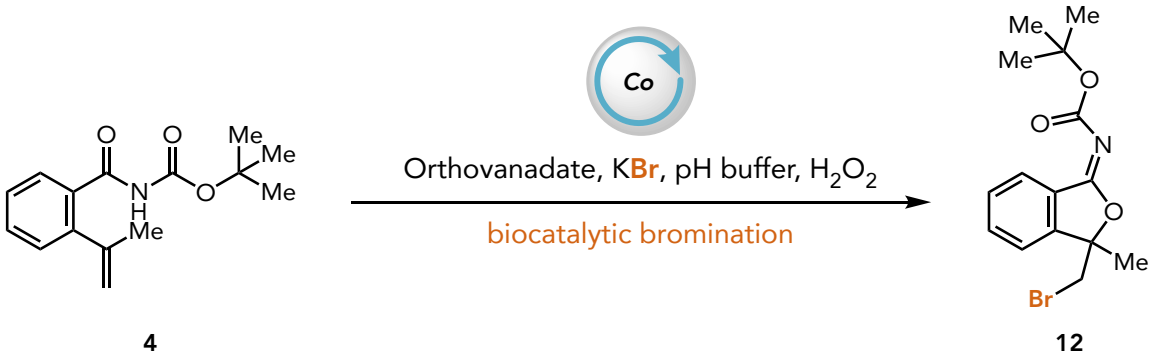

4 12

Peak	%	m/z	Ret. Time (min)
SM	>99	235	3.4
STD	>99	342	3.8
No OV	96	342	3.8

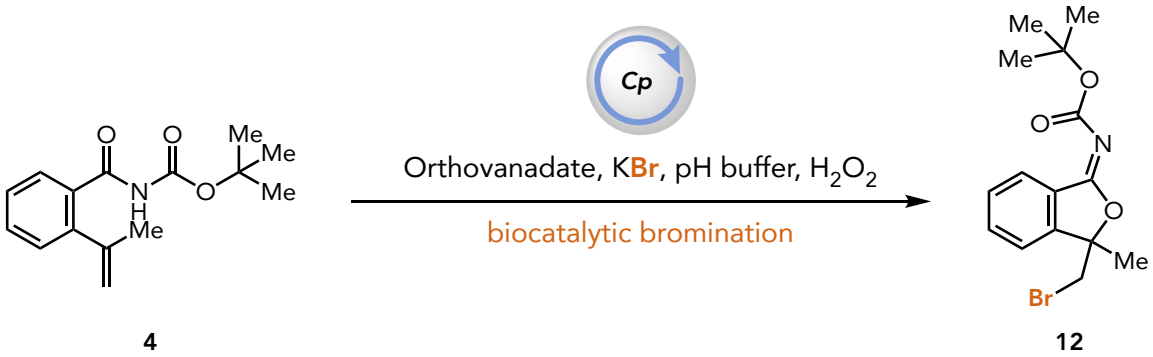

4 12

Peak	%	m/z	Ret. Time (min)
SM	>99	235	3.4
STD	43	340	3.8
No OV	96	340	3.8

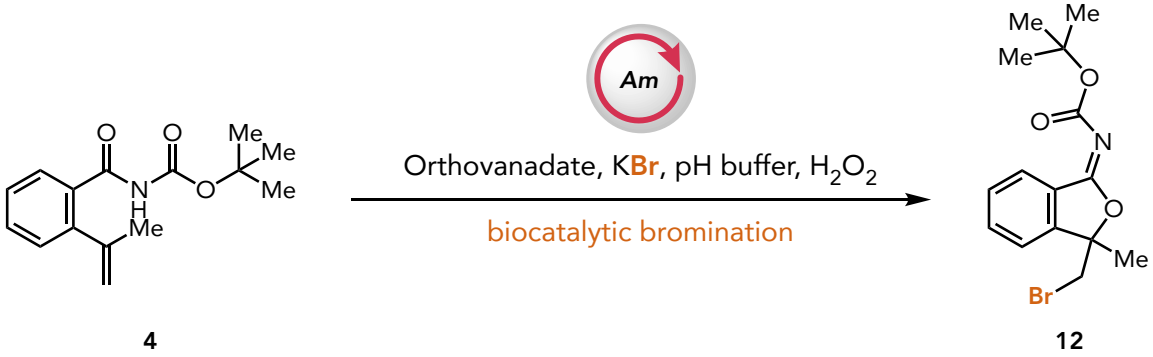

4 12

Peak	%	m/z	Ret. Time (min)
SM	>99	235	3.4
STD	88	340	3.8
No OV	27	340	3.8

The yields of the iminolactone product **(13)** are lower than the previous results with **(11)** and **(12)** (Table 3). This may be because of the large tosyl protecting group on the nitrogen. Product **(13)** is identified by mass spectrometry, *m/z* 396, whereas the starting material **(5)** has a *m/z* 316. When the enzyme was not pre-incubated with the co-factor, the results slightly contributed or harmed the conversion of product **(13)**. All enzymes shared a yield averaging 24 percent of conversion. Identical to the previous

methods mentioned above, when changing the conditions independently to no enzyme, no halide, or no peroxide it resulted in no product formation. Between the two methods of conversion, the NBS route has a higher average of product conversion than the NBS reaction. Additionally, the elution time and *m/z* of products **(9)** and **(13)** enzymatic-mediated and NBS-mediated are the same.

The amide substrate also reacted in the presence of a chloride ion instead of a bromide ion with the four vanadium haloperoxidases. Same as the amide substrate (**3**), three out of four of the enzymes did not perform, whereas under standard conditions with *C. inaequalis* results presented a yield of 28 percent of the chlorinated product **(17)**. Products under standard conditions and with no orthovanadate were confirmed by mass spectrometry. Same as the previous methods written for bromoperoxidases, we changed the conditions independently to no enzyme, no halide, or no peroxide. This resulted in no product formation. Additionally, when the amount of halide or peroxide added in the reaction increased, the percent yield did not increase more than 5 percent for the desired iminolactone product. The cyclized product **(17)** was never confirmed on enantioselectivity, nor was the product characterized by NMR. Additionally, experiments utilizing NCS for the halocyclization were not conducted to compare product formation.

Table 3 shows the comparison of conversion of the enzymatic reactions with **(5)**. The LCMS analyses of and NMRs are represented in Physical Data.

Table 3. Enzymatic Analysis with Ci, Co, Cp and Am with (5).

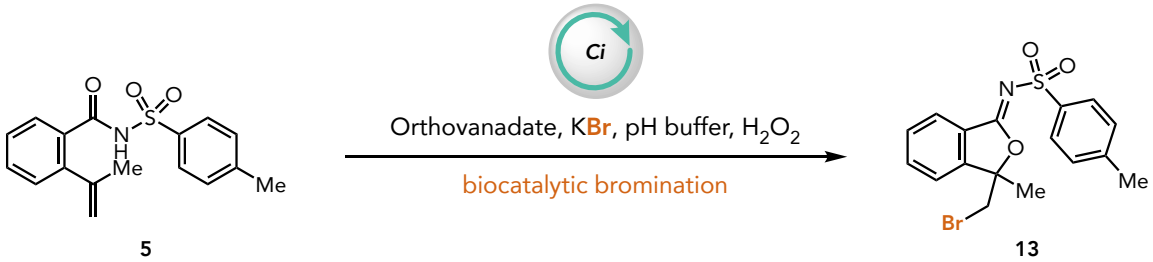

5 13

Peak	%	m/z	Ret. Time (min)
SM	>99	316	3.5
STD	24	396	3.9
No OV	27	396	3.9

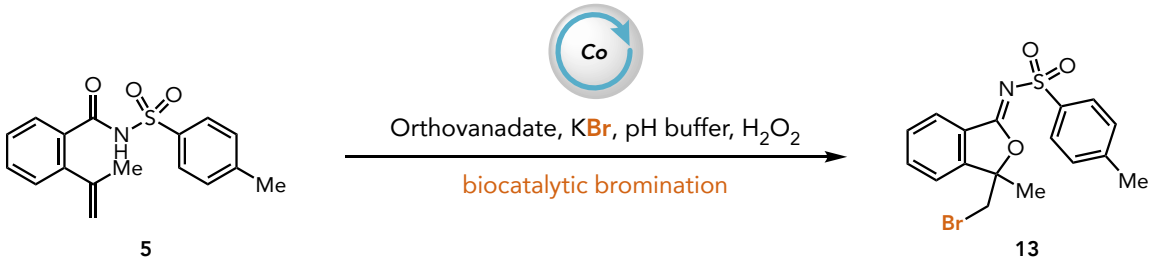

5 13

Peak	%	m/z	Ret. Time (min)
SM	>99	316	3.5
STD	23	396	3.9
No OV	29	396	3.9

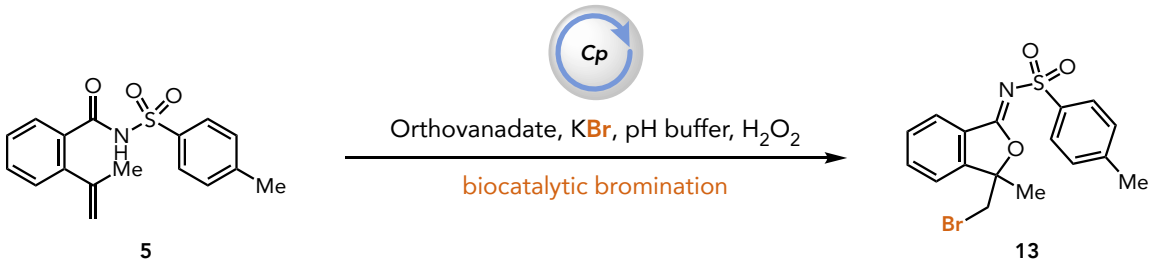

5 13

Peak	%	m/z	Ret. Time (min)
SM	>99	316	3.5
STD	22	396	3.9
No OV	20	396	3.9

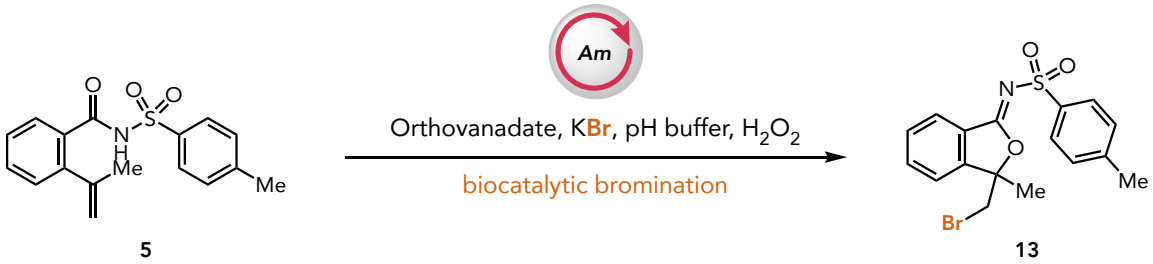

5 13

Peak	%	m/z	Ret. Time (min)
SM	>99	316	3.5
STD	24	396	3.9
No OV	19	396	3.9

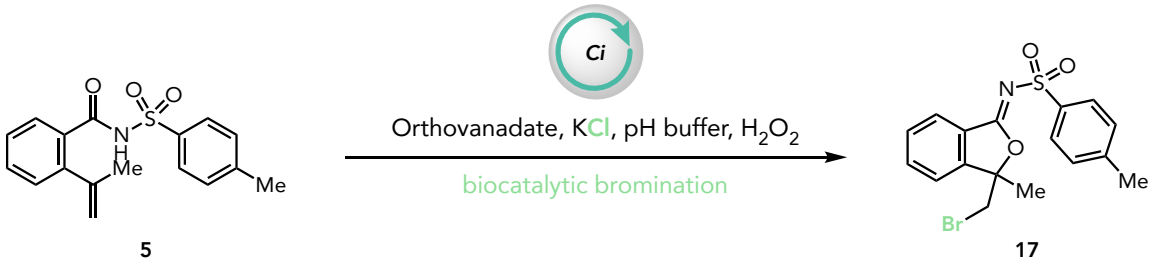

5 17

Peak	%	m/z	Ret. Time (min)
STD	28	350	3.9
No OV	26	350	3.9

The reaction of *N*-methoxy-2-(prop-1-en-2-yl)benzamide **(6)** with vanadium bromoperoxidases, *C. inaequalis, C. officinalis, C. pilulifera reported a* yield of 99 percent and greater under standard conditions and with no orthovanadate (Table 4). The iminolactone **(14)** was identified by mass spectrometry, *m/z* 270, whereas the starting material (**6**) *m/z* 192. The yields with *A. marina* significantly reduced to 44 percent under standard conditions and 28 percent with no orthovanadate. Similarly, when changing conditions independently to no enzyme, no halide, or no peroxide it resulted in no product formation. Three out of the four biocatalytic route has a higher average of

product conversion than the NBS reaction. Similarly, as the previous studies demonstrated the elution time and *m/z* of products **(10)** and **(14)** enzymatic-mediated and NBS-mediated are the same. Although the product yield in the NBS reaction is relatively close, other factors to consider is less harmful waste and faster turnover arises utilizing biocatalysis.

The amide substrate (**6**) also reacted in the presence of a chloride ion instead of a bromide ion with the four vanadium haloperoxidases. Three out of four of the enzymes did not perform, whereas under standard conditions with *A. marina* results presented a yield of 26 percent of the chlorinated product **(18)**. Products under standard conditions and with no orthovanadate were confirmed by mass spectrometry. Same as the previous methods written for bromoperoxidases, we changed the conditions independently to no enzyme, no halide, or no peroxide. This resulted in no product formation. Additionally, when the amount of halide or peroxide added in the reaction increased, the percent yield did not increase more than 5 percent for the desired iminolactone product. The cyclized product **(18)** was never confirmed on enantioselectivity, nor was the product characterized by NMR. Additionally, experiments utilizing NCS for the halocyclization were not conducted to compare product formation.

Table 4 shows the comparison of conversion of the enzymatic reactions with the starting substrate **(6)**. The LCMS analyses of and NMRs are represented in Physical Data.

Table 4. Enzymatic Analysis with Ci, Co, Cp and Am with (6).

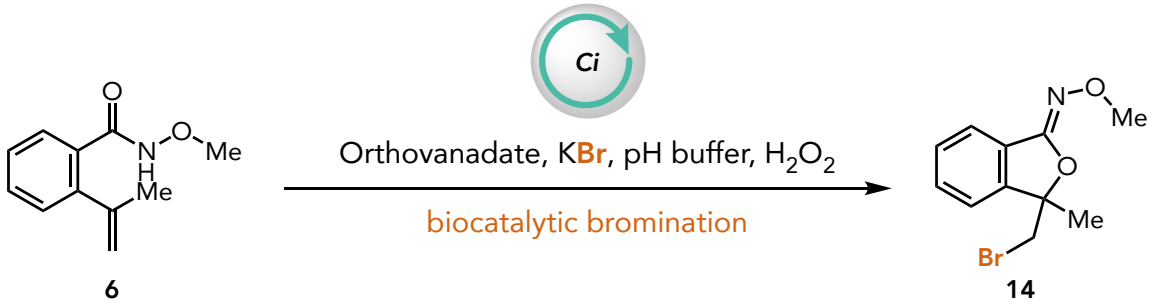

6 14

Peak	%	m/z	Ret. Time (min)
SM	>99	192	2.0
STD	>99	270	3.2
No OV	>99	270	3.2

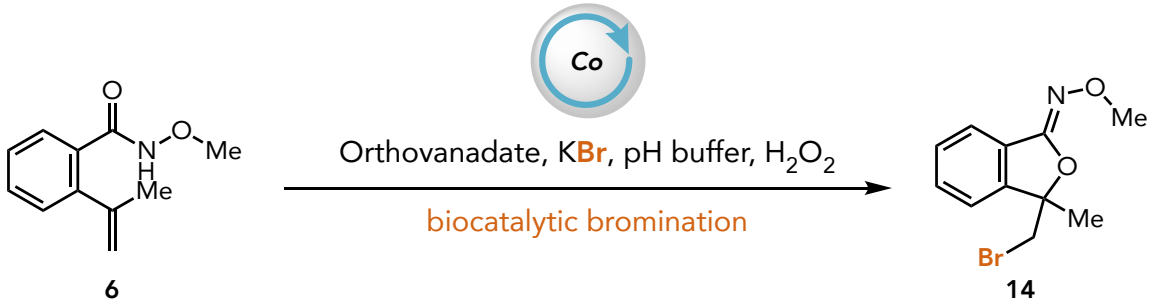

6 14

Peak	%	m/z	Ret. Time (min)
SM	>99	192	2.0
STD	>99	270	3.2
No OV	>99	270	3.2

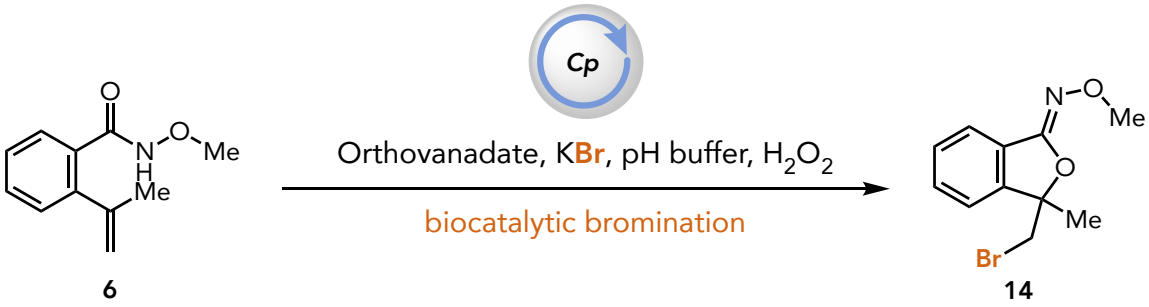

6 14

Peak	%	m/z	Ret. Time (min)
SM	>99	192	2.0
STD	>99	270	3.2
No OV	>99	270	3.2

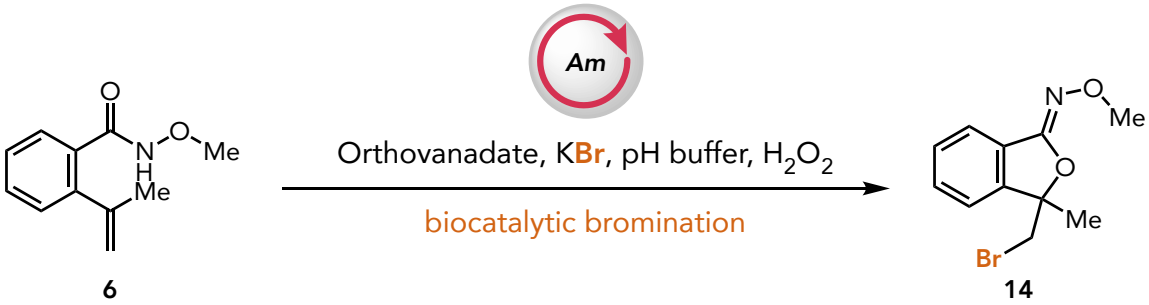

6 14

Peak	%	m/z	Ret. Time (min)
SM	>99	192	2.0
STD	44	272	3.2
No OV	28	272	3.2

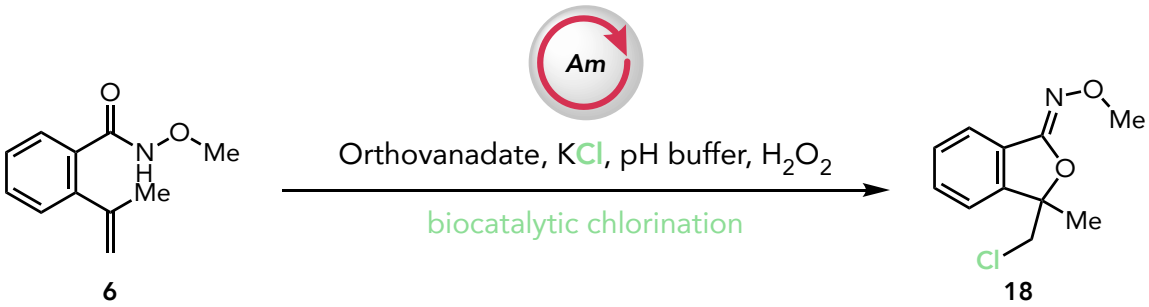

6 18

Peak	%	m/z	Ret. Time (min)
STD	26	231	2.4
No OV	18	231	2.4

To our surprise, we found that there was actually an O- vs N-alkylation (Scheme 22). Interestingly, this is also a "new to nature" reaction. Typically, carbonyl carbons are generally the furthest downfield (165– 185 ppm), due to both sp^2 hybridization and to the double bond to oxygen.[101] An imine carbon is slightly more upfield ranging between 150– 160 ppm.[102] A mechanistic study reported by Zhang *et. al* utilizes an acidic inorganic salt ($CuBr_2$ or $CuCl_2$) to perform a halocyclization of γ-unsaturated amides for the synthesis of functionalized iminolactones and lactams. Halogenation of unsaturated amides involve activation of the C=C double bond with halonium sources such as Br_2 and NBS are followed by nucleophilic O-attack or N-attack onto the halonium intermediate. The O-attack or the N-attack ring closure of unsaturated amides is typically subjected to the structure of the amides and the natures of the electrophiles.[103] Development of a standard reagent-based method for C-N bond formation is still underway. However, if we change the halide in the screen to potassium chloride, could we expect the same method of O-attack cyclization, or could we possibly undergo an N-attack cyclization?

Scheme 22. Actual Reaction Sequence for the Enzyme Catalyzed Reaction with (3).

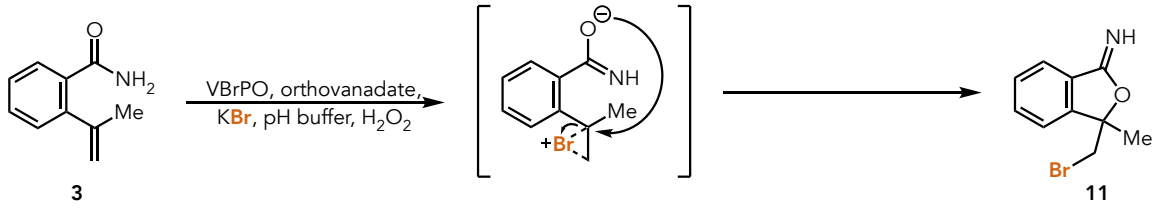

Summary and Conclusion

The synthesis of functionalized heterocyclic compounds (lactones, ethers, lactams, amides, etc.) are commonly obtained through intramolecular halo-heteroatom cyclization of inactivated olefins. Lactams are present in several biologically active natural products, pharmaceutical agents, and serve as intermediates in organic syntheses. Halogenation of unsaturated amides involves the activation of the carbon-carbon double bond with halonium sources (ex. Br_2, NBS, etc.) followed by nucleophilic attack of the oxygen or nitrogen onto the halonium intermediate. The ring closure of the amide is dependent on the amide structure or the nature of the electrophiles.[103] However, previous synthetic methods have been reported as toxic and create an abundance of waste. Additionally, some of these procedures produce several side products, causing a lower final product yield. The goal of the study was to report a vanadium haloperoxidase-catalyzed method of vicinal brominated lactams by halocyclization of amide derivatives.

In this work, a theory is reported on the catalytic cycle of the vanadium haloperoxidase enzymes. Different family enzymes were explored and analyzed to determine quicker and safer alternatives in halogenating natural products. Several conditions were measured to confirm the final enzymatic design, such as testing several different concentrations of reagents and changing time intervals. The vanadium haloperoxidases catalyzed a new-to-nature C-O bond formation method of brominative iminolactones instead of the C-N bond formation lactam product. Results showed more than 99 percent yields under standard conditions and some of the products obtained performed the same or better when orthovanadate was not added to the mixture. These results form a platform to understand better haloperoxidase activity towards different

functional groups, which will further our understanding of future development. Continuing investigations are focused on clarifying the reactivity with other amide substrates or with other functional groups (esters, carboxylic acids, etc.). Additionally, explorations should involve optimization of screening methodologies and further characterization of vanadium haloperoxidases to halogenate organic substrates.

Experimental Procedures

General Experimental Information

General: Before organic reaction setup, all glassware was flame-dried under an atmosphere of nitrogen. A rubber septum was used with an inlet and outlet needle connected to a mineral oil bubbler. Magnetic stirring was utilized for all organic reactions. However, enzymatic reactions continued using glassware that was not flame-dried before the experiment, nor was a nitrogen-closed environment needed. Additionally, magnetic stirring was not required to perform these types of reactions.

Solvents and Reagents: All solvents and reagents used in this study were obtained from commercial suppliers (Sigma-Aldrich, Oakwood Chemicals, Fisher Scientific). Dry or degassed solvents were obtained from a solvent purification system by Pure Process Technology. All enzymatic expression and purification have been done by members of the Biegasiewicz group, Logan Z. Hessefort and Jackson Tennent. Deionized water was used if water was included in the procedure.

Chromatography: Thin-layer chromatography (TLC) was performed using Unliplate GHLF 250. TLC analysis was performed using a short-wave UV lamp. Column chromatography was performed with a 250-1000 mL glass column with EMD silica gel 60 (230-400 mesh, particle size 0.040-0.063 mm), sand, and used the indicated solvent mentioned in the procedure.

Physical Data: 1H and 13C NMR spectra were recorded on a Bruker UltraShield Plus 500 spectrometer (1H 500.15 MHz, 13C 125.78 MHz). The chemical shifts are reported in

parts per million (ppm, δ) related to non-deuterated chloroform signal (1H NMR: δ = 7.26; 13C NMR: δ = 77.16). Multiplicities are denoted as follows: s (singlet), b (broad signal), d (doublet), dd (doublet of doublets), ddd (doublet of doublet of doublets), t (triplet), dt (doublet of triplets), tt (triplet of triplets), q (quartet), dq (doublet of quartets), p (pentet), m (multiplet). Additionally, LC-MS analyses were obtained using ionization techniques featuring electron impact (EI) or chemical ionization (CI) on a mass analyzer (MAT 95XL).

Synthetic Procedures for Intermediates and Substrates

Procedure for the synthesis of 2-(prop-1-en-2-yl)benzoic acid **(1)**

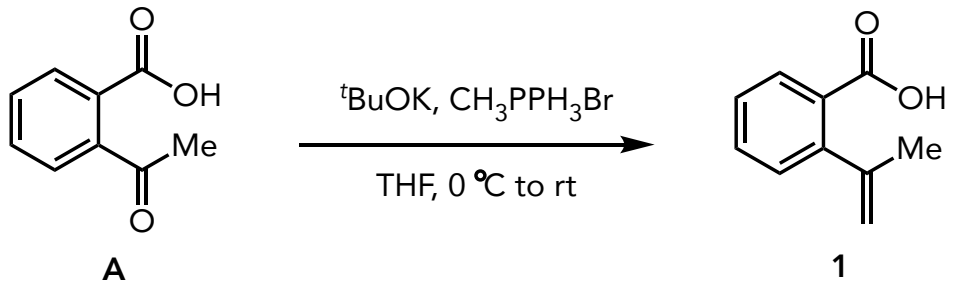

A **1**

A mixture of methyltriphenylphosphonium bromide (21.76 g) in anhydrous THF (150 mL) was stirred at 0°C under an atmosphere of nitrogen. Potassium tert-butoxide (10.25 g) was added portion-wise into the mixture and was stirred for 2 hours under 0°C before acid **A** (5.0 g) was added. The reaction mixture stirred overnight after allowing to warm to room temperature. The filtrate was then evaporated under reduced pressure and was treated with 6M NaOH (150 mL). The aqueous layer was washed with EtOAc (3 x 50 mL), and the organic extracts were washed with DI water (50 mL). The combined aqueous extracts were acidified with aq HCl (6M) to a pH of 1. The aqueous layer was extracted with EtOAc (3 x 50 mL). The combined organic extracts were wash with brine, dried over Na_2SO_4, and evaporated *in vacuo*. The residue was purified by silica gel chromatography (Hexanes/EtOAc, 4:1) to give the product as a white solid; characterization for this data have been previously reported.[104]

^{1}H NMR (500 MHz, $CDCl_3$) δ 7.97 (d, 1H), 7.51 – 7.55 (t, 1H), 7.36 – 7.40 (m, 1H), 7.30 (m, 1H), 5.16 (m, 1H), 4.93 (q, 1H), 2.15 (d, 3H)

^{13}C NMR (125 MHz, $CDCl_3$) δ 171.9, 146.6, 146.2, 132.5, 130.7, 129.7, 127.9, 127.0, 114.0, 24.3

Procedure for the synthesis of 2-(prop-1-en-2-yl)benzoyl chloride **(2)**

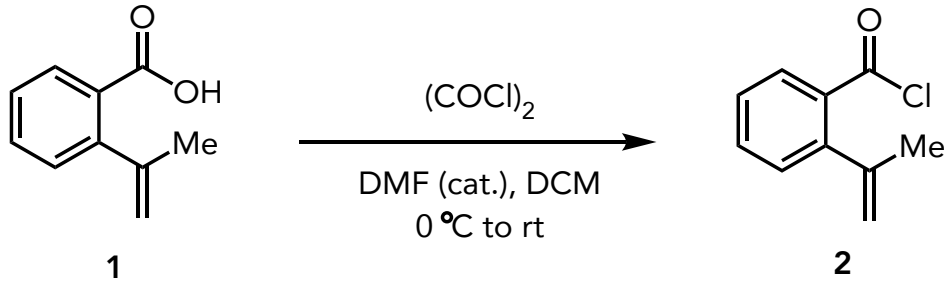

1 **2**

To a mixture of **1** (1.0 g, 6.2 mmol, 1.0 equiv.) in dry DCM (10 mL) at 0°C under an atmosphere of nitrogen was added dropwise oxalyl chloride (0.7 mL, 7.4 mmol, 1.2 equiv.) followed by a catalytic amount of dry DMF (2 drops). The reaction mixture was stirred to rt for 2 h. The filtrate was then evaporated under reduced pressure to afford the crude acid chloride **2** as a yellowish oil. The data of the compound was consistent with those reported in literature.[105]

Procedure for the synthesis of 2-(prop-1-en-2-yl)benzamide **(3)**

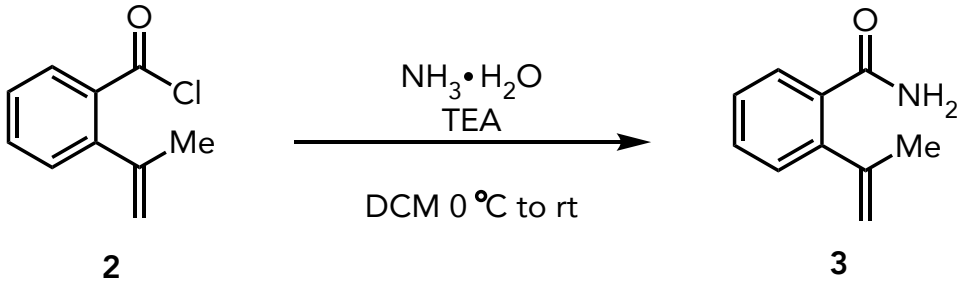

2 **3**

To a solution of ammonium hydroxide (about 28% w%, 2.6 g, 3 equiv.) in DCM (10 mL) at 0°C under an atmosphere of nitrogen. After TEA (4 equiv.) was added dropwise into the reaction mixture the reaction was allowed to stir to rt overnight. Saturated $NaHCO_3$ solution was added, and the product was extracted with EtOAc (3 x 30 mL), dried over Na_2SO_4, filtered, and evaporated *in vacuo.* Th pure product was obtained by recrystallization from hexane as a white crystal; characterization for this data have been previously reported.[105]

^{1}H NMR (500 MHz, $CDCl_3$) δ 7.77 (d, 2H), 7.76 – 7.78 (d, 1H), 7.43 – 7.46 (t, 1H), 7.36 – 7.39 (d, 1H), 7.24 – 7.26 (t, 1H), 5.27 (d, 1H), 5.13 (d, 1H), 2.15 (s, 3H)

^{13}C NMR (125 MHz, $CDCl_3$) δ 170.8, 146.9, 142.2, 132.7, 130.9, 129.0, 128.9, 127.6, 116.0, 24.4

Procedure for the synthesis of *tert*-butyl (2-(prop-1-en-2-yl)benzoyl)carbamate **(4)**

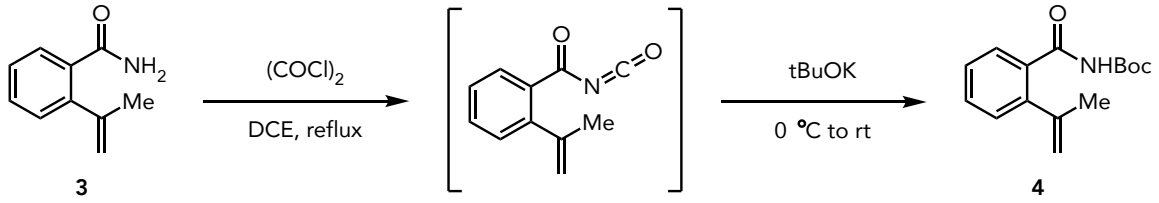

Compound **3** was synthesized from the following procedure. To a mixture of benzamide (1.0 equiv.) in DCE (6.1 mL) was slowly added oxalyl chloride (1.2 equiv.) at 0°C under an atmosphere of nitrogen. The mixture was warmed to 60 degrees Celsius and stirred for 1 h. After re-cooling the mixture to 0°C, a solution of tert-butanol in DCE was added and stirred for an additional 2 h. Saturated $NaHCO_3$ solution was added to the reaction mixture before extracting with DCM. The organic layers were combined and washed with brine before being dried over Na_2SO_4, filtered, and concentrated *in vacuo.* The crude product was purified by silica gel chromatography to afford of product **4** as a yellowish solid; characterization for this data have been previously reported. [105]

^{1}H NMR (500 MHz, $CDCl_3$) δ 7.84 (s, 1H), 7.58 (d, 1H), 7.43 – 7.48 (t, 1H), 7.35 – 7.42 (t, 1H), 7.28 – 7.30 (m, 1H), 5.28 (p, 1H), 5.10 (d, 1H), 2.14 (d, 3H), 1.48 (s, 9H)

^{13}C NMR (125 MHz, $CDCl_3$) δ 170.5, 149.4, 145.0, 141.8, 133.2, 130.9, 128.5, 128.4, 127.4, 116.6, 82.6, 28.0, 24.1

Procedure for the synthesis of 2-(prop-1-en-2-yl)-*N*-tosylbenzamide **(5)**

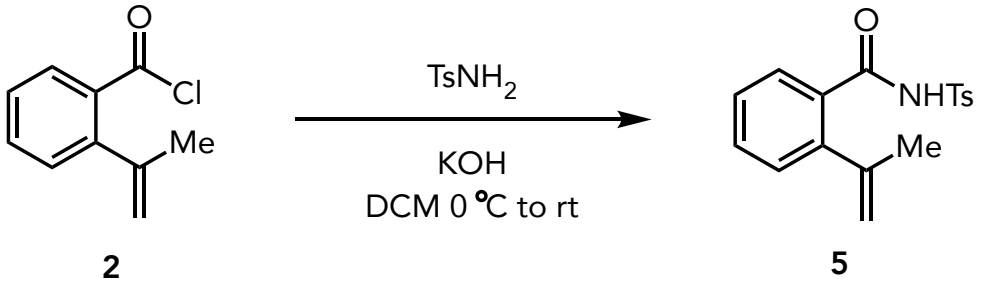

2 **5**

Compound **2** was synthesized was synthesized in the following procedure described above. The following mixture of 4-methylbenzenesulonamide (1.1 g) and powered KOH (1.0 g) in DCM (20 mL) was added to a cold suspension (0°C) of a solution of acid chloride **2** in CH_2Cl_2 (20 mL). After stirring for 2 h from 0°C to room temperature, the mixture was quenched with DI water and acidified with 1M HCl. The reaction mixture was extracted with EtOAc. The organic layers were combined and was dried over Na_2SO_4, filtered, and concentrated *in vacuo.* The residue was purified by silica gel chromatography to afford of product **5** as a yellowish oil. The data of the compound was consistent with those reported in literature. [105]

^{1}H NMR (500 MHz, $CDCl_3$) δ 8.83 (s, 1H), 8.1 – 8.05 (d, 2H), 7.69 – 7.71 (d, 1H), 7.47 – 7.53 (m, 1H), 7.35-7.39 (m, 3H), 7.22 – 7.25 (m, 1H), 5.34 (td, 1 H), 5.11 (dt, 1H), 2.47 (s, 3H), 1.99 (s, 3H)

^{13}C NMR (125 MHz, $CDCl_3$) δ 165.4, 145.9, 145.2, 142.4, 135.3, 132.3, 130.3, 129.5, 129.1, 128.7, 127.9, 117.8, 24.7, 21.7

Procedure for the synthesis of *N*-methoxy-2-(prop-1-en-2-yl)benzamide **(6)**

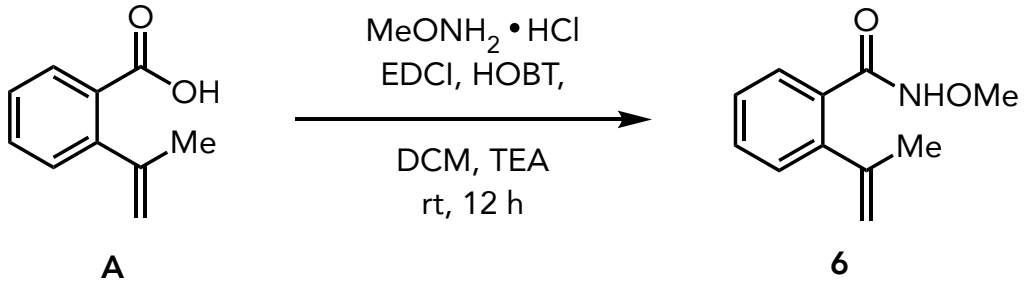

A **6**

To a suspension of **A** (1.0 g) in CH_2Cl_2 (25 mL), were added *o*-methylhydroxylamine hydrochloride (0.8 g), TEA (1 g). After stirring for 10 minutes EDCI (1.75 g) and HOBT (1.25 g) were added to the mixture and was stirred overnight at room temperature. Water and DCM were added to the reaction mixture after completion. The organic phases were combined and washed with aqueous HCl (1 M), saturated in $NaHCO_3$ solution, and washed with brine. The organic phase was dried over Na_2SO_4, filtered, and evaporated *in vacuo.* The crude was purified by silica gel chromatography to afford substrate **6** as a white solid. The data of the compound was consistent with those reported in literature.[105]

^{1}H NMR (500 MHz, $CDCl_3$) δ 8.63 (s, 1H), 7.64 – 7.66 (d, 1H), 7.43 – 7.46 (t, 1H), 7.35 – 7.38 (m, 1H), 7.26 – 7.28 (d, 1H), 5.29 (s, 1H), 5.13 (s, 1H), 3.89 (s, 3H), 2.14 (s, 3H)

General Procedure for NBS Reactions:

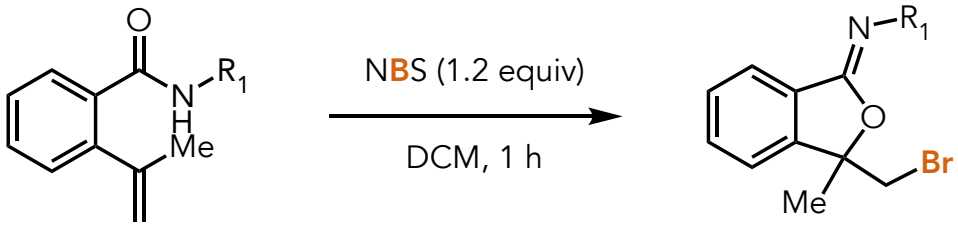

D **7-10**

The reaction must be carried out by adding, at the beginning, N-bromosuccinamide (NBS) (1.2 equiv.) to the starting material **D** (which can be compound **3** or **4** or **5**, 1 mmol) dissolved in DCM. The reaction stirred for 1 h at room temperature. The residue was purified by silica gel chromatography (Hexanes/EtOAc, 4:1) to give the products **7-10**. The data of each compound is not reported in literature. However, there was a similar source to help analyze NMR peaks.[103]

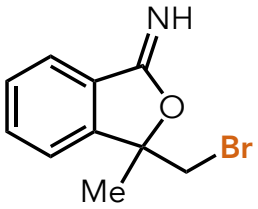

3-(bromomethyl)-3-methylisobenzofuran-1(3*H*)-imine **(7)**

White solid, 54.8% yield

^{1}H NMR (500 MHz, $CDCl_3$) δ 7.84 – 7.89 (d, 1H), 7.60 – 7.63 (t, 1H), 7.51 – 7.55 (t, 1H), 7.40 – 7.44 (d, 1H), 3.80-3.82 (d, 1H), 3.74 – 3.76 (d, 1H), 1.89 (s, 3H)

^{13}C NMR (125 MHz, $CDCl_3$) δ 168.9, 134.3, 129.8, 126.3, 126.0, 125.5, 121.5, 84.5, 37.8, 28.2

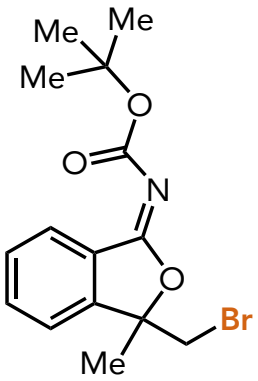

tert-butyl (*E*)-(3-(bromomethyl)-3-methylisobenzofuran-1(3*H*)-ylidene)carbamate **(8)**

Colorless oil, 72.2% yield

^{1}H NMR (500 MHz, $CDCl_3$) δ 7.91 – 7.94 (d, 1H), 7.71 – 7.75 (t, 1H), 7.58 – 7.61 (t, 1H), 7.52 – 7.55 (d, 1H), 3.75 – 3.77 (d, 1H), 3.71 – 3.74 (d, 1H), 1. 84 (s, 3H), 1.48 (s, 9H)

^{13}C NMR (125 MHz, $CDCl_3$) δ 171.2, 159.2, 148.8, 133.2, 129.7, 125.0, 125.0, 121.2, 88.7, 81.6, 37.9, 28.1, 24.2

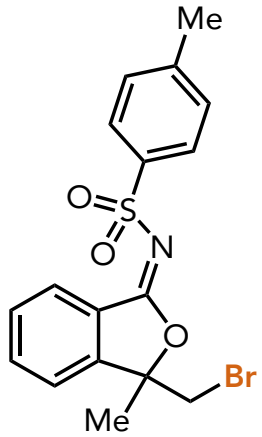

(*E*)-*N*-(3-(bromomethyl)-3-methylisobenzofuran-1(3*H*)-ylidene)-4-methylbenzenesulfonamide **(9)**

White solid, 83.0% yield

^{1}H NMR (500 MHz, $CDCl_3$) δ 8.14 – 8.18 (d, 1H), 7.79 – 7.81 (d, 1H), 7.69 – 7.72 (m, 2H), 7.49 – 7.53 (d, 1H), 7.49 – 7.51 (t, 1H), 7.34 – 7.44 (m, 2H), 4.60 – 4.62 (d, 1H), 3.94 – 3.96 (d, 1H), 2.45 (s, 3H), 2.13 (s, 3H)

^{13}C NMR (125 MHz, $CDCl_3$) δ 166.1, 149.0, 145.2, 136.1, 134.4, 129.4, 129.2, 129.2, 128.6, 124.8, 120.8, 70.2, 38.0, 24.9, 21.7

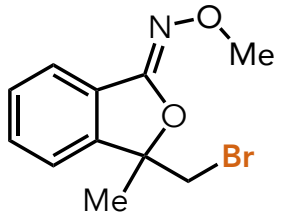

(*Z*)-3-(bromomethyl)-3-methylisobenzofuran-1(3*H*)-one *O*-methyl oxime **(10)**

Colorless oil, 93.0% yield

^{1}H NMR (500 MHz, $CDCl_3$) δ 7.69 – 7.71 (d, 1H), 7.50 – 7.53 (t, 1H), 7.45 – 7.48 (t, 1H), 7.39 – 7.40 (d, 1H), 3.99 (s, 1H), 3.74 (s, 1H), 1.85 (s, 3H)

^{13}C NMR (125 MHz, $CDCl_3$) δ 154.5, 145.6, 130.9, 129.5, 128.7, 121.8, 121.4, 89.4, 62.9, 38.5, 24.7

General Procedure for Enzymatic Halocyclization of Amide Derivatives 3 – 6

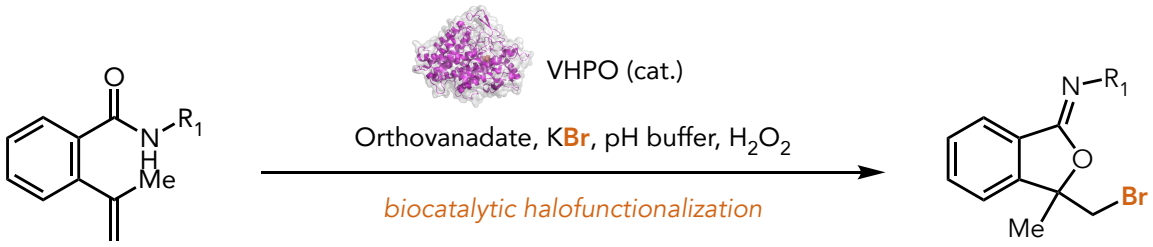

3-6 **11-14**

Each enzymatic screen has different standard measurements dependent on the enzyme (see below – *C. inaequalis, C. officinalis, C. pilulifera, A. marina*) used. Before the start of the screen, each enzyme aliquot was pre-incubated with orthovanadate (250 mM) in a PCR tube and was shaken at room temperature for ten minutes. During the ten-minute period, the halide (50 μL, 176 mM), buffer (100 μL, 50–100 mM), and DI water were added in a separate 1-dram vial. The starting amide substrate, **3–6** was dissolved in 5 mL of acetonitrile to make a stock 40mM stock solution, and 100 μL of the solution was added to the reaction mixture. After stirring for ten minutes, the haloperoxidase was added to the resulting solution. Lastly, hydrogen peroxide (2.9 μL, 10% in water, 3034 mM) was added to the vial, and the mixture was stirred vigorously at room temperature for 1 h. Next, acetonitrile (750 μL) was added to enable phase separation between the organic and aqueous layers. After centrifuging the vial (12.5 krpm), the two layers were separated, and the organic phase was extracted and transferred into a 1.5 mL LCMS vial for analysis.

C. inaequalis

Enzyme 5.0 μM *Ci* (μL)	Cofactor 250 mM OV (μL)	Halide 176 mM KBr (μL)	Buffer 100 mM pH 5 Citrate (μL)	Substrate in ACN 40 mM (μL)	DI Water (μL)	Peroxide 3034 mM (μL)
24.2	4	50	100	100	718.9	2.9

C. officinalis

Enzyme 10 μM *Co* (μL)	Cofactor 250 mM OV (μL)	Halide 176 mM KBr (μL)	Buffer 50 mM pH 6.5 Pipes (μL)	Substrate in ACN 40 mM (μL)	DI Water (μL)	Peroxide 3034 mM (μL)
24.2	4	50	100	100	718.9	2.9

C. pilulifera

Enzyme 10 μM *Cp* (μL)	Cofactor 250 mM OV (μL)	Halide 176 mM KBr (μL)	Buffer 50 mM pH 6.5 Pipes (μL)	Substrate in ACN 40 mM (μL)	DI Water (μL)	Peroxide 3034 mM (μL)
24.2	4	50	100	100	718.9	2.9

A. marina

Enzyme 10 μM *Am* (μL)	Cofactor 250 mM OV (μL)	Halide 176 mM KBr (μL)	Buffer 100 mM pH 6 Citrate (μL)	Substrate in ACN 40 mM (μL)	DI Water (μL)	Peroxide 3034 mM (μL)
24.2	4	50	100	100	718.9	2.9

Physical Data

1H and 13C NMR Analysis for Intermediates and Substrates

Wittig Product **1**

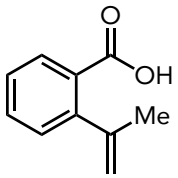

[1]H-NMR

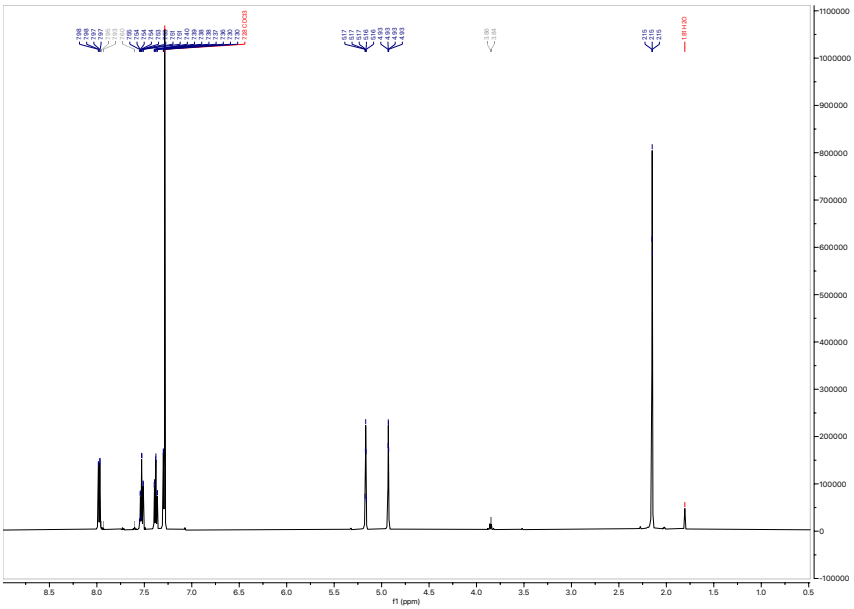

[13]C-NMR

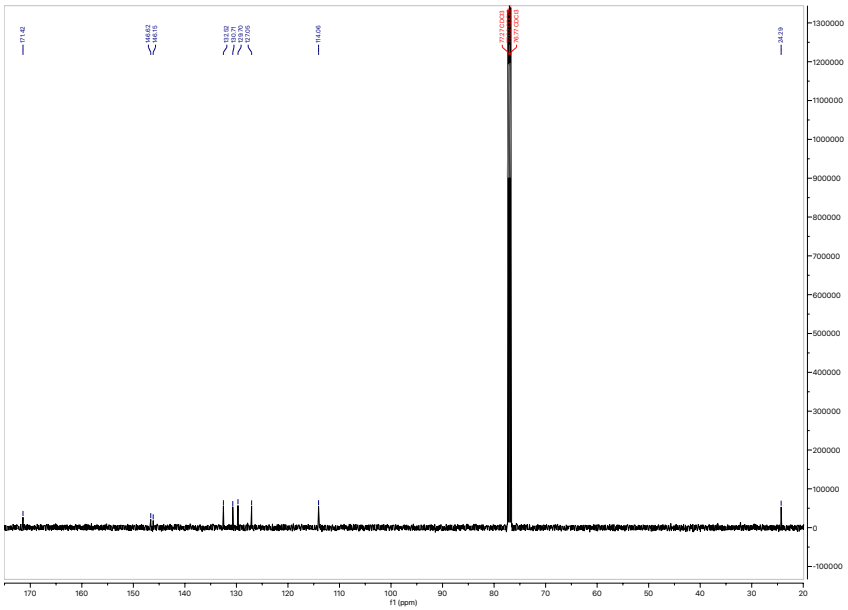

Amide Product **3**

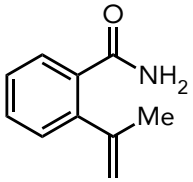

^{1}H-NMR

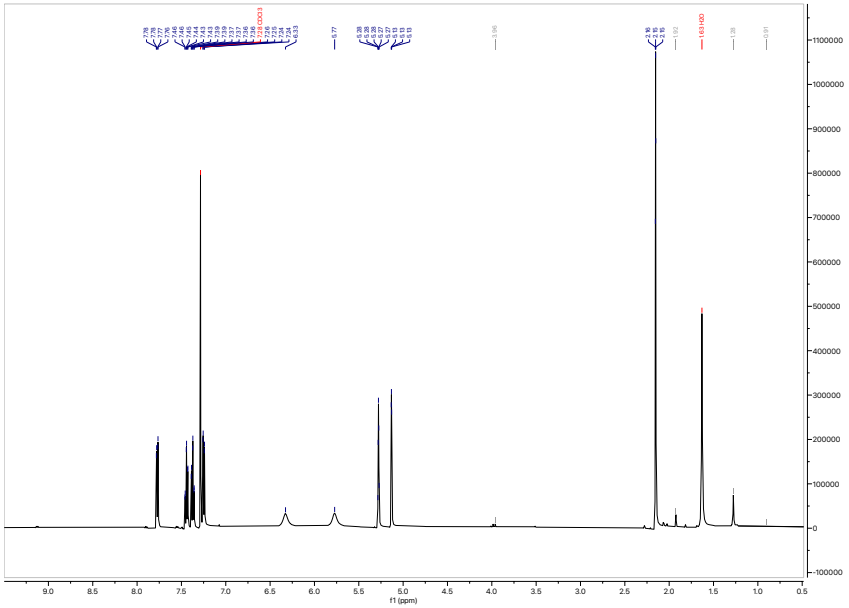

^{13}C-NMR

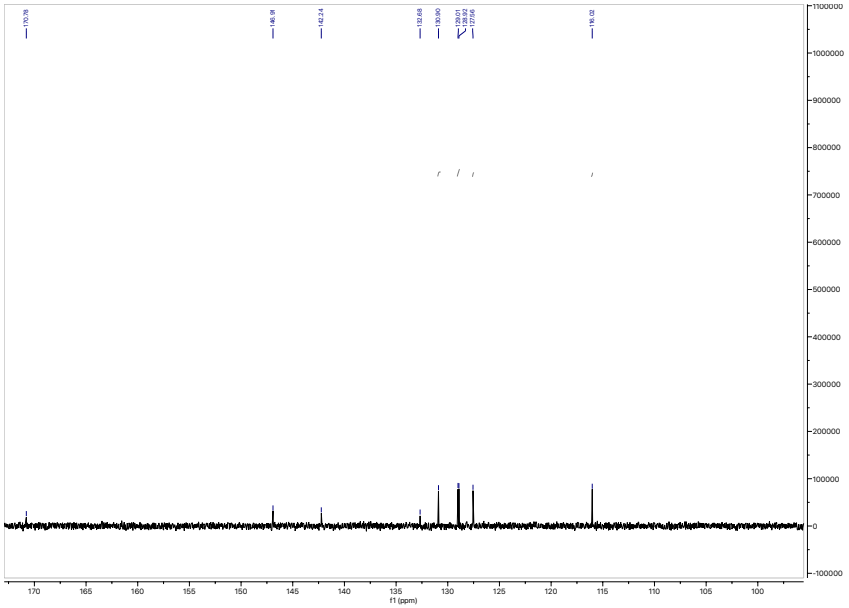

Boc Amide Product **4**

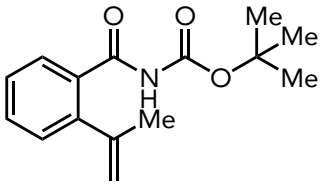

^{1}H-NMR

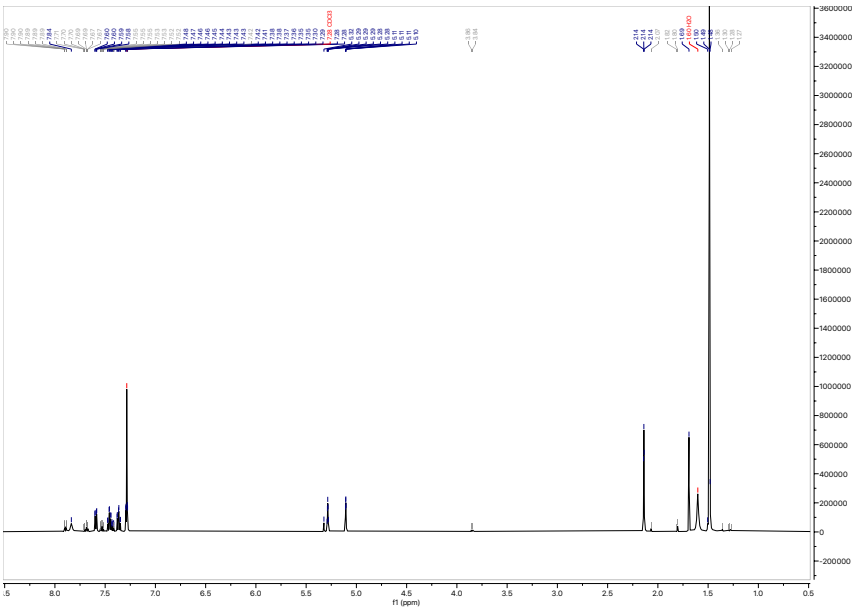

^{13}C-NMR

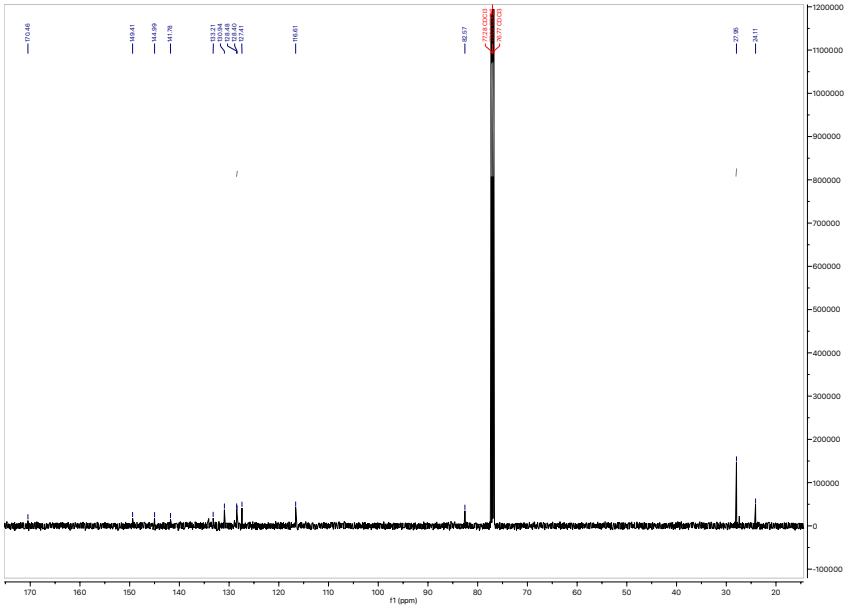

Tosyl Amide Product **5**

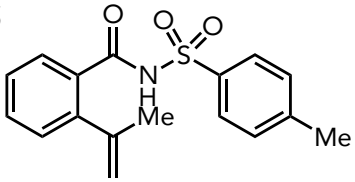

^{1}H-NMR

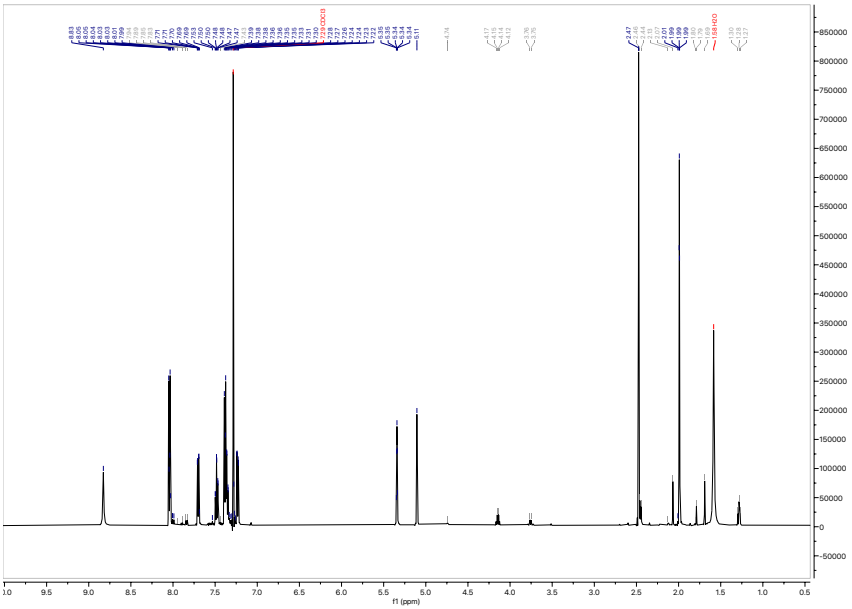

^{13}C-NMR

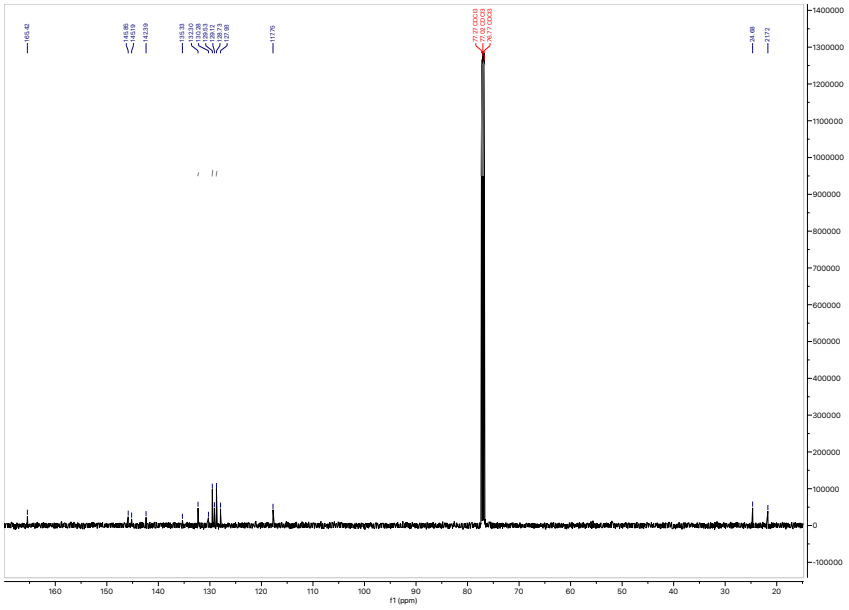

Methoxy Amide Product **6**

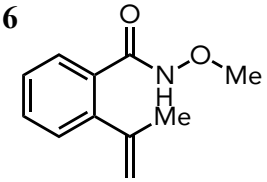

^{1}H-NMR

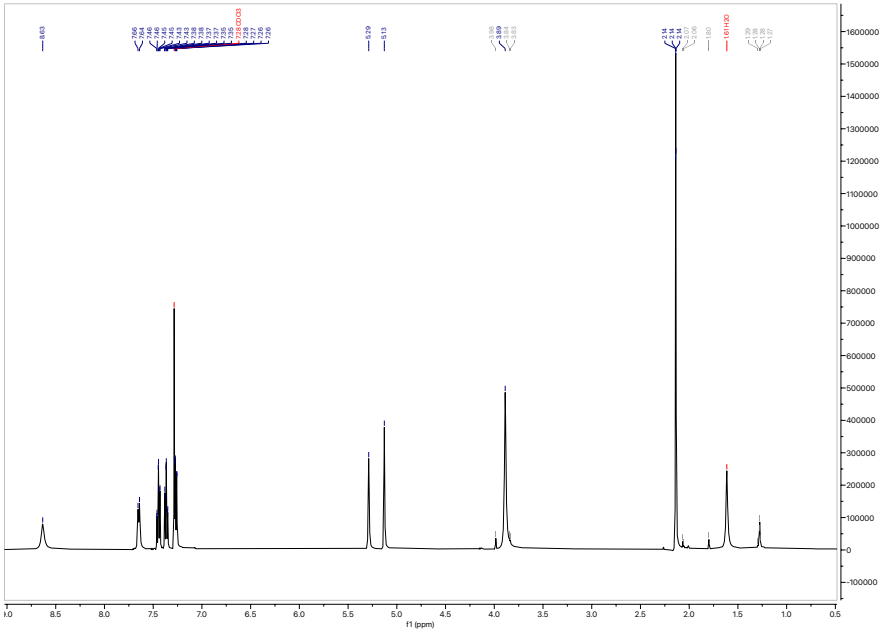

^{1}H and ^{13}C NMR Analysis for NBS Products

Amide Product **7**

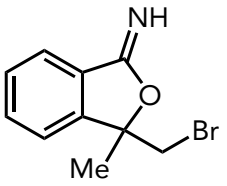

^{1}H-NMR

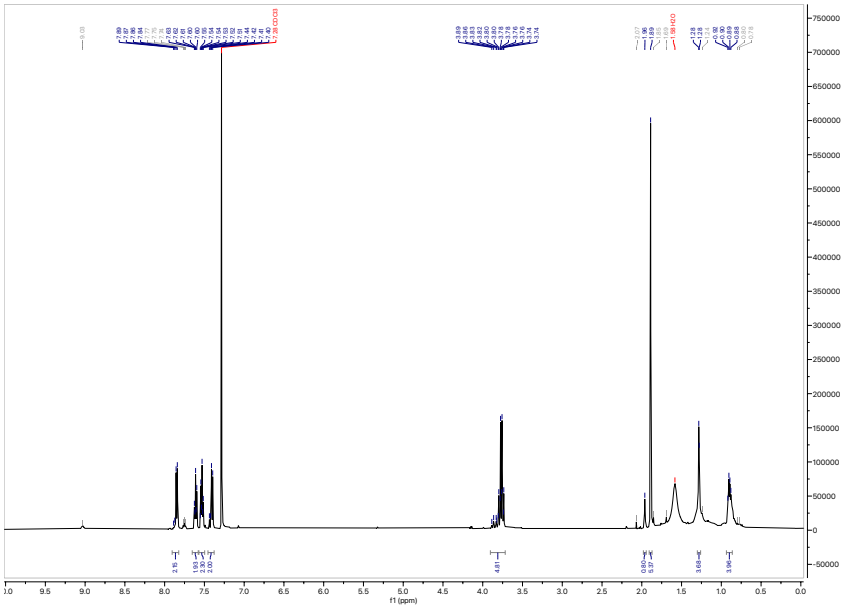

^{13}C-NMR

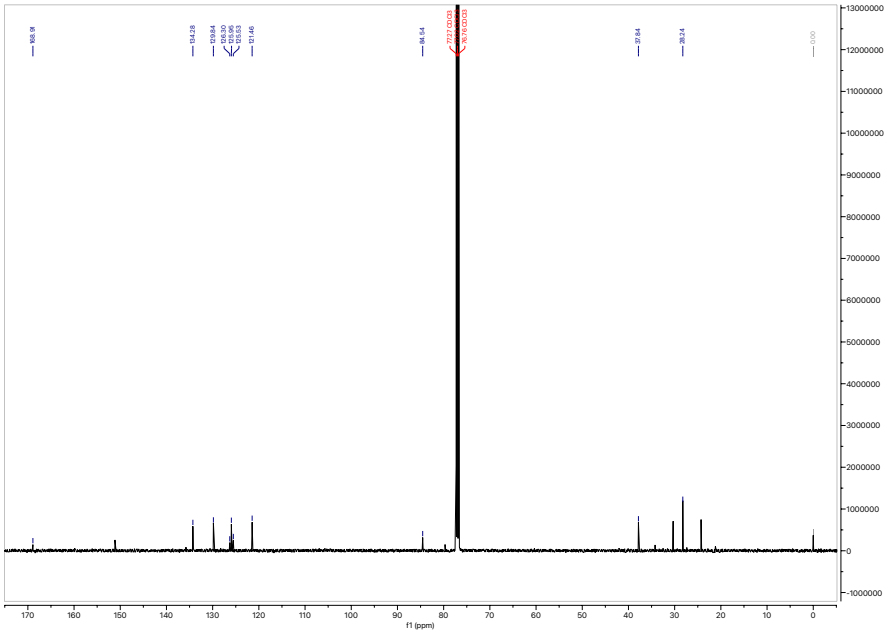

Boc Amide Product **8**

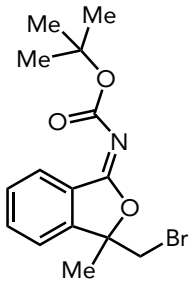

^{1}H-NMR

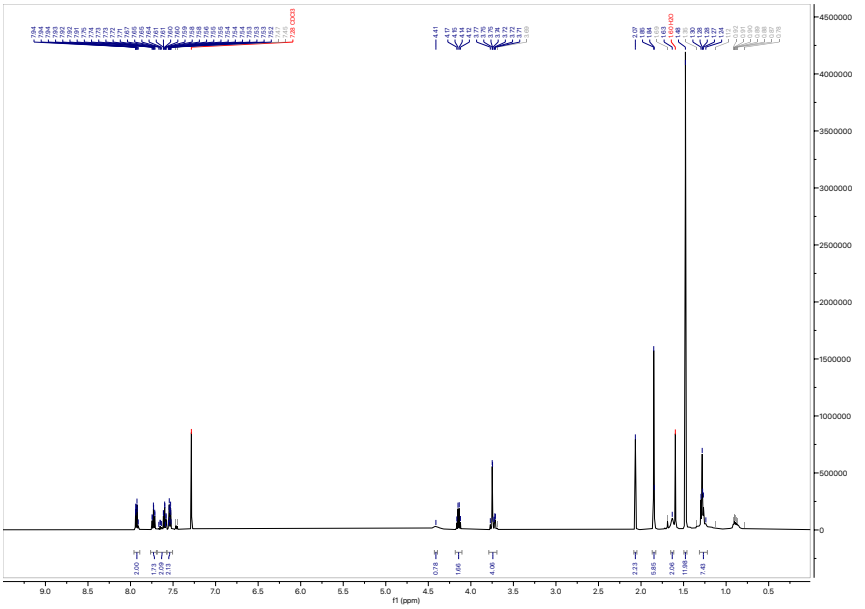

^{13}C-NMR

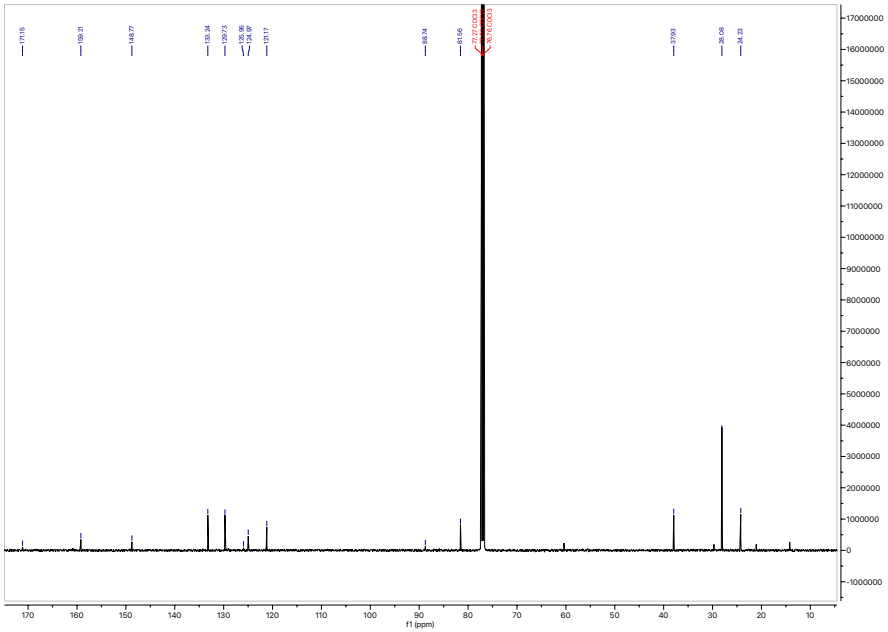

Tosyl Amide Product **9**

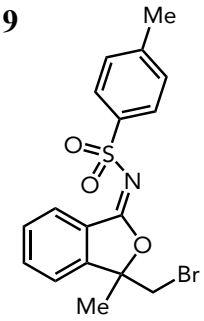

[1]H-NMR

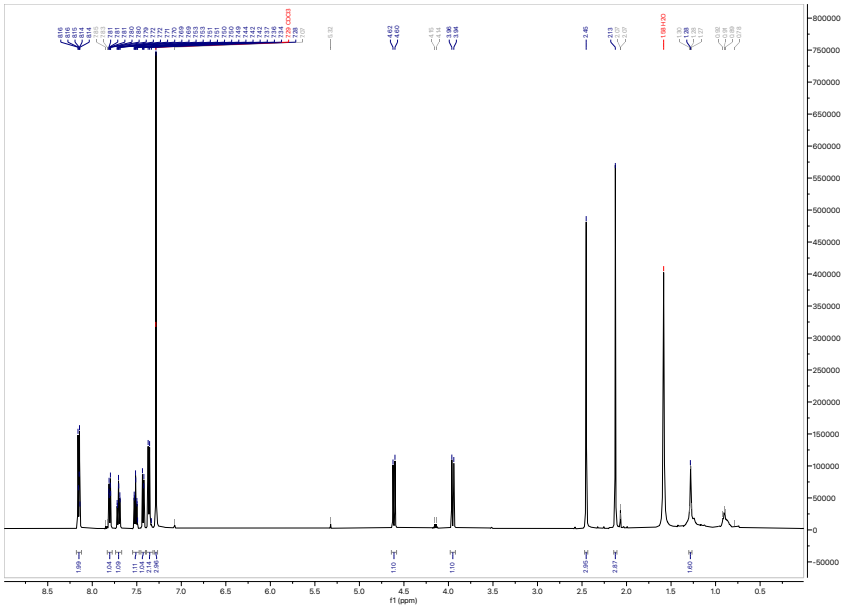

[13]C-NMR

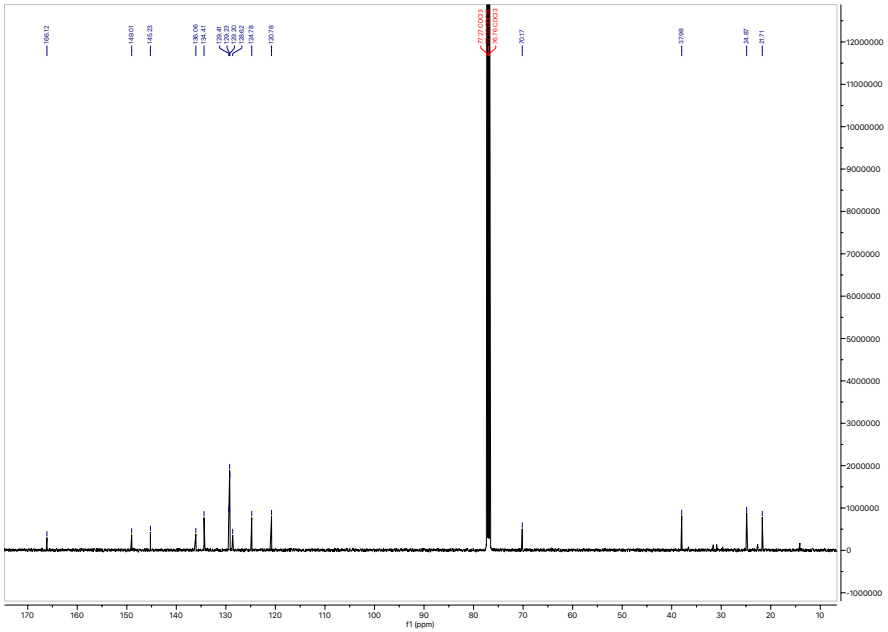

Methoxy Amide Product **10**

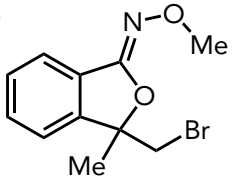

^{1}H-NMR

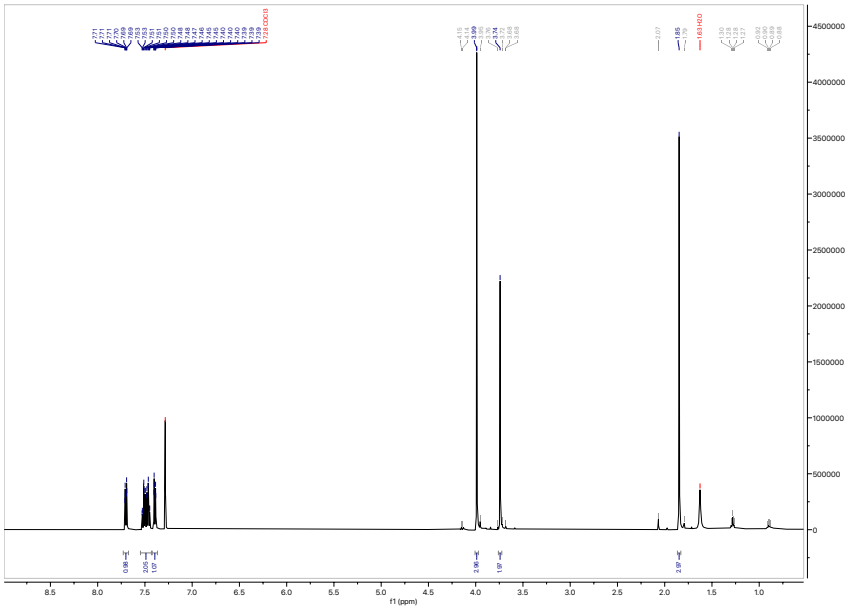

^{13}C-NMR

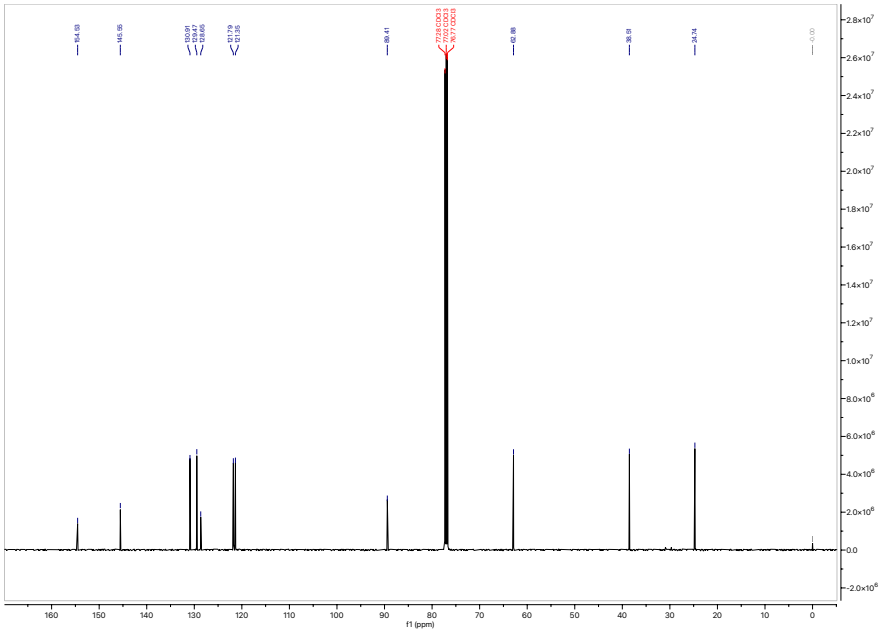

LCMS Analysis of Enzymatic Runs

Amide **3** and Enzymatic Product **11**

Analysis A: Standard Conditions

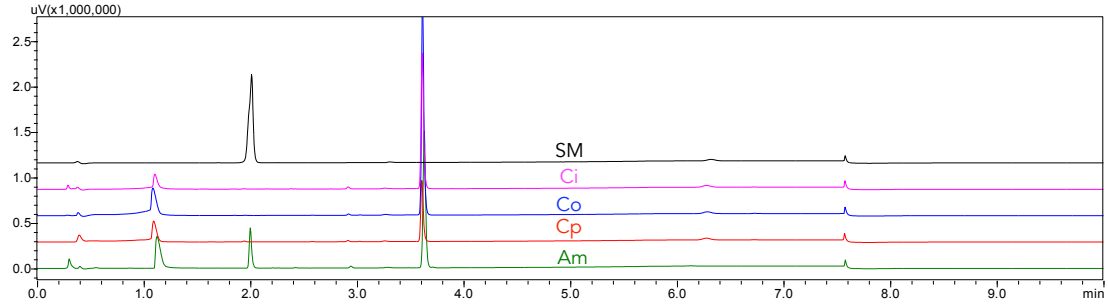

Analysis B: No OV

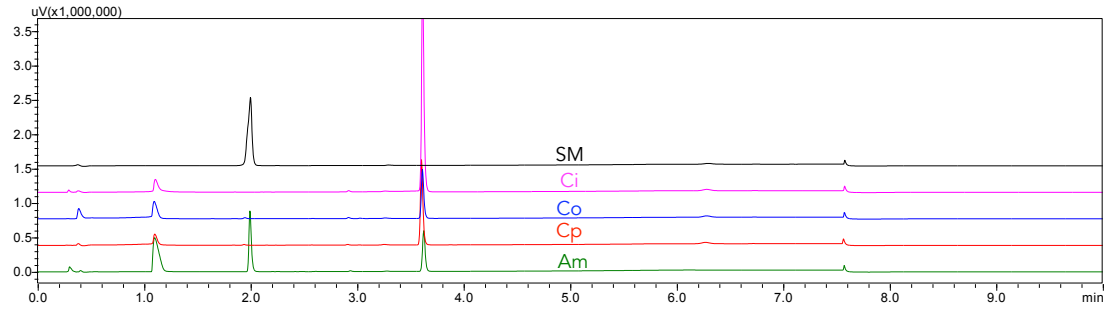

Analysis C: NBS

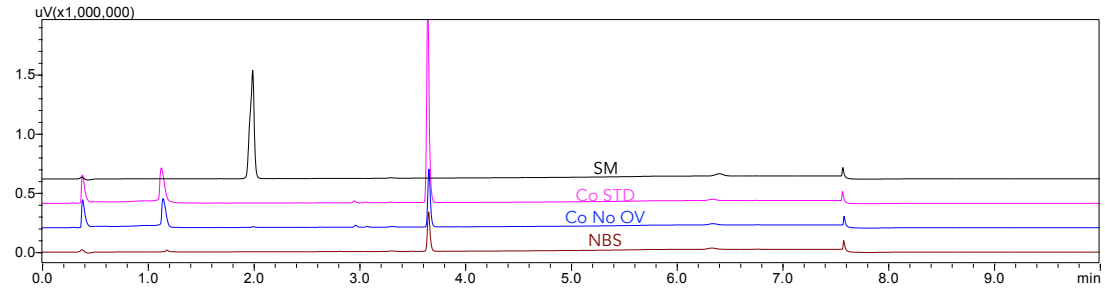

Boc Amide **4** and Enzymatic Product **12**

Analysis A: Standard Conditions

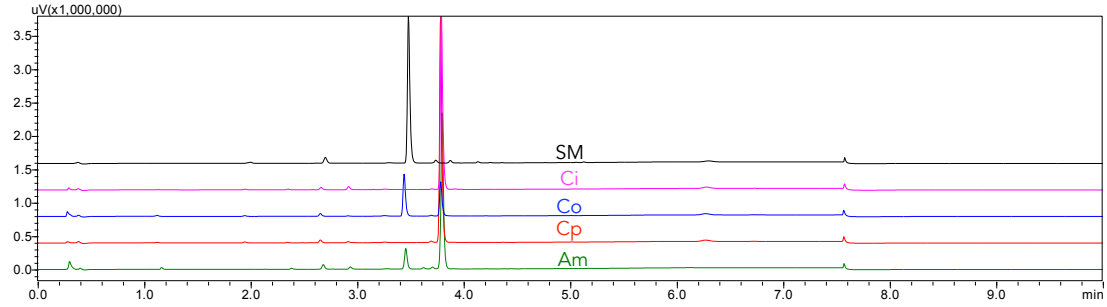

Analysis B: No OV

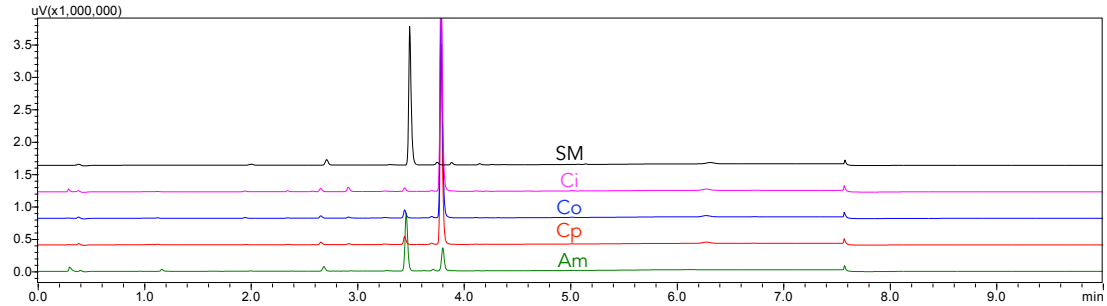

Analysis C: NBS

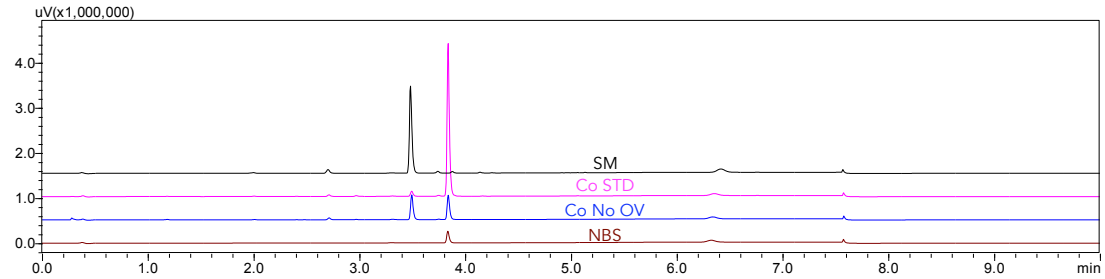

Tosyl Amide **5** and Enzymatic Product **13**

Analysis A: Standard Conditions

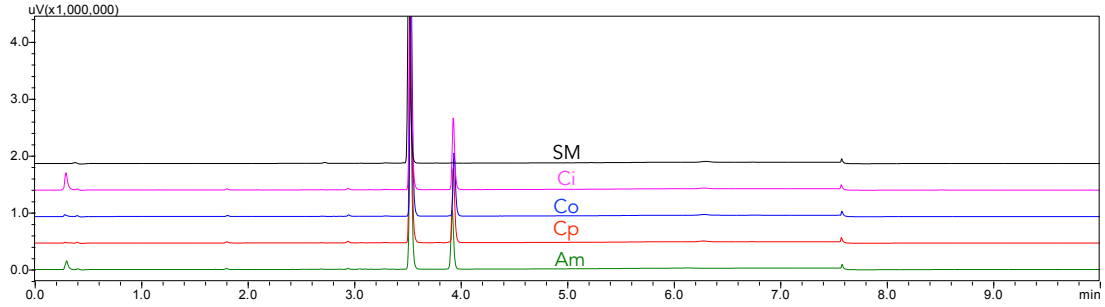

Analysis B: No OV

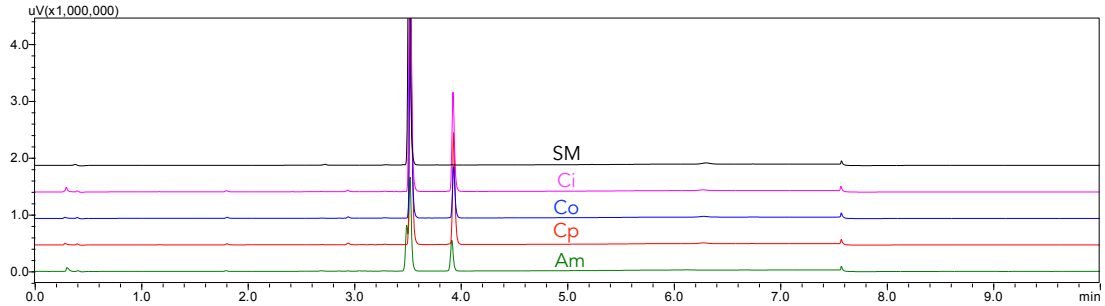

Analysis C: NBS

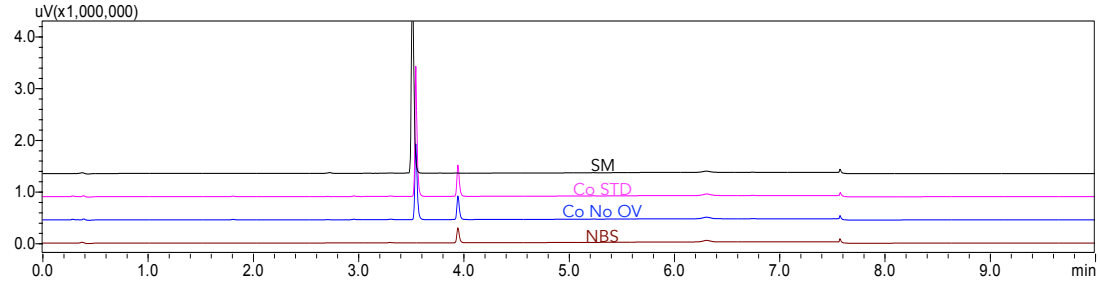

Methoxy Amide **6** and Enzymatic Product **14**

Analysis A: Standard Conditions

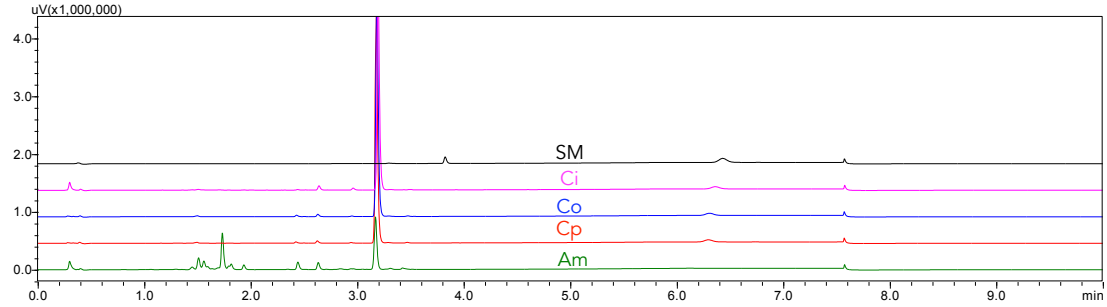

Analysis B: No OV

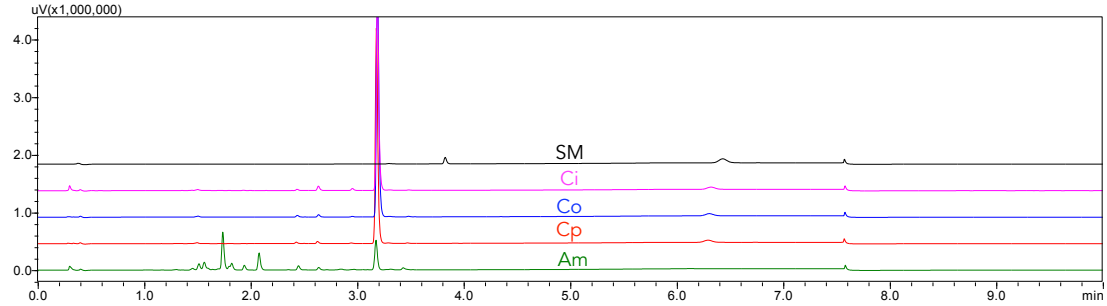

Analysis C: NBS

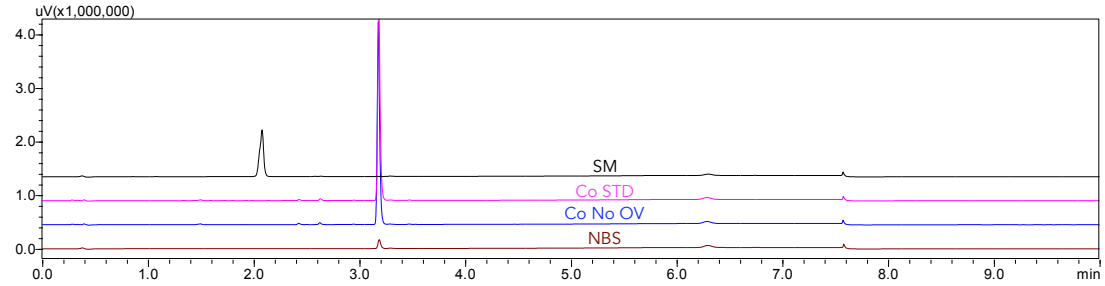

REFERENCES

[1] Saldívar-González, F.; Lenci, E.; Trabocchi, A.; L. Medina-Franco, J. Exploring the Chemical Space and the Bioactivity Profile of Lactams: A Chemoinformatic Study. *RSC Advances* **2019**, *9* (46), 27105–27116. https://doi.org/10.1039/C9RA04841C.

[2] Tahlan, K.; Jensen, S. E. Origins of the β-Lactam Rings in Natural Products. *J Antibiot (Tokyo)* **2013**, *66* (7), 401–410. https://doi.org/10.1038/ja.2013.24.

[3] Elander, R. P. Industrial Production of β-Lactam Antibiotics. *Appl Microbiol Biotechnol* **2003**, *61* (5), 385–392. https://doi.org/10.1007/s00253-003-1274-y.

[4] Lobanovska, M.; Pilla, G. Penicillin's Discovery and Antibiotic Resistance: Lessons for the Future? *Yale J Biol Med* **2017**, *90* (1), 135–145.

[5] Park, Y.; Chang, S. Asymmetric Formation of γ-Lactams via C–H Amidation Enabled by Chiral Hydrogen-Bond-Donor Catalysts. *Nat Catal* **2019**, *2* (3), 219–227. https://doi.org/10.1038/s41929-019-0230-x.

[6] Caruano, J.; Muccioli, G. G.; Robiette, R. Biologically Active γ-Lactams: Synthesis and Natural Sources. *Org. Biomol. Chem.* **2016**, *14* (43), 10134–10156. https://doi.org/10.1039/C6OB01349J.

[7] Barrett, A. G. M.; Head, J.; Smith, M. L.; Stock, N. S.; White, A. J. P.; Williams, D. J. Fleming−Tamao Oxidation and Masked Hydroxyl Functionality: Total Synthesis of (+)-Pramanicin and Structural Elucidation of the Antifungal Natural Product (−)-Pramanicin. *J. Org. Chem.* **1999**, *64* (16), 6005–6018. https://doi.org/10.1021/jo9905672.

[8] Bhuma, N.; Vangala, M.; Nair, R. J.; Sabharwal, S. G.; Dhavale, D. D. Halogenated D-Xylono-δ-Lactams: Synthesis and Enzyme Inhibition Study. *Carbohydrate Research* **2015**, *402*, 215–224. https://doi.org/10.1016/j.carres.2014.10.023.

[9] Kowalczyk, P.; Gawdzik, B.; Trzepizur, D.; Szymczak, M.; Skiba, G.; Raj, S.; Kramkowski, K.; Lizut, R.; Ostaszewski, R. δ-Lactones—A New Class of Compounds That Are Toxic to E. Coli K12 and R2–R4 Strains. *Materials (Basel)* **2021**, *14* (11), 2956. https://doi.org/10.3390/ma14112956.

[10] Cantillo, D.; Kappe, C. O. Halogenation of Organic Compounds Using Continuous Flow and Microreactor Technology. *React. Chem. Eng.* **2017**, *2* (1), 7–19. https://doi.org/10.1039/C6RE00186F.

[11] Benedetto Tiz, D.; Bagnoli, L.; Rosati, O.; Marini, F.; Sancineto, L.; Santi, C. New Halogen-Containing Drugs Approved by FDA in 2021: An Overview on Their Syntheses and Pharmaceutical Use. *Molecules* **2022**, *27* (5), 1643. https://doi.org/10.3390/molecules27051643.

[12] *Infographic: The Drugs That Bring in the Most Pharma Revenue*. Statista Infographics. https://www.statista.com/chart/18311/sales-revenues-of-drug-classes/ (accessed 2022-06-16).

[13] Reeves, E. K.; Entz, E. D.; Neufeldt, S. R. Chemodivergence between Electrophiles in Cross-Coupling Reactions. *Chemistry – A European Journal* **2021**, *27* (20), 6161–6177. https://doi.org/10.1002/chem.202004437.

[14] Paik, A.; Paul, S.; Bhowmik, S.; Das, R.; Naveen, T.; Rana, S. Recent Advances in First-Row Transition-Metal-Mediated C−H Halogenation of (Hetero)Arenes and Alkanes. *Asian Journal of Organic Chemistry* **2022**, *11* (5), e202200060. https://doi.org/10.1002/ajoc.202200060.

[15] Denmark, S. E.; Kuester, W. E.; Burk, M. T. Catalytic, Asymmetric Halofunctionalization of Alkenes—A Critical Perspective. *Angewandte Chemie International Edition* **2012**, *51* (44), 10938–10953. https://doi.org/10.1002/anie.201204347.

[16] Qi, C.; Force, G.; Gandon, V.; Lebœuf, D. Hexafluoroisopropanol-Promoted Haloamidation and Halolactonization of Unactivated Alkenes. *Angew. Chem. Int. Ed.* **2021**, *60* (2), 946–953. https://doi.org/10.1002/anie.202010846.

[17] *Enzymatic Halogenation: A Timely Strategy for Regioselective C−H Activation - Schnepel - 2017 - Chemistry – A European Journal - Wiley Online Library*. https://chemistry-europe.onlinelibrary.wiley.com/doi/10.1002/chem.201701209.

[18] M. Abdelraheem, E. M.; Busch, H.; Hanefeld, U.; Tonin, F. Biocatalysis Explained: From Pharmaceutical to Bulk Chemical Production. *Reaction Chemistry & Engineering* **2019**, *4* (11), 1878–1894. https://doi.org/10.1039/C9RE00301K.

[19] *Biocatalytic Asymmetric Synthesis of Chiral Amines from Ketones Applied to Sitagliptin Manufacture*. https://www-science-org.ezproxy1.lib.asu.edu/doi/epdf/10.1126/science.1188934 (accessed 2022-09-06).

[20] Biocatalytic Cascades Go Viral. *Science* **2019**, *366* (6470), 1199–1200. https://doi.org/10.1126/science.aaz7376.

[21] Huffman, M. A.; Fryszkowska, A.; Alvizo, O.; Borra-Garske, M.; Campos, K. R.; Canada, K. A.; Devine, P. N.; Duan, D.; Forstater, J. H.; Grosser, S. T.; Halsey, H. M.; Hughes, G. J.; Jo, J.; Joyce, L. A.; Kolev, J. N.; Liang, J.; Maloney, K. M.; Mann, B. F.; Marshall, N. M.; McLaughlin, M.; Moore, J. C.; Murphy, G. S.; Nawrat, C. C.; Nazor, J.; Novick, S.; Patel, N. R.; Rodriguez-Granillo, A.; Robaire, S. A.; Sherer, E. C.; Truppo, M. D.; Whittaker, A. M.; Verma, D.; Xiao, L.; Xu, Y.; Yang, H. Design of an in Vitro Biocatalytic Cascade for the Manufacture of Islatravir. *Science* **2019**, *366* (6470), 1255–1259. https://doi.org/10.1126/science.aay8484.

[22] Senn, H. M. Insights into Enzymatic Halogenation from Computational Studies. *Front Chem* **2014**, *2*, 98. https://doi.org/10.3389/fchem.2014.00098.

[23] Yeh, E.; Blasiak, L. C.; Koglin, A.; Drennan, C. L.; Walsh, C. T. Chlorination by a Long-Lived Intermediate in the Mechanism of Flavin-Dependent Halogenases,. *Biochemistry* **2007**, *46* (5), 1284–1292. https://doi.org/10.1021/bi0621213.

[24] Crowe, C.; Molyneux, S.; Sharma, S. V.; Zhang, Y.; Gkotsi, D. S.; Connaris, H.; Goss, R. J. M. Halogenases: A Palette of Emerging Opportunities for Synthetic Biology–Synthetic Chemistry and C–H Functionalisation. *Chem Soc Rev 50* (17), 9443–9481. https://doi.org/10.1039/d0cs01551b.

[25] O'Hagan, D.; Schaffrath, C.; Cobb, S. L.; Hamilton, J. T. G.; Murphy, C. D. Biosynthesis of an Organofluorine Molecule. *Nature* **2002**, *416* (6878), 279–279. https://doi.org/10.1038/416279a.

[26] Eustáquio, A. S.; Pojer, F.; Noel, J. P.; Moore, B. S. Discovery and Characterization of a Marine Bacterial SAM-Dependent Chlorinase. *Nat Chem Biol* **2008**, *4* (1), 69–74. https://doi.org/10.1038/nchembio.2007.56.

[27] Aik, W.; McDonough, M. A.; Thalhammer, A.; Chowdhury, R.; Schofield, C. J. Role of the Jelly-Roll Fold in Substrate Binding by 2-Oxoglutarate Oxygenases. *Current Opinion in Structural Biology* **2012**, *22* (6), 691–700. https://doi.org/10.1016/j.sbi.2012.10.001.

[28] *SyrB2 in syringomycin E biosynthesis is a nonheme FeII α-ketoglutarate- and O2-dependent halogenase*. https://www.pnas.org/doi/10.1073/pnas.0504412102 (accessed 2022-06-30). https://doi.org/10.1073/pnas.0504412102.

[29] *In Vitro Analysis of Cyanobacterial Nonheme Iron-Dependent Aliphatic Halogenases WelO5 and AmbO5 | Elsevier Enhanced Reader*. https://reader.elsevier.com/reader/sd/pii/S007668791830082X?token=68D54B6978BDB8CECF3A466A9FFAD38CAEECFD05413C9CBC262D1582B7577CEC13DE15BA5A8D7D2983D8B10C58EE3339&originRegion=us-east-1&originCreation=20220630191352 (accessed 2022-06-30). https://doi.org/10.1016/bs.mie.2018.02.015.

[30] Hillwig, M. L.; Liu, X. A New Family of Iron-Dependent Halogenases Acts on Freestanding Substrates. *Nat Chem Biol* **2014**, *10* (11), 921–923. https://doi.org/10.1038/nchembio.1625.

[31] Mitchell, A. J.; Zhu, Q.; Maggiolo, A. O.; Ananth, N.; Hillwig, M. L.; Liu, X.; Boal, A. K. Structural Basis for Halogenation by Iron- and 2-Oxo-Glutarate-Dependent Enzyme WelO5. *Nat Chem Biol* **2016**, *12* (8), 636–640. https://doi.org/10.1038/nchembio.2112.

[32] Nakano, Y.; Biegasiewicz, K. F.; Hyster, T. K. Biocatalytic Hydrogen Atom Transfer: An Invigorating Approach to Free-Radical Reactions. *Current Opinion in Chemical Biology* **2019**, *49*, 16–24. https://doi.org/10.1016/j.cbpa.2018.09.001.

[33] Hillwig, M. L.; Liu, X. A New Family of Iron-Dependent Halogenases Acts on Freestanding Substrates. *Nat Chem Biol* **2014**, *10* (11), 921–923. https://doi.org/10.1038/nchembio.1625.

[34] Dauben, H. J.; McCoy, L. L. N-Bromosuccinimide. I. Allylic Bromination, a General Survey of Reaction Variables1-3. *J. Am. Chem. Soc.* **1959**, *81* (18), 4863–4873. https://doi.org/10.1021/ja01527a027.

[35] Dairi, T.; Nakano, T.; Aisaka, K.; Katsumata, R.; Hasegawa, M. Cloning and Nucleotide Sequence of the Gene Responsible for Chlorination of Tetracycline. *Bioscience, Biotechnology, and Biochemistry* **1995**, *59* (6), 1099–1106. https://doi.org/10.1271/bbb.59.1099.

[36] van Pée, K.-H.; Patallo, E. P. Flavin-Dependent Halogenases Involved in Secondary Metabolism in Bacteria. *Appl Microbiol Biotechnol* **2006**, *70* (6), 631–641. https://doi.org/10.1007/s00253-005-0232-2.

[37] Yeh, E.; Blasiak, L. C.; Koglin, A.; Drennan, C. L.; Walsh, C. T. Chlorination by a Long-Lived Intermediate in the Mechanism of Flavin-Dependent Halogenases,. *Biochemistry* **2007**, *46* (5), 1284–1292. https://doi.org/10.1021/bi0621213.

[38] Flecks, S.; Patallo, E. P.; Zhu, X.; Ernyei, A. J.; Seifert, G.; Schneider, A.; Dong, C.; Naismith, J. H.; van Pée, K.-H. New Insights into the Mechanism of Enzymatic Chlorination of Tryptophan. *Angew. Chem. Int. Ed.* **2008**, *47* (49), 9533–9536. https://doi.org/10.1002/anie.200802466.

[39] Blasiak, L. C.; Drennan, C. L. Structural Perspective on Enzymatic Halogenation. *Acc. Chem. Res.* **2009**, *42* (1), 147–155. https://doi.org/10.1021/ar800088r.

[40] Wilcken, R.; Zimmermann, M. O.; Lange, A.; Joerger, A. C.; Boeckler, F. M. Principles and Applications of Halogen Bonding in Medicinal Chemistry and Chemical Biology. *J. Med. Chem.* **2013**, *56* (4), 1363–1388. https://doi.org/10.1021/jm3012068.

[41] Olah, G. A.; Bollinger, J. Martin. Stable Carbonium Ions. XLVIII. Halonium Ion Formation via Neighboring Halogen Participation. Tetramethylethylene Halonium Ions. *J. Am. Chem. Soc.* **1967**, *89* (18), 4744–4752. https://doi.org/10.1021/ja00994a031.

[42] Brown, R. S.; Nagorski, R. W.; Bennet, A. J.; McClung, R. E. D.; Aarts, G. H. M.; Klobukowski, M.; McDonald, R.; Santarsiero, B. D. Stable Bromonium and Iodonium Ions of the Hindered Olefins Adamantylideneadamantane and Bicyclo[3.3.1]Nonylidenebicyclo[3.3.1]Nonane. X-Ray Structure, Transfer of Positive Halogens to Acceptor Olefins, and Ab Initio Studies. *J. Am. Chem. Soc.* **1994**, *116* (6), 2448–2456. https://doi.org/10.1021/ja00085a027.

[43] Haas, J.; Piguel, S.; Wirth, T. *Reagent* -Controlled Stereoselective Iodolactonizations. *Org. Lett.* **2002**, *4* (2), 297–300. https://doi.org/10.1021/ol0171113.

[44] Hennecke, U.; Müller, C. H.; Fröhlich, R. Enantioselective Haloetherification by Asymmetric Opening of *Meso* -Halonium Ions. *Org. Lett.* **2011**, *13* (5), 860–863. https://doi.org/10.1021/ol1028805.

[45] Huang, D.; Wang, H.; Xue, F.; Guan, H.; Li, L.; Peng, X.; Shi, Y. Enantioselective Bromocyclization of Olefins Catalyzed by Chiral Phosphoric Acid. *Org. Lett.* **2011**, *13* (24), 6350–6353. https://doi.org/10.1021/ol202527g.

[46] Inoue, T.; Kitagawa, O.; Ochiai, O.; Shiro, M.; Taguchi, T. Catalytic Asymmetric Iodocarbocyclization Reaction. *Tetrahedron Letters* **1995**, *36* (51), 9333–9336. https://doi.org/10.1016/0040-4039(95)02021-G.

[47] Kitagawa, O.; Hanano, T.; Tanabe, K.; Shiro, M.; Taguchi, T. Enantioselective Halocyclization Reaction Using a Chiral Titanium Complex. *J. Chem. Soc., Chem. Commun.* **1992**, No. 14, 1005. https://doi.org/10.1039/c39920001005.

[48] Kang, S. H.; Lee, S. B.; Park, C. M. Catalytic Enantioselective Iodocyclization of γ-Hydroxy-Cis-Alkenes. *J. Am. Chem. Soc.* **2003**, *125* (51), 15748–15749. https://doi.org/10.1021/ja0369921.

[49] Kwon, H. Y.; Park, C. M.; Lee, S. B.; Youn, J.-H.; Kang, S. H. Asymmetric Iodocyclization Catalyzed by Salen–CrIIICl: Its Synthetic Application to Swainsonine. *Chem. Eur. J.* **2008**, *14* (3), 1023–1028. https://doi.org/10.1002/chem.200701199.

[50] Ning, Z.; Jin, R.; Ding, J.; Gao, L. Enantioselective Iodolactonizations of 4-Pentenoic Acid Derivatives Mediated by Chiral Salen-Co(II) Complex. *Synlett* **2009**, *2009* (14), 2291–2294. https://doi.org/10.1055/s-0029-1217806.

[51] Soedjak, H. S.; Butler, A. Characterization of Vanadium Bromoperoxidase from Macrocystis and Fucus: Reactivity of Vanadium Bromoperoxidase toward Acyl and Alkyl Peroxides and Bromination of Amines. *Biochemistry* **1990**, *29* (34), 7974–7981. https://doi.org/10.1021/bi00486a028.

[52] Winter, J. M.; Moore, B. S. Exploring the Chemistry and Biology of Vanadium-Dependent Haloperoxidases *. *Journal of Biological Chemistry* **2009**, *284* (28), 18577–18581. https://doi.org/10.1074/jbc.R109.001602.

[53] Soedjak, H. S.; Walker, J. V.; Butler, A. Inhibition and Inactivation of Vanadium Bromoperoxidase by the Substrate Hydrogen Peroxide and Further Mechanistic Studies. *Biochemistry* **1995**, *34* (39), 12689–12696. https://doi.org/10.1021/bi00039a027.

[54] Butler, A.; Carter-Franklin, J. N. The Role of Vanadium Bromoperoxidase in the Biosynthesis of Halogenated Marine Natural Products. *Nat. Prod. Rep.* **2004**, *21* (1), 180–188. https://doi.org/10.1039/B302337K.

[55] Martinez, J. S.; Carroll, G. L.; Tschirret-Guth, R. A.; Altenhoff, G.; Little, R. D.; Butler, A. On the Regiospecificity of Vanadium Bromoperoxidase. *J. Am. Chem. Soc.* **2001**, *123* (14), 3289–3294. https://doi.org/10.1021/ja004176c.

[56] Wever, R., 2012. "Structure and Function of Vanadium Haloperoxidases." In: Michibata H. (eds) Vanadium. Springer, Dordrecht. https://doi.org/10.1007/978-94-007-0913-3.

[57] Tschirret-Guth, R. A.; Butler, A. Evidence for Organic Substrate Binding to Vanadium Bromoperoxidase. *J. Am. Chem. Soc.* **1994**, *116* (1), 411–412. https://doi.org/10.1021/ja00080a063.

[58] Rehder, D. The Coordination Chemistry of Vanadium as Related to Its Biological Functions. **1999**, 26.

[59] Crans, D. C.; Smee, J. J.; Gaidamauskas, E.; Yang, L. The Chemistry and Biochemistry of Vanadium and the Biological Activities Exerted by Vanadium Compounds. *Chem. Rev.* **2004**, *104* (2), 849–902. https://doi.org/10.1021/cr020607t.

[60] Vilter, H. PEROXIDASES FROM PHAEOPHYCEAE: A VANADIUM(V)-DEPENDENT PEROXIDASE FROM ASCOPH LZLUA4 NODOSUM. 4.

[61] Butler, Alison.; Walker, J. V. Marine Haloperoxidases. *Chem. Rev.* **1993**, *93* (5), 1937–1944. https://doi.org/10.1021/cr00021a014.

[62] Burns, R. C. NITROGENASFEROMVANADIUM-GROWANEOTOBACTERIS: OLATION, CHARACTERISTICSA, NDMECHANISTICIMPLICATIONS. *BIOCHEMICAL AND BIOPHYSICAL RESEARCH COMMUNICATIONS* **1971**, *42* (3), 6.

[63] Schweitzer, A.; Gutmann, T.; Wächtler, M.; Breitzke, H.; Buchholz, A.; Plass, W.; Buntkowsky, G. 51V Solid-State NMR Investigations and DFT Studies of Model Compounds for Vanadium Haloperoxidases. *Solid State Nuclear Magnetic Resonance* **2008**, *34* (1–2), 52–67. https://doi.org/10.1016/j.ssnmr.2008.02.003.

[64] Butler, A.; Sandy, M. Mechanistic Considerations of Halogenating Enzymes. *Nature* **2009**, *460* (7257), 848–854. https://doi.org/10.1038/nature08303.

[65] Hu, Y. and Ribbe, M.W., 2011. Historic overview of nitrogenase research. In *Nitrogen Fixation* (pp. 3-7). Humana Press.

[66] Hoffman, B. M.; Lukoyanov, D.; Dean, D. R.; Seefeldt, L. C. Nitrogenase: A Draft Mechanism. *Acc. Chem. Res.* **2013**, *46* (2), 587–595. https://doi.org/10.1021/ar300267m.

[67] Vollenbroek, E. G. M.; Simons, L. H.; van Schijndel, J. W. P. M.; Barnett, P.; Balzar, M.; Dekker, H.; van der Linden, C.; Wever, R. Vanadium Chloroperoxidases Occur Widely in Nature. *Biochemical Society Transactions* **1995**, *23* (2), 267–271. https://doi.org/10.1042/bst0230267.

[68] Plat, H.; Krenn, B. E.; Wever, R. The Bromoperoxidase from the Lichen *Xanthoria Parietina* Is a Novel Vanadium Enzyme. *Biochemical Journal* **1987**, *248* (1), 277–279. https://doi.org/10.1042/bj2480277.

[69] Messerschmidt, A.; Wever, R. X-Ray Structure of a Vanadium-Containing Enzyme: Chloroperoxidase from the Fungus Curvularia Inaequalis. *Proc. Natl. Acad. Sci. USA* **1996**, 5.

[70] Messerschmidt, A.; Prade, L.; Wever, R. Implications for the Catalytic Mechanism of the Vanadium-Containing Enzyme Chloroperoxidase from the Fungus Curvularia Inaequalis by X-Ray Structures of the Native and Peroxide Form. *Biological Chemistry* **1997**, *378* (3–4). https://doi.org/10.1515/bchm.1997.378.3-4.309.

[71] Macedo-Ribeiro, S.; Hemrika, W.; Renirie, R.; Wever, R.; Messerschmidt, A. X-Ray Crystal Structures of Active Site Mutants of the Vanadium-Containing Chloroperoxidase from the Fungus Curvularia Inaequalis. *J Biol Inorg Chem* **1999**, *4* (2), 209–219. https://doi.org/10.1007/s007750050306.

[72] McLauchlan, C. C.; Murakami, H. A.; Wallace, C. A.; Crans, D. C. Coordination Environment Changes of the Vanadium in Vanadium-Dependent Haloperoxidase Enzymes. *Journal of Inorganic Biochemistry* **2018**, *186*, 267–279. https://doi.org/10.1016/j.jinorgbio.2018.06.011.

[73] Weyand, M.; Schomburg, D. X-Ray Structure Determination of a Vanadium-Dependent Haloperoxidase from Ascophyllum Nodosum at 2.0 AÊ Resolution. 17.

[74] Isupov, M. N.; Dalby, A. R.; Brindley, A. A.; Izumi, Y.; Tanabe, T.; Murshudov, G. N.; Littlechild, J. A. Crystal Structure of Dodecameric Vanadium-Dependent Bromoperoxidase from the Red Algae Corallina Officinalis 1 1Edited by R. Huber. *Journal of Molecular Biology* **2000**, *299* (4), 1035–1049. https://doi.org/10.1006/jmbi.2000.3806.

[75] Hemrika, W.; Renirie, R.; Dekker, H. L.; Barnett, P.; Wever, R. From Phosphatases to Vanadium Peroxidases: A Similar Architecture of the Active Site. *Proc. Natl. Acad. Sci. U.S.A.* **1997**, *94* (6), 2145–2149. https://doi.org/10.1073/pnas.94.6.2145.

[76] Figure made my Logan Z. Hessefort

[77] Rehder, D. The Role of Vanadium in Biology. *Metallomics* **2015**, *7* (5), 730–742. https://doi.org/10.1039/C4MT00304G.

[78] Arber, J.M., De Boer, E., Garner, C.D., Hasnain, S.S. and Wever, R., **1989**. "Vanadium K-Edge X-Ray Absorption Spectroscopy of Bromoperoxidase from Ascophyllum Nodosum."*Biochemistry*, 28(19), pp.7968-7973.

[79] Vilter, H. Peroxidases from Phaeophyceae: A Vanadium(V)-Dependent Peroxidase from Ascophyllum Nodosum. *Phytochemistry* **1984**, *23* (7), 1387–1390. https://doi.org/10.1016/S0031-9422(00)80471-9.

[80] Van Schijndel, J.W., Barnett, P., Roelse, J., Vollenbroek, E.G. and Wever, R., **1994**. "The Stability and Steady-state Kinetics of Vanadium Chloroperoxidase from the Fungus *Curvularia Inaequalis*." *European Journal of Biochemistry* 225 (1): 151-157.

[81] de Boer, E.; van Kooyk, Y.; Tromp, M. G. M.; Plat, H.; Wever, R. Bromoperoxidase from Ascophyllum Nodosum: A Novel Class of Enzymes Containing Vanadium as a Prosthetic Group? *Biochimica et Biophysica Acta (BBA) - Protein Structure and Molecular Enzymology* **1986**, *869* (1), 48–53. https://doi.org/10.1016/0167-4838(86)90308-0.

[82] Coupe, E. E.; Smyth, M. G.; Fosberry, A. P.; Hall, R. M.; Littlechild, J. A. The Dodecameric Vanadium-Dependent Haloperoxidase from the Marine Algae Corallina Officinalis: Cloning, Expression, and Refolding of the Recombinant Enzyme. *Protein Expression and Purification* **2007**, *52* (2), 265–272. https://doi.org/10.1016/j.pep.2006.08.010.

[83] ten Brink, H. B.; Dekker, H. L.; Schoemaker, H. E.; Wever, R. Oxidation Reactions Catalyzed by Vanadium Chloroperoxidase from Curvularia Inaequalis. *Journal of Inorganic Biochemistry* **2000**, *80* (1), 91–98. https://doi.org/10.1016/S0162-0134(00)00044-1.

[84] *Functional Models for Vanadium Haloperoxidase: Reactivity and Mechanism of Halide Oxidation | Journal of the American Chemical Society*. https://pubs.acs.org/doi/10.1021/ja953791r (accessed 2022-09-06).

[85] Raugei, S.; Carloni, P. Structure and Function of Vanadium Haloperoxidases. *J. Phys. Chem. B* **2006**, *110* (8), 3747–3758. https://doi.org/10.1021/jp054901b.

[86] Amadio, E.; Di Lorenzo, R.; Zonta, C.; Licini, G. Vanadium Catalyzed Aerobic Carbon–Carbon Cleavage. *Coordination Chemistry Reviews* **2015**, *301–302*, 147–162. https://doi.org/10.1016/j.ccr.2015.06.004.

[87] De Boer, E.; Boon, K.; Wever, R. Electron Paramagnetic Resonance Studies on Conformational States and Metal Ion Exchange Properties of Vanadium Bromoperoxidase. *Biochemistry* **1988**, *27* (5), 1629–1635. https://doi.org/10.1021/bi00405a036.

[88] Carter-Franklin, J. N.; Butler, A. Vanadium Bromoperoxidase-Catalyzed Biosynthesis of Halogenated Marine Natural Products. *J. Am. Chem. Soc.* **2004**, *126* (46), 15060–15066. https://doi.org/10.1021/ja047925p.

[89] Carter-Franklin, J. N.; Parrish, J. D.; Tschirret-Guth, R. A.; Little, R. D.; Butler, A. Vanadium Haloperoxidase-Catalyzed Bromination and Cyclization of Terpenes. *J. Am. Chem. Soc.* **2003**, *125* (13), 3688–3689. https://doi.org/10.1021/ja029271v.

[90] Winter, J. M.; Moffitt, M. C.; Zazopoulos, E.; McAlpine, J. B.; Dorrestein, P. C.; Moore, B. S. Molecular Basis for Chloronium-Mediated Meroterpene Cyclization: CLONING, SEQUENCING, AND HETEROLOGOUS EXPRESSION OF THE NAPYRADIOMYCIN BIOSYNTHETIC GENE CLUSTER *. *Journal of Biological Chemistry* **2007**, *282* (22), 16362–16368. https://doi.org/10.1074/jbc.M611046200.

[91] Okwu, M. U.; Olley, M.; Akpoka, A. O.; Izevbuwa, O. E. Methicillin-Resistant Staphylococcus Aureus (MRSA) and Anti-MRSA Activities of Extracts of Some Medicinal Plants: A Brief Review. *AIMS Microbiol* **2019**, *5* (2), 117–137. https://doi.org/10.3934/microbiol.2019.2.117.

[92] McKinnie, S. M. K.; Miles, Z. D.; Jordan, P. A.; Awakawa, T.; Pepper, H. P.; Murray, L. A. M.; George, J. H.; Moore, B. S. Total Enzyme Syntheses of Napyradiomycins A1 and B1. *J. Am. Chem. Soc.* **2018**, *140* (51), 17840–17845. https://doi.org/10.1021/jacs.8b10134.

[93] van Schijndel, J. W. P. M.; Vollenbroek, E. G. M.; Wever, R. The Chloroperoxidase from the Fungus Curvularia Inaequalis; a Novel Vanadium Enzyme. *Biochimica et Biophysica Acta (BBA) - Protein Structure and Molecular Enzymology* **1993**, *1161* (2), 249–256. https://doi.org/10.1016/0167-4838(93)90221-C.

[94] Barnett, P.; Hemrika, W.; Dekker, H. L.; Muijsers, A. O.; Renirie, R.; Wever, R. Isolation, Characterization, and Primary Structure of the Vanadium Chloroperoxidase from the Fungus Embellisia Didymospora *. *Journal of Biological Chemistry* **1998**, *273* (36), 23381–23387. https://doi.org/10.1074/jbc.273.36.23381.

[95] Barnett, P.; Kruitbosch, D. L.; Hemrika, W.; Dekker, H. L.; Wever, R. The Regulation of the Vanadium Chloroperoxidase from Curvularia Inaequalis. *Biochimica et Biophysica Acta (BBA) - Gene Structure and Expression* **1997**, *1352* (1), 73–84. https://doi.org/10.1016/S0167-4781(96)00238-2.

[96] Butler, A. Mechanistic Considerations of the Vanadium Haloperoxidases. *Coordination Chemistry Reviews* **1999**, *187* (1), 17–35. https://doi.org/10.1016/S0010-8545(99)00033-8.

[97] Ligtenbarg, A. Catalytic Oxidations by Vanadium Complexes. *Coordination Chemistry Reviews* **2003**, *237* (1–2), 89–101. https://doi.org/10.1016/S0010-8545(02)00308-9.

[98] China, H.; Kumar, R.; Kikushima, K.; Dohi, T. Halogen-Induced Controllable Cyclizations as Diverse Heterocycle Synthetic Strategy. *Molecules* **2020**, *25* (24), 6007. https://doi.org/10.3390/molecules25246007.

[99] De Boer, E.; Boon, K.; Wever, R. Electron Paramagnetic Resonance Studies on Conformational States and Metal Ion Exchange Properties of Vanadium Bromoperoxidase. *Biochemistry* **1988**, *27* (5), 1629–1635. https://doi.org/10.1021/bi00405a036.

[100] Thompson, K. Coordination Chemistry of Vanadium in Metallopharmaceutical Candidate Compounds. *Coordination Chemistry Reviews* **2001**, *219–221*, 1033–1053. https://doi.org/10.1016/S0010-8545(01)00395-2.

[101] Starkey, L. 13C NMR Chemical Shifts. https://www.cpp.edu/~lsstarkey/courses/NMR/NMRshifts13C.pdf

[102] Chu, G.; Li, C. Convenient and Clean Synthesis of Imines from Primary Benzylamines. *Org. Biomol. Chem.* **2010**, *8* (20), 4716–4719. https://doi.org/10.1039/C0OB00043D.

[103] Zhang, Z.-Q.; Liu, F. CuX_2 -Mediated Oxybromination/Aminochlorination of Unsaturated Amides: Synthesis of Iminolactones and Lactams. *Org. Biomol. Chem.* **2015**, *13* (24), 6690–6693. https://doi.org/10.1039/C5OB00520E.

[104] Han, C.; Feng, X.; Du, H. Asymmetric Halocyclizations of 2-Vinylbenzyl Alcohols with Chiral FLPs. *Org. Lett.* **2021**, *23* (19), 7325–7329. https://doi.org/10.1021/acs.orglett.1c02361.

[105] Palladium-Catalyzed Aerobic Aminooxygenation of Alkenes for Preparation of Isoindolinones | *Organic Letters*. https://pubs.acs.org/doi/full/10.1021/acs.orglett.5b02703 (accessed 2022-06-16).